MODELING DISSOLVED PHOSPHORUS TRANSPORT FROM AGRICULTURAL WATERSHEDS IN CENTRAL NEW YORK

A Dissertation

Presented to the Faculty of the Graduate School

of Cornell University

In Partial Fulfillment of the Requirements for the Degree of

Doctor of Philosophy

by

Josephine A. Archibald

January 2015

MODELING DISSOLVED PHOSPHORUS TRANSPORT FROM AGRICULTURAL WATERSHEDS IN CENTRAL NEW YORK

Josephine A. Archibald, Ph. D.

Cornell University 2015

An important cause of freshwater contamination in the United States, soluble reactive phosphorus (SRP) loss from agriculture often occurs when overland runoff transports phosphorus (P) from manures and fertilizers to receiving waters. Because of the importance of overland runoff in transporting P, models that allow us to pinpoint the location and timing of overland runoff are an important tool for reducing SRP transport in overland runoff. We created a simple regional model that allows us to predict the timing and location of runoff in the northeastern United States. In addition, we conducted soil box experiments which indicate that SRP concentrations decline rapidly over time after manure fertilization, and this decline in P availability is affected by temperature. We developed an SRP model which predicts the SRP concentration after manure application, which, combined with the spatially explicit watershed model, allows for prediction of SRP loss from agriculture under a variety of manure timing scenarios. We find that in a 326 km^2 watershed where farmers apply P to match crop needs, simply changing the timing of manure application to avoid periods of runoff have the potential to reduce manure-derived SRP in runoff by up to 40%.

BIOGRAPHICAL SKETCH

Josephine Archibald was born in England in 1982, the third of five children. She moved with her family to the United States when she was three, and lived in New Rochelle, NY until attending college first at Edinburgh University in Scotland, and then Oberlin College, OH, where she received her bachelors in Environmental Studies and Biology. After college Josephine served as a US Peace Corps volunteer in a rural shepherding community in Morocco, where she helped the community implement a number of projects aimed at clean water access, income generation, women's empowerment, and health education. Josephine is an enthusiastic proponent of co-operative living and enjoying life's journeys, preferably by foot, bike or paddle.

This dissertation is dedicated to my grandmother, Valerie Archibald, whose insatiable interest in all questions, big and small, has been a constant source of inspiration to me.

ACKNOWLEDGMENTS

This work was funded by USDA Land/Sea Grant number 2012-67019019434, and from Cornell University Teaching and Research Assistantships.

I am very grateful to my advisers, Todd Walter, Brian Richards and Rebecca Schneider, for their continual support, thoughtful ideas, and encouragement. Thanks to Dan Fuka for all his help with programming, data access, and thinking outside the box. Thanks to Shree Giri for his invaluable help with chemical analysis, and Chris Berry for helping to set up the web-interface for the online tool that motivated so much of this work. I'd also like to thank Rebecca Marjerison for her patient and helpful explanations for all things GIS, and Brian Buchanan for his continual help creating usable map layers for the spatial analyses. Thanks to all members of the Soil and Water Lab group for creating such an inspirational and positive work environment.

I'd also like to thank my parents, Jean and Giles, and my siblings, Catherine, Mary, Henry and Isabella, for all their love and support through the years.

TABLE OF CONTENTS

LIST OF FIGURES

LIST OF TABLES

LIST OF ABBREVIATIONS

AWC	Available water capacity of the soil
DD	Degree days
DEM	Digital elevation model
ET	Evapotranspiration
HSM	Hydrologically sensitive moments, periods when water quality is most at risk
LIDAR	Light Detection and Ranging – a remote sensing method to map the earth's surface
NPS	Nonpoint source, coming from a variety of undefined locations.
NSE	Nash-Sutcliffe efficiency, a measure of fitness for streamflow, in which 1 signifies a perfect fit, and values less than 0 imply that using the average of the observations would be better than the model
P	Phosphorus
PBIAS	Percent bias, the average tendency of a model to be larger or smaller than the observations
PET	Potential evapotranspiration, the amount of water we would expect to evaporate given an unlimited supply of water.
RMSE	Root mean square error
RSR	Ratio of the root mean square error to the standard deviation of observations
SRP	Soluble reactive phosphorus
STI	Soil topographic index
STP	Morgan-extractable Soil Test Phosphorus
SWAT	Soil and Water Assessment Tool, a commonly used watershed model
SW_d	Soil water depth on day d
TDR	Time domain reflectometry, a method for determining soil moisture
VSA	Variable source areas, dynamic landscape locations that contribute to runoff
VSLF	Variable Source Loading Function, a watershed model that distributes runoff spatially
WEP	Water extractable P, the most-readily accessible P pool in soil or manure

INTRODUCTION

Phosphorus (P) loss from agriculture or other non-point sources is an important cause of freshwater contamination in the United States. In particular, the form of P that has highest potential to cause eutrophication is soluble reactive P (SRP), which is most readily available to aquatic life. Modeling the transport of SRP from diffuse sources across an agricultural watershed is complex because of the many interacting sources, sinks and pathways for P movement. However, the problem can be simplified by conceptualizing P transport as the sum of two main pathways – chronic, usually low-level transport in baseflow, and short periods of intense SRP transport during overland runoff. In agricultural watersheds where manure fertilization is common, the high-level P-transfers during runoff events become further compounded when recent fertilization coincides with runoff events. In these cases, it is especially important to correctly model when and where runoff is occurring in a watershed to accurately predict P transport.

One of the challenges of controlling non-point source pollution is that these sources of P can be anywhere in a watershed. If models are going to help us tackle the problem, they need to be easily applicable to a variety of watersheds, even those without data to allow model initiation and validation. Chapter 1 presents a simple watershed model that has been tested in ten watersheds in the northeastern US and can predicts timing and runoff locations without calibration.

Once runoff locations are known, it is important to understand how the availability of phosphorus for transport changes over time after manure application on soil. Chapter 2 presents results of soil box experiments which examine the interplay between timing of manure application, temperature, and soil moisture in impacting the concentration of SRP in runoff during simulated rain events.

Using the results from chapters 1 and 2, we can model the impact of timing changes in manure management in SRP delivery from agricultural land in an agricultural watershed in

central New York State. These results have implications for the use of affordable farming best management strategies, in which farmers would avoid spreading manure during times of high runoff potential.

CHAPTER 1

A simple model for predicting nonpoint source areas in the Northeastern US [1]

Introduction

Many stakeholders are involved in addressing the persistent challenge of mitigating nonpoint source (NPS) pollution to protect receiving water resources, including scientists, farmers and landowners. For NPS pollutants that are transported disproportionately in runoff such as phosphorus (P), a useful strategy for minimizing water contamination would be to avoid polluting activities like manure fertilization in areas that are expected to generate overland runoff in the near future (Walter et al., 2000). In the northeastern US, storm runoff is most commonly generated in parts of the landscape prone to soil saturation; because these areas are dynamic in time and space they are commonly referred to as variable source areas (VSAs) (e.g., Dunne and Black, 1970). Several methods of predicting storm runoff locations in active agricultural lands have already been proposed (Agnew et al., 2006; Gburek et al., 2000; Marjerison et al., 2011). However, these methods generally ignore the dynamic behavior of VSAs, and this variability in time is arguably a more critical factor in contaminant transport. For example, McDowell and Srinivasan (2009) found that over 75% of P loading during a 20 month period came from three rainfall-runoff events. Such timing influence suggests that planners need to be concerned about hydrologically sensitive "moments" (HSM) in addition to hydrologically sensitive areas and avoid manure-fertilizer or other contaminant applications at these times and locations.

Concepts aligned with HSMs are gaining traction among decision makers and planners. Researchers studying P transport (e.g. Kleinman et al., 2011) and flood risk (e.g. Van

[1] Archibald, J.A., B.P. Buchanan, D.F. Fuka, C.B. Georgakakos, S.L. Lyon, and M.T. Walter. 2014. A simple, regionally parameterized model for predicting nonpoint source areas in the Northeastern US. J. Hydrol. Reg. Stud. 1(C): 74–91. DOI: 10.1016/j.ejrh.2014.06.003

Steenbergen and Willems, 2013) suggest using dynamic decision support systems (DSS) to deal with these issues. One example of this is the Wisconsin Manure Management Advisory System (DATCP, 2013). This is a dynamic agricultural nonpoint source DSS that addresses the timing component of runoff risk using weather forecasts to determine the potential risk of runoff on a watershed scale (on average 500 km^2). However, while knowledge of watershed-wide risk(s) is useful, it does not allow farmers or other land managers to target the highest-risk runoff-generating areas. The reality of farm manure management with finite-capacity manure storage facilities (e.g., manure lagoons) is that there are times when there is a pressing need to spread manure regardless of watershed-scale risk forecasts. Therefore, producers with limited manure storage are often left with little guidance about when and where runoff is predicted in order to prioritize risks at the farm scale.

In looking ahead to the next generation of watershed NPS-mitigation tools to provide farm and field-scale predictions of storm runoff risks, one challenge is developing a simple model with enough of a physical basis to correctly predict where and when storm runoff will be generated. Simplicity is important in models because excessive parameterization or calibration may be prohibitively complex for conservation planners, and could lead to over-calibration and a fundamental misrepresentation of the processes involved in runoff generation (e.g. Kirchner, 2006).

Considerable work has already been devoted to reducing the number of calibration parameters in a variety of watershed models (Pradhan and Ogden, 2010; Seibert, 1999). In order to do this, we often need to make some assumptions about the dominant underlying processes driving runoff in

our watersheds of interest. For example, if we are primarily interested in the humid, well-vegetated northeastern USA, as is the case in this study, we can assume that saturation-excess is the main processes driving runoff and is expressed via shallow, lateral subsurface flows (a.k.a., interflows) that are a primary control on VSAs (Dunne and Black, 1970; Dunne and Leopold, 1978; Walter et al., 2003). From this standpoint, the goal of this study is to develop and test a minimally parameterized model for the northeastern USA. This model is designed to predict VSAs and hydrological response from readily obtainable watershed characteristics and forcing data that does not need to be calibrated. Specifically, we are interested in reducing the number of parameters and removing the need for watershed-specific calibration. To do this, we combine modeling concepts from STOPMODEL (Walter et al., 2002) and the Variable Source Loading Function (VSLF) model, which has been shown to work well in the northeastern US (Schneiderman et al., 2007). Although the model simulates stream discharge at the watershed outlet, our focus is on predicting the locations and timing of runoff generation.

A major advantage to STOPMODEL and VSLF is that they predict runoff generation in time and at spatial resolutions relevant to farmers (sub-field), which is our main goal in this application. As such, we extend a semi-distributed approach to watershed modeling that maintains a "lumped" watershed water balance and redistributes runoff based on soil topographic index (STI), as defined by Walter et al. (2002). The STI is useful for pinpointing runoff generating landscape locations in humid regions (Lyon et al., 2004). In fact, Dahlke et al. (2013) successfully used this approach to calibrate a prototype of a DSS that is capable of using weather forecasts to predict saturated areas in a watershed. Here, we modify the Dahlke et al. (2013) model structure to create a simple VSA model that relies on three runoff parameters (a daily

storage coefficient, and two parameters to determine the daily hydrograph shape). The resulting model is computationally efficient enough to be applied at large spatial scales and yet yields spatially explicit results that are useful for conservation planners tasked with targeting sub-field scale management practices. In addition to predicting when and where storm runoff will occur, this model uses open source coding (R-programming language, R Core Team 2013) and information (e.g., USGS and USDA geographical information) in a manner that is easily applicable to web-based applications.

Conceptual Model Description

Water Budget

The modeling approach adopted here is similar to that used by the early forms of TOPMODEL (Beven and Kirkby, 1979), STOPMODEL (Walter et al., 2002), and VSLF (Schneiderman et al., 2007) in which the soil- and ground-water budgets are maintained at the watershed scale (Figure 1.1) while storm runoff is distributed according to topographic position within the watershed. The soil water budget that forms the backbone of the model was first proposed by Thornthwaite and Mather (1955). Daily modeled soil water and evapotranspiration (ET) are based on soil water status and potential evapotranspiration (*PET*):

$$SW_d = SW_{d-1} \exp\left(\frac{I_d - C_C PET_d}{AWC}\right) \quad \text{for } I_d - C_c PET_d < 0 \qquad (1.1a)$$

$$SW_d = SW_{d-1} + (I_d - C_C PET_d) - D \quad \text{for } I_d - C_c PET_d \geq 0 \qquad (1.1b)$$

$$D = SW_{d-1} + (I_d - C_C PET_d) - AWC$$

$$\text{for } SW_{d-1} + (I_d - C_C PET_d) > AWC \qquad (1.1c)$$

where SW_d is soil water depth on day d (mm), AWC is the watershed-wide average available water capacity of the soil (mm), I_d is water input on day d (rain + snowmelt – Q_d) (mm), C_c is a generalized crop coefficient to scale PET under various effective vegetative covers (adopted from Shuttleworth, 1992), D *is* drainage to the groundwater (mm), and Q_d is storm runoff on day d (mm). Storm runoff is estimated using Eq. 2 (discussed in the next paragraph).The watershed-average AWC is calculated from the area-averaged AWC-percentage (mm water per mm of soil depth) and soil depths from the NRCS SSURGO database (NRCS, 2013). Daily PET is calculated using the Priestley-Taylor (1972) equation using daily maximum and minimum air temperature to estimate net radiation (Archibald and Walter, 2013). A similar method is used to model daily snow (Walter et. al., 2005; Fuka et al.,2012). Baseflow is modeled using a linear reservoir model adopting an average regional coefficient of 0.1 day^{-1} based on recession flow analysis of streams in the northeastern US (Frankenberger et al., 1999).

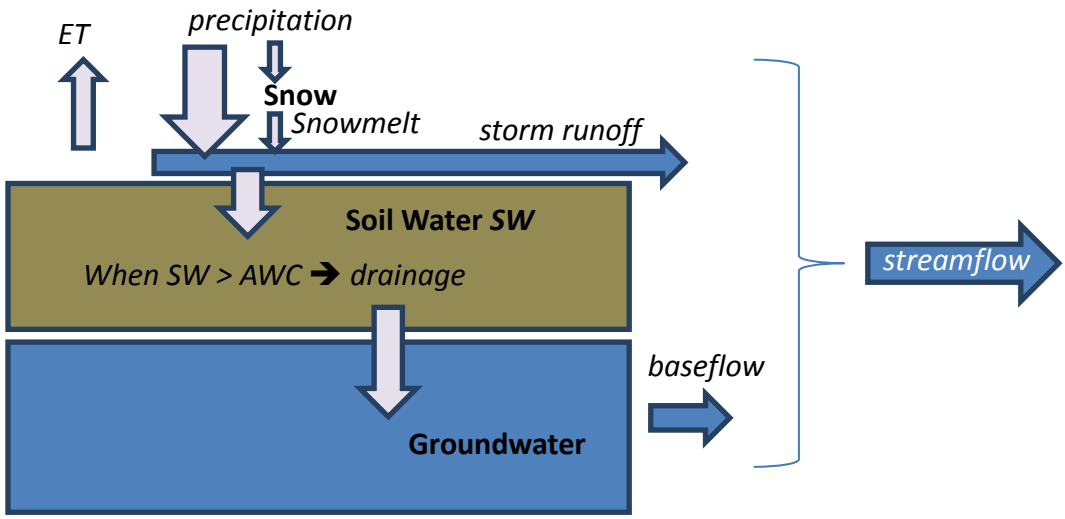

Figure 1.1: Schematic of the lumped water budget model.

Storm Runoff

Storm runoff is estimated using the SCS Curve Number equation (e.g. USDA-NRCS, 2004):

$$Q_d = \frac{{P_d}^2}{P_d + S_d} \quad (1.2)$$

where Q_d is runoff on day d (mm), P_d is the effective precipitation and/or snowmelt (mm) for that day defined as rain plus snowmelt minus an initial abstraction – here we use initial abstraction = $0.05S_d$ for the Northeast (similar to Shaw and Walter, 2009) -- and S_d is the storage parameter (mm), which changes in the model on a daily time-step based on average watershed soil water status, SW_d. Eq. 1.2 has been shown to be consistent with VSA hydrology (e.g., Steenhuis et al., 1995; Lyon et al., 2004; Schneiderman et al., 2007; Easton et al., 2008; Dahlke et al., 2012). However, the tabulated parameters for determining S are inconsistent with the VSA concept and do not work well in the Northeast (Shaw and Walter, 2009). Here we test a linear relationship between S_d and soil water deficit, SWD_d = AWC - SW_d.

Runoff Hydrograph

Although simulating stream discharge is not the main objective of this model, the storm hydrograph is used to simulate storm water temporarily retained in the landscape after the storm is over, before ultimately draining to the river. In order to model runoff timing, we adapt a variation of the SCS synthetic unit hydrograph (USDA-NRCS 2004) in which the hydrograph shape has a linear rising limb from the beginning of the storm to the time to peak, T_p, and an exponential falling limb characterized by a hydrograph shape parameter, b. We estimate T_p as an empirical, linear function of the time of concentration, T_c, (Kirpich, 1940);

$$T_c = T_c\,(hrs) = 0.00032L^{0.77}(\Delta E/L)^{-0.385}$$

where L is the longest flow path (m) and ΔE is the elevation change over L (m).

Spatial Distribution of Runoff:

Modeled storm runoff is distributed across the watershed based on the approach proposed by Lyon et al. (2004) and used by Schneiderman et al. (2007). Briefly, runoff distribution follows the soil topographic index (STI) (Walter et al., 2002), which indicates the relative propensity of a particular location to saturate and generate runoff:

$$\lambda = \ln\left(\frac{a}{T\tan(\beta)}\right) \quad (1.3)$$

where λ is the soil topographic index [ln(day m^{-1})], a is the upslope contributing area per unit length of contour (m), T *is* transmissivity (m^2 day^{-1}) of the soil defined as the product of soil depth and saturated hydraulic conductivity, and β(m m^{-1}) is the local slope (see Buchanan et al., 2013 for optimal ways to calculate these terms for northeastern US landscapes). The fractional area, A_f (dimensionless) of the watershed that is generating storm runoff (e.g., Steenhuis et al., 1995; Lyon et al., 2004) is given as:

$$A_f = 1 - \frac{{S_d}^2}{(P_d+S_d)^2} \quad (1.4)$$

We divide each watershed into wetness classes based on the quantiles of the STI (Eq. 3); starting with the first wetness class corresponding to the wettest quantile of the watershed. We then calculate the amount of soil water storage that is available in each wetness class using (Schneiderman et al., 2007):

$$\sigma_{w,d} = \left(S_d \sqrt{\frac{1}{1-A_s}} - 1\right) \quad (1.5)$$

where $\sigma_{w,d}$ (mm) is the daily effective soil water content for a particular wetness class, *w*, of the watershed and A_S is fractional area of the watershed of all wetness classes up to and including wetness class *w* (dimensionless, between 0-1) (For more details see Schneiderman et al., 2007). This method allows us to have different effective soil water contents throughout the watershed based on wetness classification; these values change over time based on S_d. The amount of storm runoff generated from each fractional area is then simply P_d - $\sigma_{w,d}$. Areas of a watershed where $\sigma_{w,d} \geq P_d$ do not generate storm runoff. This semi-distributed VSA model is included in the EcoHydRology package in R (Fuka et al., 2013b).

Determining Regional Model Parameters

The conceptual model described here has three unknown parameters, S_d (Eq. 1.2), and T_p and *b*, which characterize the storm hydrograph. All other parameters in the study were obtained independently from open source and commonly available data, e.g., soil properties (i.e., *AWC*, *T*) from the USDA-NRCS SSURGO or STATSGO databases, and watershed characteristics (i.e., *a*, tan(β), watershed area, etc.) determined from a USGS digital elevation model (DEM). We used ten USGS-gauged watersheds in New Jersey (NJ), Pennsylvania (PA), and New York (NY) in the northeastern USA (Figure 1.2) to develop methods for regionally estimating the unknown parameters. Watersheds varied in size from approximately 10 km^2 (Biscuit Brook, NY) to over 4000 km^2 (Allegheny River, NY, PA) (Table 1).

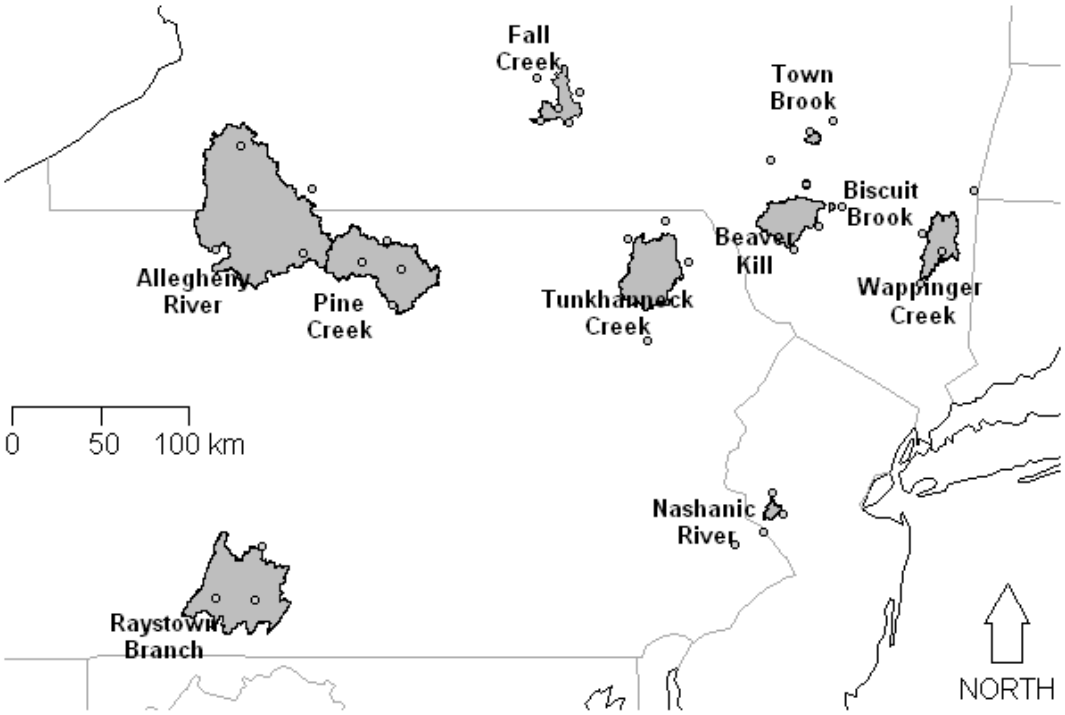

Figure 1.2. Locations of the ten watersheds used in this study, and the GHCN gauges used to model streamflow and saturation extent in the watersheds (open circles). Note, not all the gauges recorded precipitation and temperature data for all years between 1990-2010, so an average value of temperature and precipitation was recorded for each day using available data from the closest 2-4 gauges.

Table 1.1: Characteristics of the ten watersheds used in this study

Watershed	USGS ID	Size (km^2)	Soil Depth (mm)*	*AWC* (mm)*
Biscuit Brook (NY)	01434025	9.6	500	50
Town Brook (NY)	01421618	37	1,470	120
Neshanic River (NJ)	01398000	66	1,140	160
Fall Creek (NY)	04234000	330	1,990	110
Wappinger Creek (NY) (1999-2000)	01372500	470	1,880	280
Beaver Kill (NY)	01420500	620	1,200	100
Tunkhannock Creek (PA)	01534000	990	1,950	170
Pine Creek (PA)	01548500	1600	1,580	130
Raystown Branch Juniata River (PA)	01562000	2000	1,120	120
Allegheny River (NY,PA)	03011020	4200	1,560	160

* Area weighted averages based on SSURGO (USDA-NRCS)

We used daily measurements of precipitation and maximum and minimum temperatures as inputs for the model (NOAA, 2013). Daily streamflow measurements at these sites were from the USGS (2013). Watershed characteristics determined by topography, average soil depth, average available water capacity, and latitude were from the USDA and the USGS (USDA-NRCS, 2013; USGS, 2013). These watersheds were used to develop regional relationships between a watershed-wide soil water deficit, SWD_d, and S_d. They were also used to determine a relationship between watershed size and topography, and T_p .

To develop a regional relationship for S_d, we identified 532 isolated events from all the watersheds considered. Because Eq. 2 is most accurate in larger precipitation events (USDA-NRCS, 2004), we only considered events with daily rain and/or snowmelt events that were at least 20 mm and associated with an isolated rise in the streamflow hydrograph. From these, we estimated the storm runoff using a one-pass baseflow separation filter (Lyne and Hollick, 1979) (Appendix A.1). We calculated S_d-values (by rearranging Eq. 1.2) from these events using the technique described by Shaw and Walter (2009). We used Eq. 1 to estimate SW_d continuously to determine SWD_d, which we then correlated with the back-calculated S_d-values. We used the take-one-out methodology to ensure that no single watershed was biasing the S_d-SWD_d relationship.

To develop regionalized functions to describe the storm hydrograph, which has two parameters, T_p and b, we identified 214 well-defined events from the ten watersheds. The criteria defining these events were: rain (+ snowmelt) > 10 mm and no days with more than 2 mm for the two preceding and the five following days. These criteria allowed us to balance identifying many hydrographs while minimizing the impacts of rain and snowmelt before and after an event on the

hydrograph shape. The *b* parameter determines the overall shape of the runoff hydrograph, and for this study we found that a constant value of 4.5 allowed us to reproduce the overall runoff pattern for all watersheds after manual calibration. Based on the proportion of runoff that reached the outlet on each of the five days following a rain or snowmelt event, we were able to determine a best-fit T_p which minimized the root-mean-square error between the predicted and observed runoff shape (see Appendix A.1 for further details). We used the take-one-out approach to evaluate the degree to which any one watershed influenced the relationships between the best-fit T_p and T_c.

Model Application

We performed three independent tests on our model: (1) we used a leave-one-out approach to see how well our model would predict the hydrograph of a watershed that was not used to determine the regional model parameters, (2) we compared our predicted storm runoff locations to shallow water table measurements, and (3) we compared our predicted storm runoff locations to measured soil moisture.

Test 1: Hydrograph Analysis

To understand how the model would perform in ungauged watersheds, we considered the recalculated relationships between S and SWD_d and *between* T_c and T_p, determined by systematically excluding one watershed in a leave-one-out approach (Arlot and Celisse, 2010). We then used these relationships to model the excluded watershed and compare the predicted and observed discharge hydrographs; note, in the earlier part of this paper we were only investigating how sensitive the parameters were to any one watershed and here we are evaluating

model performance. The values of the coefficients for the relationships between measured and model parameters when excluding each watershed are reported in Table 1.2.

Modeled results were compared to USGS daily streamflow measurements at each location. In addition to the Nash-Sutcliffe efficiencies (NSE), we determined the ratio of the root mean square error to the standard deviation of observed streamflow (RSR) and the percent bias (PBIAS) for each watershed (Nash and Sutcliffe, 1970). Moriasi et al. (2007) proposed that a model is satisfactory if NSE > 0.50, RSR < 0.70, and has an absolute PBIAS < 25%. We also calculated NSE on an event basis, where runoff events were initiated by a one day rise in the observed USGS hydrograph after at least two days of decreasing flows.

Test 2: Water Table Analysis

We created a LIDAR-derived STI (Figure 1.3) for comparison to water table height measurements from Town Brook Watershed, using: (i) a 3m LIDAR-derived DEM from the NY Department of Environmental Protection (DEP), (ii) maximum triangular slope (Tarboton, 1997), (iii) the Multiple Triangular Flow Direction method (Seibert and McGlynn, 2007) as per Buchanan et al. (2013). We then binned STI values into equal-area wetness classes, such that low-numbered wetness classes are wetter areas (large STI values) and high wetness classes signify dry areas of the watershed (low STI values). This allowed us to assign a location as "wet" or "dry" during a storm event based on the saturated extent predicted by the model.

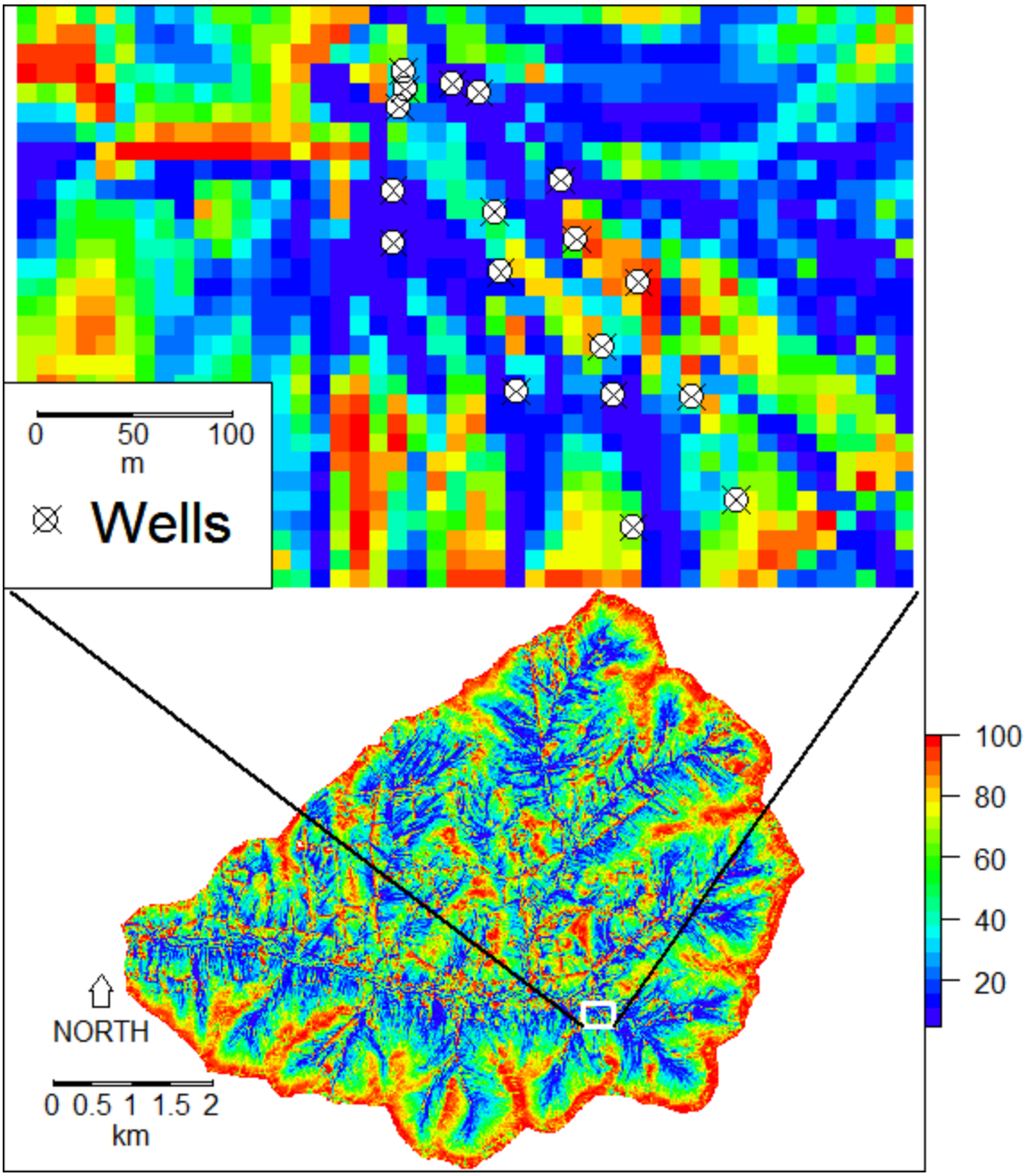

Figure 1.3: Town Brook watershed broken into 100 equal area wetness classes based on a 3m LIDAR DEM. Wet areas are blue and have a low number wetness class, while dry areas are labeled red and have high wetness class values (see color ramp). The top map shows the locations of the shallow water table wells used in this analysis (Lyon et al., 2006).

Lyon et al. (2006) collected 6 months of 15-minute interval shallow water table measurements in a 2 ha near-stream region in the Town Brook, NY watershed (inset, Figure 1.3). We used maximum daily water level measured in 18 wells (Lyon et al., 2006) recorded via WT-HR 500 capacitance probes (TruTrack, Inc, New Zealand). We ran the watershed model using precipitation data measured on-site and temperature data from Delhi, NY. On days when runoff was predicted, we divided the wells into "wet" locations where our model predicted runoff generation and "dry" locations where our model predicted no runoff generation to compare water table depths between groups.

Test 3: Soil Moisture Analysis:

Volumetric soil moisture measurements were taken at two field sites in Fall Creek and Cascadilla Creek watersheds (near Ithaca, NY) over the course of Fall 2012 and Spring 2013 (Figure 1.4). Measurements were taken in triplicate using a TDR probe over a range of wetness classes (Buchanan et al., 2013). We assigned a wetness class to each sampling location using a 3-m LIDAR derived STI value (same method as in Test 2). For each measurement date, we modeled the extent of saturated areas in the contributing watershed that were predicted to generate runoff on that particular date. Using this breakdown, we assigned each soil moisture measurement point a predicted value of "wet" and "dry" based on whether the model predicted the point to be generating runoff or not, respectively. This was compared to the soil moisture status of these wet and dry locations. The number of wet and dry locations changed on each measurement date, depending on the extent of saturation predicted for that day. We estimated the porosity of the soil as 53% assuming minimal organic matter using the bulk density reported in the USDA SSURGO data set (USDA-NRCS, 2013).

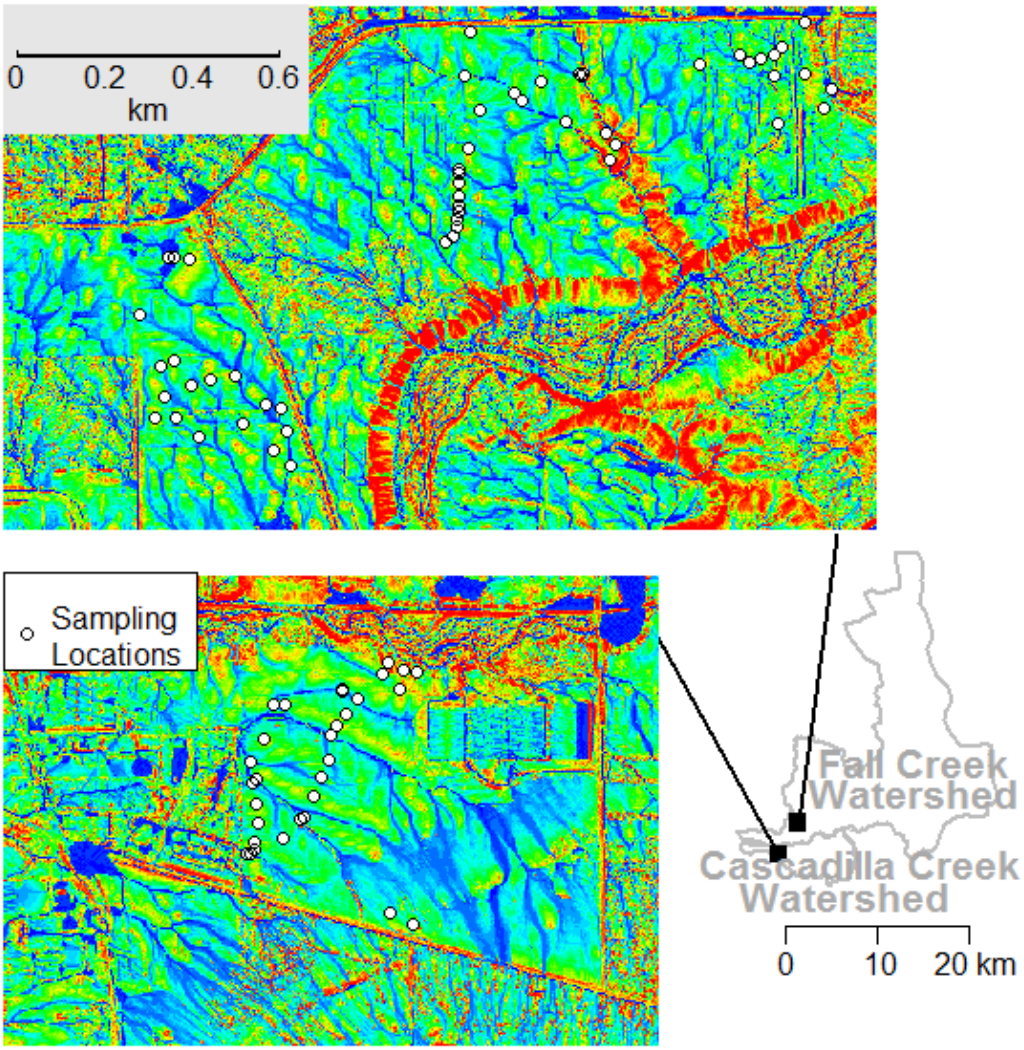

Figure 1.4. Wetness class maps of the soil moisture measurement sites in Fall Creek and Cascadilla Creek watersheds. Blue areas have a low wetness class value and are most likely to generate runoff, while red areas have high wetness class values and are expected to remain dry (see color ramp in Figure 1.3). Note: the linear wet and dry features represent the effects of roads and roadside ditches (i.e. linear blue areas are road ditches and red linear features are the downslope, drying-out effects due to the ditches).

Determining Regional Model Parameters

Calculating the Curve Number S (S_d) from a watershed-wide Soil Water Deficit (SWD_d)

We found there was a significant ($p<0.001$) linear relationship between S_d *and* SWD_d, which is represented by equation 6 and overall coefficients reported in Table 1.2.

$$S_d = S_{min} + C_1(SWD_d) \quad (1.6)$$

We recalculated this relationship by excluding data from each watershed individually, and found that the relationship remained significant at the $p<0.001$ level for each watershed excluded, with the intercept, S_{min}, varying between 78 to 86 mm, and the slope, C_1, varying between 3.3 and 3.5 (Table 1.2, Figure 1.5). This suggests that we can use Eq. 1.6 to determine S_d from SWD_d directly, without needing to calibrate unique coefficients for individual watersheds, i.e., we can use the average values for S_{min} and C_1.

Table 1.2. S_{min} and C_1 are the intercept and slope of the relationship between S_d and SWD_d (Eq. 6) calculated excluding values from each watershed; C_2 and C_3 are the coefficients used in the linear equation relating T_c to T_p (Eq. 7) when excluding data for each watershed and $T_{p,TOO}$ is the time to peak calculated (Eq. 7) using the C_2 and C_3 based on the other nine watersheds.

Watershed	Period Modeled	S_{min} (mm)	C_1	C_2	C_3 (hr)	T_c (hr)	$T_{p,TOO}$* (hr)
Biscuit Brook	1990-2010	78	3.4	0.32	3.6	0.53	3.8
Town Brook	1997-2010	82	3.4	0.33	3.5	1.4	4.0
Neshanic River	1990-2010	86	3.3	0.31	3.8	2.8	4.7
Fall Creek	1990-2010	84	3.5	0.33	3.5	8.7	6.4
Wappinger Creek	1999-2010	82	3.4	0.33	3.1	8.9	6.0
Beaver Kill	1990-2010	80	3.4	0.33	3.5	7.3	5.9
Tunkhannock Creek	1990-2010	82	3.5	0.33	3.3	8.4	6.1
Pine Creek	1990-2010	81	3.5	0.33	3.5	14	8.2
Raystown Branch	1990-2010	83	3.4	0.28	3.6	21	9.5
Allegheny River	1990-2010	81	3.5	0.46	2.6	30	16
All Watersheds		82	3.4	0.33	3.4		-

* T_P determined using the take-one-out approach. Note that these are different from the best-fit T_p values shown in Figure 1.5.

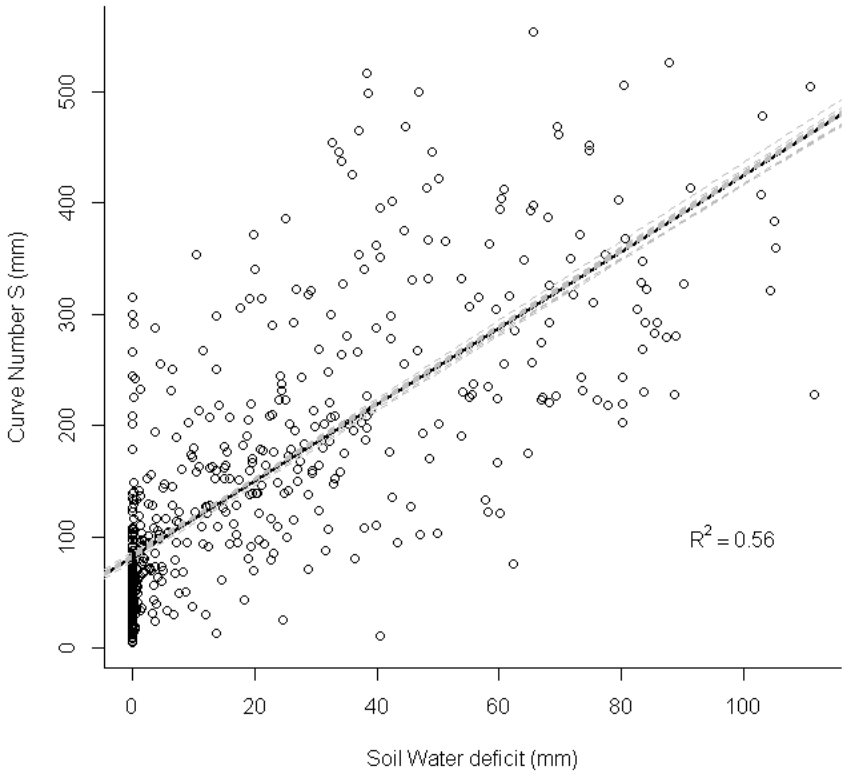

Figure 1.5: Observed S_d verses soil water deficit (SWD_d) on the day preceding runoff initiation. The dashed grey lines are the relationships found when removing one watershed at a time from the 10-watershed dataset. Intercept varied between 78 to 86, slope between 3.3-3.5 (Table 1.2); the relationship was always significant, p-value < 0.001 (even when all 110 points with SWD_d = zero are removed).

Estimating the hydrograph shape using watershed characteristics

The best-fit T_P values were well correlated (R^2 = 0.80, p<0.01) to T_C (Figure 1.6), and we determined a linear relationship that allows us to estimate T_p based on T_c:

$$T_{P,c} = C_2 T_C + C_3 \quad (1.7)$$

where $T_{P,C}$ is the calculated time to peak (hr), C_2 is a fitted slope of 0.33 (unitless), and C_3 is the fitted intercept of 3.4 (hrs). We recalculated C_2 and C_3 using the leave-one-out method (Figure

1.6); R^2 varied between 0.77 to 0.88 for the various combinations of nine watersheds, C_2 varied between 0.28 and 0.46, and C_3 varied between 2.6 and 3.76 hours (Table 1.2).

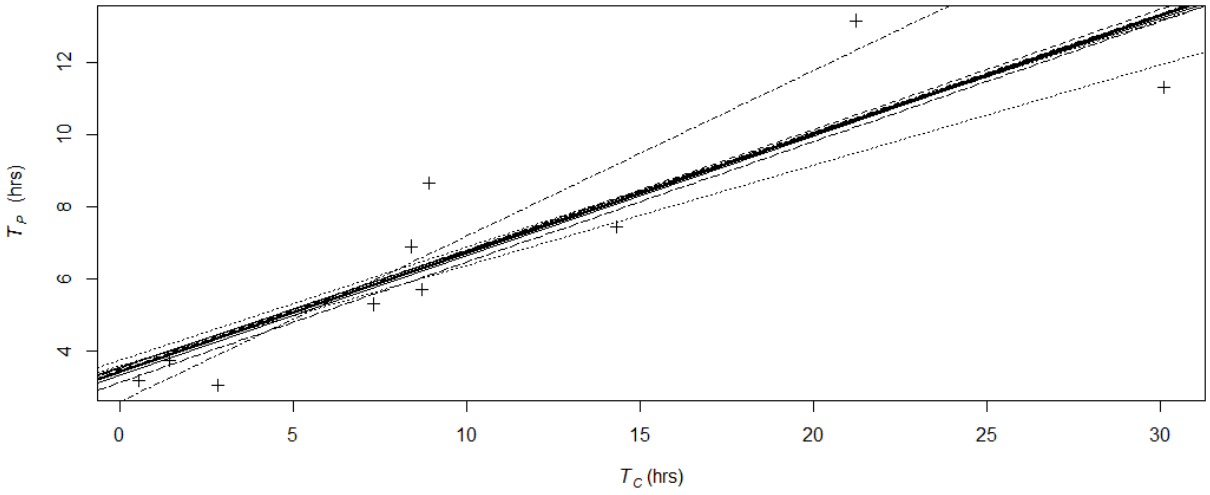

Figure 1.6: Relationship between the best fit-determined T_P and T_C calculated for each watershed. The dashed lines are the relationship recalculated by dropping each watershed from the data. This take-one-out approach is useful for applying the relationship for each watershed without including data taken from that particular watershed.

Model Application

Test 1: Hydrograph Analysis

Modeled flow compared reasonably well to observed flow at nine of the ten gauges (Table 1.3, Figure 1.7). These values improved during time periods when there was a rain gauge inside the watershed. For example, the Wappinger Creek NSE improved to 0.64 from 0.57 for daily flow after 2004, when a NOAA gauge is active inside the watershed. Using these measures, the model appears acceptable in nine of the ten watersheds, although it fails in the Neshanic River, NJ in all three metrics. Interestingly, event flow analyses showed better performance relative to daily for the small watersheds and no change or worse performance for the larger watersheds.

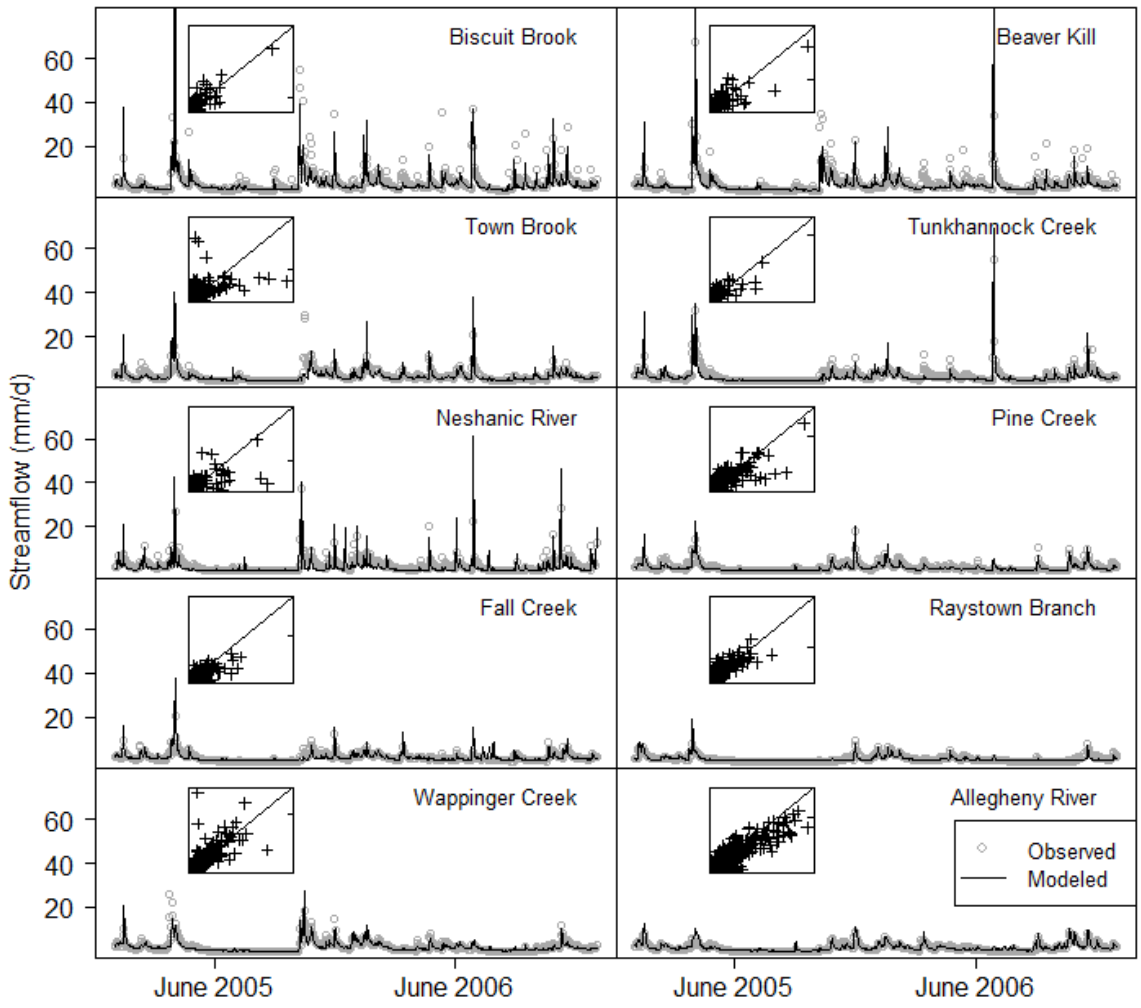

Figure 1.7. Observed and modeled streamflow during the 2-year period between 2005-2006. Observed flow is shown as grey open symbols, while modeled flow is the black line. Inset scatter plots are modeled flow on the vertical axis against measured streamflow on the horizontal axis, the line shows the 1-1 relationship.

Table 1.3. Model results for the ten USGS gauges used in this study based on a take-one-out approach. Daily NSE values in parentheses are during periods that include additional precipitation gauges inside the watershed (if applicable). RSR is the ratio of the root mean square error to the standard deviation of observed streamflow, and PBIAS is the percent bias (Moriasi et al., 2007). The average gauge distance from watershed was calculated by assigning a distance of zero for all gauges inside the watershed, and using the dist2Line function in the R-package geosphere (Robert J. Hijmans et al., 2012) to calculate the minimum distance from a gauge to the closest point along the watershed's boundary.

Watershed	Event NSE	Daily NSE	RSR	PBIAS	Average gauge distance from watershed (km)
Biscuit Brook	0.71	0.55	0.68	-3.9%	14
Town Brook	0.64	0.50	0.70	7.2%	15
Neshanic River	0.48	0.18	0.90	-33%	8
Fall Creek	0.72	0.67	0.58	-1.2%	2
Wappinger Creek	0.56	0.57 (0.64)	0.66	-17%	5- 6
Beaver Kill	0.59	0.61	0.63	-4.6%	5
Tunkhannock Creek	0.55	0.67	0.58	-17%	8
Pine Creek	0.66	0.67	0.57	-6.9%	0.4
Raystown Branch	0.56	0.56	0.67	-16%	0.5
Allegheny River	0.62	0.64 (0.68)	0.60	5.5%	0.4 -2
AVERAGE	0.61	0.56	0.66	-9.8%	3.5

Test 2: Water Table Analysis

Over the 6 month period of observations in Town Brook watershed, the model predicted 16 occurrences of overland runoff. During 15 of those events, the median water table depth for locations estimated as being "wet" was less than 100 mm from the soil surface, while the median dry wells remained at or below a depth of 100 mm during all events (Figure 1.8). This corroborates previous findings that overland runoff in the Northeast is initiated once the water table is within approximately 100 mm of the surface (Lyon et al., 2006; Dahlke et al., 2012).

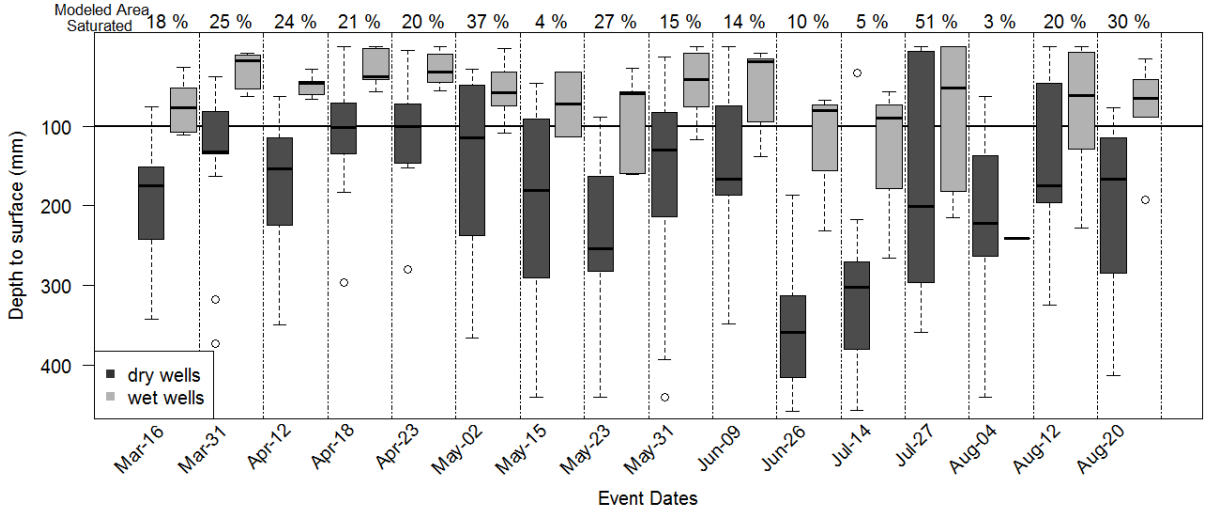

Figure 1.8: Water table depths in the 18 wells in Town Brook Watershed during runoff events, categorized by model predictions of wet area extent distributed using a 3m LIDAR-derived STI. The numbers along the top signify the percentage of the watershed that was predicted to be wet for that event. The cutoff line between dry and wet wells is 100 mm, with only one occurrence of the median occurring below, on August 4th.

Over the course of the 16 events, we compared 288 separate predictions of wet or dry conditions to field measurements. In 18 cases (6%), we predicted a well to be wet when the water table at that location was below 100 mm and in 55 (19%) cases we predicted a well to be dry when the water table depth was within 100 mm of the soil surface. The remaining 215 (75%) predictions

correctly identified a location as wet or dry based on modeled results. On days when no runoff was predicted, the average depth to the water table of all wells was 240 mm.

Test 3: Soil Moisture Analysis

At the Fall Creek site, four out of the 13 measurement dates were predicted to have saturated areas contributing to storm runoff. In three of the four dates, the median volumetric soil moisture reading in the modeled wet locations was above saturation, (i.e. $\geq$ 53%), while dry locations had median values below saturation (Figure 1.9, top). On the date that the "wet" wells were below the saturated value (June 26, 2013), the observed streamflow at the outlet did not show a discernible rise in the hydrograph, highlighting the difficulty in correctly modeling small storm runoff events. The Cascadilla Creek site only had one instance of measurements being taken in locations predicted to be wet, and on this date, the wet sites had a median soil moisture status above saturation (Figure 1.9, bottom).

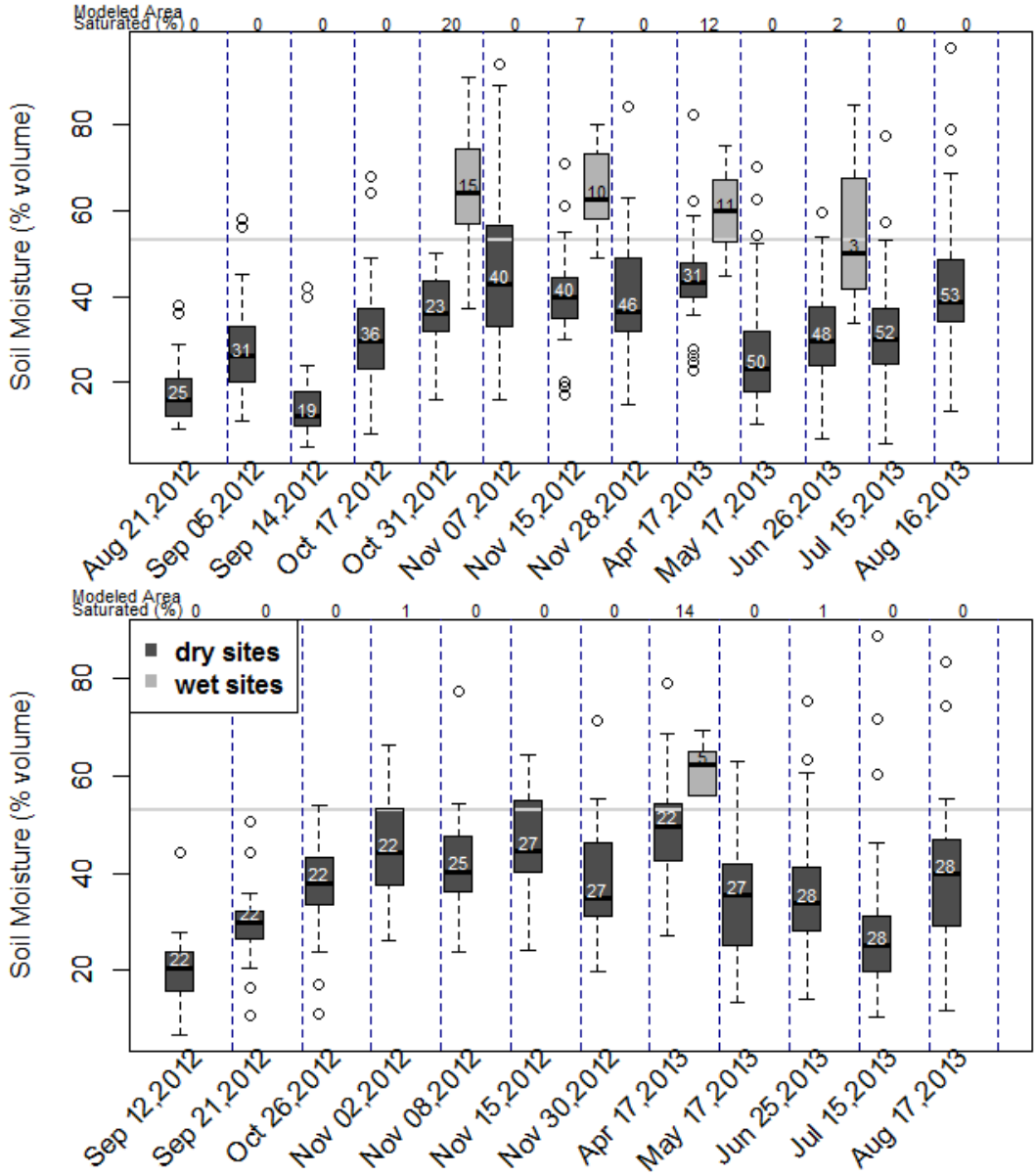

Figure 1.9: Soil moisture readings at the Fall Creek (top), and Cascadilla Creek (bottom) sites. On the days that runoff was predicted, sites were categorized as "wet" if their STI value put them within the wettest modeled percentage of watershed predicted to be contributing to runoff on that day. Light grey box-plots are measurements at locations that were labeled as wet by the model, dark grey boxes are locations that were predicted to be dry. The numbers along the top of the graph are the percentage of the watershed predicted to be contributing to runoff on that day. The numbers above the median line in the boxes are the number of measurements. The grey horizontal line is the estimated porosity of the soil, 53%, and we assume that measurements above this signify saturation.

Discussion

The model presented here shows promise as a simple tool allowing for spatial prediction of saturation-excess runoff locations in the northeastern US. Areas that were predicted to generate overland runoff had higher average soil moisture status and an elevated water table compared to areas modeled to be dry within three watersheds. As such, this model may serve as an effective screening tool for identifying sub-field scale runoff source areas or VSAs. It is particularly important to identify these VSAs when modeling contaminants that are disproportionately transported in overland flow, such as P.

Further, the model correctly identified dry locations and periods, indicating the model's ability to reflect HSMs and potential runoff source area variability. This has important implications for management as it indicates that this approach could be implemented as a real-time, spatiotemporally-dynamic runoff risk tool at the sub-basin and sub-field scale (similar to Dahlke et al., 2013). This would contrast with other real-time watershed tools, such as the Wisconsin Manure Management Advisory System, that advise users of risks on a watershed-wide basis (DATCP, 2013). These prediction tools would be most useful in the context of trying to minimize phosphorus or sediment losses in runoff.

It is instructive to look at the two watersheds where model performance was the worst, Neshanic River and Town Brook watersheds, as it allows us to use the model as a hypothesis testing tool. Both of these watersheds are small and have no internal rain gauges and, thus, the amount of rain we are assuming is occurring in the watershed may be incorrect. Fuka et al. (2013a) demonstrate that when a weather gauge is greater than 10km from a small basin, even a short term weather

forecast may result in better model performance relative to using the weather station. In particular, the Neshanic River streamflow response was poorly modeled and this could also indicate that some of our underlying assumptions about runoff processes in this watershed are incorrect, i.e. infiltration excess runoff could have a larger impact in this basin because of its relatively large urban footprint.

In the Town Brook site, there were a number of instances when we incorrectly categorized wells during runoff events. Interestingly, each well was mis-categorized at least once in the 18 runoff events. This is instructive, because it suggests that we are not so much mis-categorizing some wells entirely (which would be caused by an inaccurate STI), but instead that the water table dynamics are more variable than we are able to capture with this simple model. This is consistent with findings from Harpold et al. (2010) who, using an end-member mixing analysis, determined that lateral preferential flow paths were redistributing water beyond what is predicted by VSA models.

One limitation of this semi-distributed model is that the static nature of the STI classifications does not allow us to distinguish between upland wet sites and the lowland sites directly contributing to tributaries. We expect upland areas to show a much flashier response to precipitation inputs than lowland areas when their STI values are similar. Archibald (2010) found that water tables in lowland wetlands remained high, within 100 mm of the soil surface, for 7 months of the year, while upland wetland water tables in locations with similar STI values became saturated and drained within a few days of a rain event throughout the year. The next generation of runoff prediction tools could move away from the lumped approach and distribute

runoff over the landscape on a daily basis; however, if the end goal is a web-based mapping tool, this will require addressing the challenges of higher computer processing power and daily creation of unique map layers.

The empirical relationships developed here for the two variable model storm runoff parameters (S_d, T_P) appear to be regionally generalizable within the context of rural watersheds. We suggest this model as a potential tool for predicting flows in ungauged watersheds in the northeastern US. A beta website using the methodology described here is available for the Owasco Lake Watershed in upstate NY (Cornell Soil and Water Lab, 2013).

Conclusions

This study developed and applied a parsimonious semi-distributed hydrologic model (Lumped VSA model) across a variety of watersheds and field sites. The model performed well over multiple scales of validation and was able to simulate both watershed-scale streamflow response and groundwater table and soil moisture dynamics at the sub-field scale. Given the relatively simple model structure, transparent theoretical underpinnings and minimal calibration, the model is useful not only for predicting hydrologic response but also for testing its underlying assumptions about the dominant hydrological processes. As the model yields predictions of runoff generating zones, it forms the basis for a decision support tool for identifying critical runoff source areas in combination with "hydrologically sensitive moments" that have a high potential for targeted management practices. It is important to note that users interested in using this model should verify that saturation-excess runoff processes are important in their region. If not, it is likely that a simpler approach of avoiding polluting activities in areas that have low

infiltration capacities or during times of the year when high intensity storms are expected would be more effective.

In addition, model predictions are limited by the resolution of the DEMs underlying the STI maps. Small-scale flow paths such as ditches can radically alter surface water dynamics, but are not always identified in STIs created from USGS 10m DEMs. Instead, LIDAR– derived STIs are more likely to capture small scale spatial wetness patterns (Buchanan et al, 2013). Additionally, we expect tile drains to prevent overland runoff in areas the model will predict to be wet. However, because tile drains create an alternate rapid pathway for water, they also have potential to transport P and other pollutants from agricultural fields (Geohring, 2001), and so the prediction of runoff generation in these areas could be a useful indication of another rapid transport mechanism to stream outlets.

Acknowledgements

Funding for this research came from the USDA through NIFA Land Grant number 2012-67019-19434. It was supported in part by Agriculture and Food Research Initiative Competitive Grant No. 2010-03869 from the USDA National Institute of Food and Agriculture. We gratefully acknowledge the USGS, USDA, NOAA data sources used in this study, and the R-project and associated packages that greatly helped in the analysis of the data (R-Project, including the packages RSAGA, rgdal, maps, PBSmapping, raster, and GISTools).

WORKS CITED

Agnew, L.J., Lyon, S., Gérard-Marchant, P., Collins, V.B., Lembo, A.J., Steenhuis, T.S., Walter, M.T., 2006. Identifying hydrologically sensitive areas: Bridging the gap between science and application. J. Environ. Manage. 78, 63–76.

Archibald, J.A., Walter, M.T., 2013. Comment on "Assessing temperature-based PET equations under a changing climate in temperate, deciduous forests" by Shaw and Riha. Hydrological Processes 27(24):3511-3515 [doi: 10.1002/hyp.9971].

Archibald, J.A. 2010. Dissolved Phosphorus in Shallow Groundwater. MS Thesis, Cornell University.

Arlot, S., Celisse, A., 2010. A survey of cross-validation procedures for model selection. Statist. Surv. 4, 40-79. [doi:10.1214/09-SS054]

Beven, K.J., Kirkby, M.J., 1979. A physically based, variable contributing area model of basin hydrology / Un modèle à base physique de zone d'appel variable de l'hydrologie du bassin versant. Hydrol. Sci. Bull. 24, 43–69.

Buchanan, B.P., Fleming, M., Schneider, R.L., Richards, B.K., Archibald, J., Qiu, Z., Walter, M.T., 2013. Evaluating topographic wetness indices across central New York agricultural landscapes. Hydrol. Earth Syst. Sci. Discuss. 10, 14041–14093.

Cornell Soil and Water Lab, 2013. HSA-DSS Tool [WWW Document]. URL http://hsadss.bee.cornell.edu/OwascoLake/ (accessed 11.23.13).

Dahlke, H., Easton, Z., Fuka, D., Walter, M., Steenhuis, T., 2013. Real-Time Forecast of Hydrologically Sensitive Areas in the Salmon Creek Watershed, New York State, Using an Online Prediction Tool. Water 5, 917–944.

Dahlke, H.E., Easton, Z.M., Walter, M.T., Steenhuis, T.S., 2012. Field Test of the Variable Source Area Interpretation of the Curve Number Rainfall-Runoff Equation. J. Irrig. Drain. Eng. 138, 235–244.

DATCP, 2013. Runoff Risk Advisory Forecast [WWW Document]. Wis. Manure Manag. Advis. Syst. URL http://144.92.93.196/app/events/runoff_forecast (accessed 10.14.13).

Dunne, T., Black, R.D., 1970. Partial area contributions to storm runoff in a small New England watershed. Water Resour. Res. 6, 1296–1311.

Dunne, T., Leopold, L.B., 1978. Water in Environmental Planning. W.H. Freeman, New York, NY.

Easton, Z.M., Fuka, D.R., Walter, M.T., Cowan, D.M., Schneiderman, E.M., Steenhuis, T.S., 2008. Re-conceptualizing the Soil and Water Assessment Tool (SWAT) model to predict saturation excess runoff from variable source areas. Journal of Hydrology 348(3-4): 279-291

ESRI (Environmental Systems Resource Institute). 2009. ArcMap 9.2. ESRI, Redlands, California.

Frankenberger, J.R., Brooks, Erin S., Walter, M. Todd, Walter, Michael F., Steenhuis, Tammo S., 1999. A GIS-based variable source area hydrology model. Hydrol. Process. 13, 805–822.

Fuka, D.R., Easton, Z.M., Brooks, E.S., Boll, J., Steenhuis, T.S., Walter, M.T., 2012. A Simple Process-Based Snowmelt Routine to Model Spatially Distributed Snow Depth and Snowmelt in the SWAT Model1. JAWRA J. Am. Water Resour. Assoc. 48, 1151–1161.

Fuka, D.R., Walter, M.T., MacAlister, C., Degaetano, A.T., Steenhuis, T.S., Easton, Z.M., 2013. Using the Climate Forecast System Reanalysis as weather input data for watershed models: Using CFSR as weather input data for watershed models. Hydrol. Process. DOI: 10.1002/hyp.10073.

Fuka, D.R., Walter, M. T., Archibald, J., Steenhuis, T. S., Easton, Z., 2013. EcoHydRology: A community modeling foundation for Eco-Hydrology. http://cran.r-project.org/web/packages/EcoHydRology/EcoHydRology.pdf

Gburek, W.J., Sharpley, A.N., Heathwaite, L., Folmar, G.J., 2000. Phosphorus management at the watershed scale: A modification of the phosphorus index. J. Environ. Qual. 29, 130–144.

Geohring, L.D., McHugh,O.V., Walter, M.T., Steenhuis, T.S., Akhtar, M.S., Walter, M.F., 2001. Phosphorus transport into subsurface drains by macropores after manure applications: Implications for best manure management practices. Soil Science. 166(12): 896-909.

Harpold, A. A., Lyon, S.W., Troch, P.A., Steenhuis, T. S., 2010. Effects of preferential hydrological pathways in a glaciated watershed in the Northeastern USA. Vadose Zone J 9, 397–414.

Hijmans, R.J., Williams, E., Vennes, C., 2012. geosphere: Spherical Trigonometry. package version 1.3-8. http://CRAN.R-project.org/package=geosphere

Kirchner, J.W., 2006. Getting the right answers for the right reasons: Linking measurements, analyses, and models to advance the science of hydrology. Water Resour. Res. 42, n/a–n/a.

Kirpich, P.Z., 1940. Time of concentration of small agricultural watersheds. Civ. Eng. 10, 362.

Kleinman, P.J.A., Sharpley, A.N., McDowell, R.W., Flaten, D.N., Buda, A.R., Tao, L., Bergstrom, L., Zhu, Q., 2011. Managing agricultural phosphorus for water quality protection: principles for progress. Plant Soil 349, 169–182.

Lyne, V., Hollick, M., 1979. Stichastic Time-Variable Rainfall-Runoff Modelling. IE Aust Natl Conf Publ.

Lyon, S.W., Lembo, A.J., Walter, M.T., Steenhuis, T.S., 2006. Defining probability of saturation with indicator kriging on hard and soft data. Adv. Water Resour. 29, 181–193.

Lyon, S.W., Walter, M.T., Gérard-Marchant, P., Steenhuis, T.S., 2004. Using a topographic index to distribute variable source area runoff predicted with the SCS curve-number equation. Hydrol. Process. 18, 2757–2771.

Marjerison, R.D., Dahlke, H., Easton, Z.M., Seifert, S., Walter, M.T., 2011. A Phosphorus Index transport factor based on variable source area hydrology for New York State. J. Soil Water Conserv. 66, 149–157.

McDowell, R.W., Srinivasan, M.S., 2009. Identifying critical source areas for water quality: 2. Validating the approach for phosphorus and sediment losses in grazed headwater catchments. J. Hydrol. 379, 68–80.

Moriasi, D.N., Arnold, J.G., Van Liew, M.W., Bingner, R.L., Harmel, R.D., Veith, T.L., 2007. Model evaluation guidelines for systematic quantification of accuracy in watershed simulations. Trans. ASABE 50, 885–900.

NOAA, NOAA - National Oceanic and Atmospheric Administration - Weather [WWW Document]. URL http://www.noaa.gov/wx.html (accessed 11.22.13).

NRCS, SSURGO/STATSGO2 Structural Metadata and Documentation | NRCS Soils [WWW Document]. URL http://soils.usda.gov/survey/geography/ssurgo/ (accessed 11.1.13).

Nash, J.E., Sutcliffe, J.V., 1970. River Flow Forecasting through conceptual models, Part I - A Discussion of Principles. J. Hydrol. 10, 282-290.

Pradhan, N.R., Ogden, F.L., 2010. Development of a one-parameter variable source area runoff model for ungauged basins. Adv. Water Resour. 33, 572–584.

Priestley, C. H. B., Taylor, R. J., 1972. On the Assessment of Surface heat Flux and Evaporation Using Large-Scale Parameters. Mon. Weather Rev. 100.

R Core Team, 2013. R: A language and environment for statistical computing. Vienna, Austria.

Schneiderman, E.M., Steenhuis, T.S., Thongs, D.J., Easton, Z.M., Zion, M.S., Neal, A.L., Mendoza, G.F., Walter, M.T., 2007. Incorporating variable source area hydrology into a curve-number-based watershed model. Hydrol. Process. 21, 3420–3430.

Seibert, J., 1999. Regionalisation of parameters for a conceptual rainfall-runoff model. Agric. For. Meteorol. 98, 279–293.

Seibert, J., McGlynn, B.L., 2007. A new triangular multiple flow direction algorithm for computing upslope areas from gridded digital elevation models. Water Resour. Res. 43

Shaw, S.B., Walter, M.T., 2009. Improving runoff risk estimates: Formulating runoff as a bivariate process using the SCS curve number method. Water Resour. Res. 45,

Shuttleworth, W. J., 1992. Evaporation, in: David R. Maidment (Ed.), Handbook of Hydrology. McGraw-Hill, USA, pp. 4.1 – 4.53.

Steenhuis, T.S., Winchell, M., Rossing, J., Zollweg, J.A., Walter, M.F., 1995. SCS Runoff Equation Revisited for Variable-Source Runoff Areas. J. Irrig. Drain. Eng. 234–238.

Tarboton, D.G., 1997. A new method for the determination of flow directions and upslope areas in grid digital elevation models. Water Resour. Res. 33, 309–319.

Thornthwaite, C.W., Mather, J.R., 1955. The Water Balance. Publ. Climatol. 8.

USDA-NRCS, 2004. National Engineering handbook (NEH), Section 4, Hydrology. US Government Press, USDA.

USDA-NRCS, 2013. Soil Data Viewer [WWW Document]. URL http://soildataviewer.nrcs.usda.gov/

USGS, 2013. USGS Water Data for the Nation [WWW Document]. USGS Water Data Nation. URL http://waterdata.usgs.gov/nwis (accessed 12.6.13).

Van Steenbergen, N., Willems, P., 2013. Increasing river flood preparedness by real-time warning based on wetness state conditions. J. Hydrol. 489, 227–237.

Walter, M.T., Mehta, V.K., Marrone, A.M., Boll, J., Gérard-Marchant, P., Steenhuis, T.S., Walter, M.F., 2003. Simple estimation of prevalence of Hortonian flow in New York City watersheds. J. Hydrol. Eng. 8, 214–218.

Walter, M.T., Steenhuis, T.S., Mehta, V.K., Thongs, D., Zion, M., Schneiderman, E., 2002. Refined conceptualization of TOPMODEL for shallow subsurface flows. Hydrol. Process. 16, 2041–2046.

Walter, M.T., Walter, M.F., Brooks, E.S., Steenhuis, T.S., Boll, J., Weiler, K., 2000. Hydrologically sensitive areas: Variable source area hydrology implications for water quality risk assessment. J. Soil Water Conserv. 55, 277–284.

Walter, M. T., M., Brooks, E.S., McCool, D.K., King, L.G., Molnau, M., Boll, J., 2005. Process-based snowmelt modeling: does it require more input data than temperature-index modeling? J. Hydrol. 300, 65–75.

CHAPTER 2

Decline in soluble phosphorus mobility from land-applied dairy manure – modeling and practical applications[2]

Introduction

The loss of phosphorus (P) in runoff from agricultural systems is not only a significant water quality concern (Correll, 1998; Chappell, 2014), but also an issue of food security, since minable P is expected to run out within the next 100 years (Cordell et al., 2009). Reducing the need for P inputs to agricultural systems involves keeping P in fields where it is needed for crop production and minimizing P lost in overland and subsurface runoff. Recycling animal waste to use as fertilizer can be part of the solution, but can also lead to over fertilization with P. Because several studies have shown that soluble P in animal wastes becomes less available for transport over time (Greenhill et al., 1983; Austin et al., 1996; Shigaki et al., 2006), one possibility for reducing P lost in overland runoff is to try to avoid P fertilization in areas where runoff is common (Walter et al., 2001; Gburek et al., 2002; Agnew et al., 2006) or forecast in the near future (Dahlke et al., 2013).

However, a critical knowledge gap is our understanding of why there is a decline in P concentration in overland runoff over time. Two potential explanations are: (1) infiltrating water transfers manure P to the soil where it is less available to entrainment into storm runoff (Vadas et al., 2004) or (2) manure P is biogeochemically immobilized regardless of infiltration (Olander and Vitousek, 2005). Explanation (1) suggests that the observed decline in P concentration is related to the amount of P infiltrating with water; while explanation (2) could be correlated to

[2] Archibald, Josephine A., Peterson, Maxwell, Richards, Brian K., Giri, Shree K., and M. Todd Walter. (in preparation) Decline in soluble phosphorus mobility from land-applied dairy manure – modeling and practical applications. *Journal of Environmental Quality*

temperature, which is a prominent control on chemical and biological processes and has been shown to affect P sorption in soils (Gardner and Jones, 1973). A number of researchers have shown a decline in fertilizer P loads over time or after subsequent rain events (e.g. Austin et al., 1996; Walter et al., 2001; Shigaki et al., 2006). Kleinman and Sharpley (2003) simulated rainfall on manure-fertilized soil boxes and noted a decline in runoff P concentrations over the course of the experiment, which they attributed to P losses through soil infiltration and runoff – an idea supported by other researchers (e.g. Sharpley and Moyer, 2000). However, Kleinman et al. (2004) subsequently found that soil boxes with different infiltration capacities had similar P concentration in runoff, suggesting that in fact infiltration was not a driving factor in the decline in P mobility. The question of what is driving P decline in storm runoff after fertilization has important implications for modeling and management strategies.

The ambiguity of the major factor responsible for the declining P runoff concentrations over time is reflected in water quality models. Vadas et al. (2004) proposed a model on the basis that decreasing P concentrations were due to the amount of P that had been previously leached from the manure and either infiltrated into the soil or lost in runoff. Later versions of this model (Vadas et al., 2007, 2011) incorporated biogeochemical P immobilization, but it is not clear how the two processes were independently resolved. The Soil and Water Assessment Tool (SWAT) also combines P biogeochemistry and P leaching with similar ambiguity (Arnold, 2006). Easton et al. (2009), on the other hand, modeled the decline in P availability based primarily on an empirical, black-box P decline as a function of time with minor losses in runoff. The Easton et al. (2009) methodology is based on a model by Gérard-Marchant et al. (2005) that was developed, in part, from the Sharpley and Moyer (2000) experiments of manure P leaching from manures placed on filter papers, i.e., manure did not contact soil.

Based on the current literature, it is difficult to separate the effect of time-exposed-to-the-environment from the impact of P loss during previous rain events in determining the best modeling strategy for predicting runoff P concentrations for various P fertilizer types. Here, we attempt to distinguish between the two scenarios for dairy manure applications using soil boxes spread with manure spread between 4 hours and 7 days before the first rain and runoff event. To investigate the role of infiltration of leached P, we used wet and dry treatments to simulate low and high infiltration, respectively. To investigate exposure we used cold and warm treatments to see how these interact with exposure time before the first rain after manure spreading.

Methods

Experimental Design:

We conducted two soil box experiments designed to isolate the roles of time, temperature and infiltration on soluble reactive phosphorus (SRP) export in storm runoff after manure amendments. The first experiment had two temperature treatments – one "cold" treatment, where boxes were kept outside in the early spring of Ithaca, NY and average daily temperatures varied between -4° C and 13° C (NRCC, 2014), and a "warm" treatment, in which soils were kept indoors at a constant temperature of 22° C (Figure 2.1a). In the second experiment, all boxes were kept indoors, with "wet" boxes stored in a 1 cm water bath which kept the soil moisture higher than the "dry" treatment. During the wet-dry experiment, we measured soil moisture of the control boxes in each treatment before the rain event using Time Domain Reflectometry (TDR) probes (Figure 2.1b). Each treatment group (Cold, Warm, Wet, Dry) consisted of ten soil

boxes, which included two replicates each of boxes spread with manure seven days, three days, one day and four hours before the first rain event, and two control boxes with no manure added.

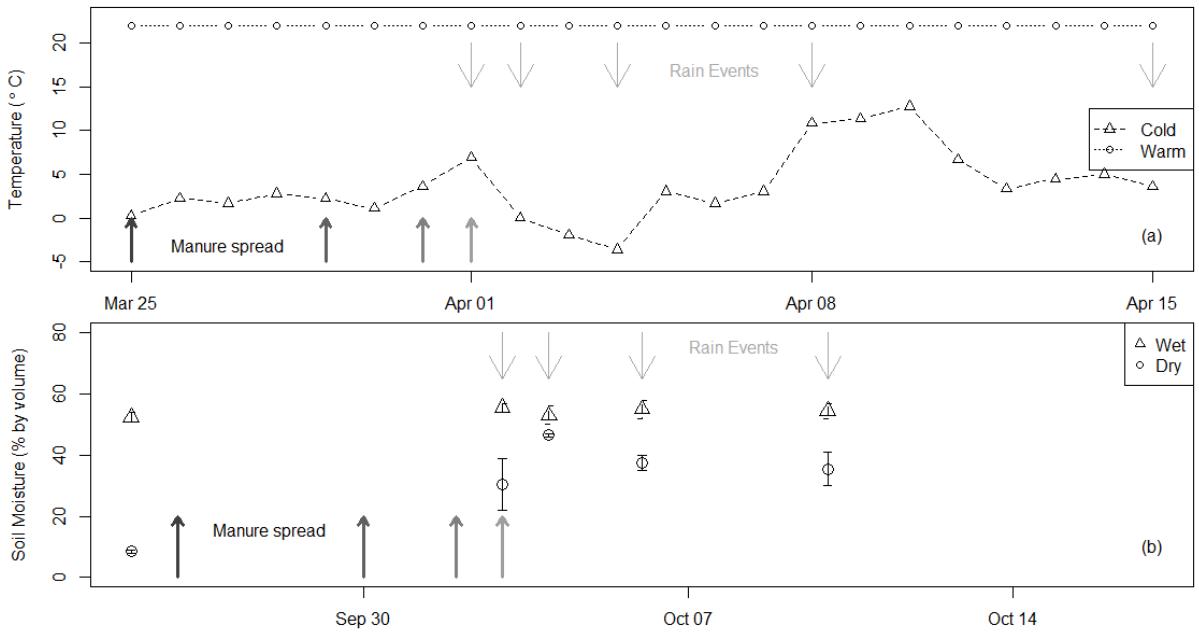

Figure 2.1: Air temperatures for the "Cold" and "Warm" treatment groups (a), and volumetric soil moisture of the control boxes in the "Wet-Dry experiment (b). Thick upward arrows represent the timing of manure applications to a subset of the boxes, while grey downward arrows indicate when a rain even occurred. Soil analysis for both experiments occurred following the rain experiments.

For all experimental groups, soil boxes 9 cm deep by 17.5 cm by 41.5 cm were packed with a poorly drained Dalton/Madalin silt loam from 50-year fallow agricultural land in central NY (Figure 2.2). The soil had very low initial concentration of Morgan-extractable P; this and other soil properties determined by Cornell Agro-One Soils Laboratory are reported in Table 2.1. All boxes had a hole just above the soil surface, to allow runoff to flow through a tube into sample bottles for analysis after each rain event. The boxes were kept at a 5% incline during the rain events, and a small channel near the outlet directed flow into the collection tubing.

Table 2.1. Average soil analysis for soils used in the runoff boxes.

SOIL TYPE	Dalton/Madalin
Aggregate Stability (%)	89.6
Available Water Capacity (m/m)	0.28
Surface Hardness (psi)	75
Subsurface Hardness (psi)	168
Organic Matter (%)	6.6
Active Carbon (ppm)	767
Potentially Mineralizable N (µgN/ gdwsoil/week)	35.6
Root Health Rating (1-9)	3.9
pH	5.6
Extractable Phosphorus (ppm)	1
Extractable Potassium (ppm)	72
Magnesium (ppm)	143
Iron (ppm)	38
Manganese (ppm)	11
Zinc (ppm)	0.6
Sand (%)	20
Clay (%)	13
Silt (%)	67
Textural Class	silt loam

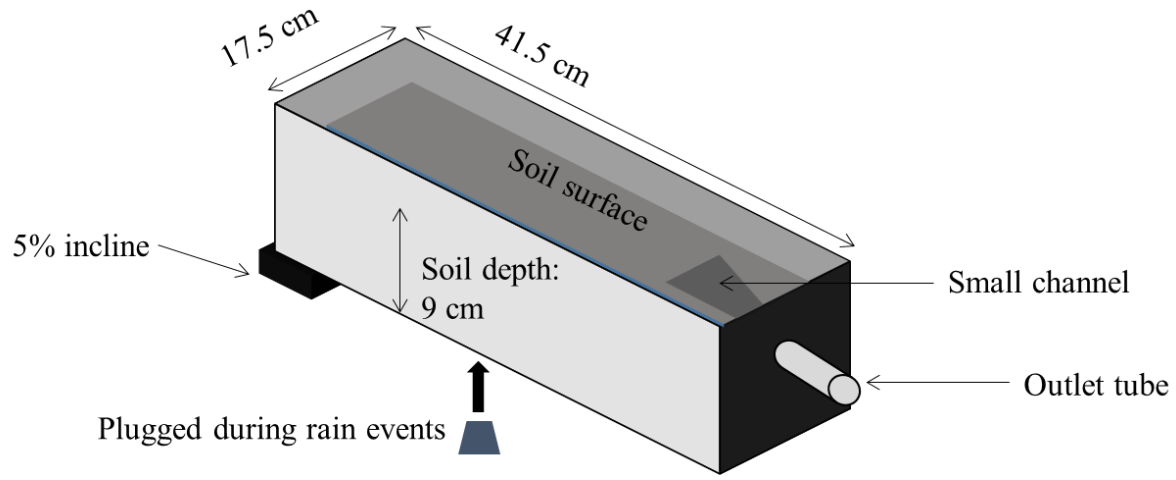

Figure 2.2. Diagram showing the set-up of soil boxes during rain events.

Each treatment (Cold, Warm, Wet, Dry) had ten soil boxes with duplicate boxes of five manure spreading strategies; control (no manure), and boxes spread with manure 4 hours – 7 days before the first rain. The manure-fertilized boxes each had 300 ml (345g) of 17 - 18% solids dairy manure spread over them, containing between 5.9 – 10 kg of water extractable phosphorus

(WEP) per ha; WEP increased over time in the refrigerated manure between applications, and the manure collected for the second experiment had a lower overall initial WEP content (Table 2.2). The manure was spread at variable times: seven days, three days, one day and four hours before the first rain event. Subsequent rain events occurred one, four, seven and 14 days after this first rain event (Table 2.2).

Table 2.2: Manure application and rain event schedule for the two experiments.

Action	Group	Cold-Warm Experiment:		Wet-Dry Experiment	
		Date	**WEP (mg/m^2)**	**Date**	**WEP (mg/m^2)**
Manure application	Control	-	0	-	0
	7 days before	3/25/2013	702	9/26/2013	590
	3 days before	3/29/2013	891	9/30/2013	640
	1 day before	3/31/2013	954	10/2/2013	721
	Day of rain	4/1/2013	1021	10/3/2013	725
Rain Events	All groups	4/1/2013	-	10/3/2013	-
		4/2/2013	-	10/4/2013	-
		4/4/2013	-	10/6/2013	-
		4/8/2013	-	10/10/2013	-
		4/15/2013	-	-	-

Rain events:

Rain intensity over the boxes averaged 57 mm/hr with a standard deviation of 17 mm/hr, and was lower than the infiltration capacity of the soil, based on visual observations of the soil boxes after rainfall initiation. Because of the variable rain intensity, for each rain event we randomly assigned soil boxes to positions under the rain-maker to minimize the sustained impact of this variable on any one box. We simulated saturation excess overland flow by plugging the drainage under the box, and allowing the boxes to saturate and generate runoff. Once runoff was initiated over at least 3 boxes, rain continued for 15 minutes. This rain simulation resulted in runoff occurring from all boxes except in two cases. Approximately 45 ml of the well-mixed runoff

water was filtered through a 0.45 um membrane for colorimetric SRP analysis. The unfiltered runoff was analyzed for total P after persulfate digestion.

Before and after each rain event, we weighed the plugged boxes to determine the amount water that infiltrated during the rain event. Then we unplugged the boxes and collected the drainage water, which was filtered and analyzed for SRP. In the first experiment we did not weigh the boxes again after draining, so the volume drained was inferred from the difference between field capacity soils (taken from the pre-rain weight on April 2), and the weight after rain on a particular date. In the second experiment, we weighed the boxes after at least one hour of drainage and drainage rate was less than 1 drip per 10 seconds.

Water Analysis:

SRP was determined by the ascorbic-acid colorimetric method (Murphy and Riley, 1962) on filtered samples within 24 hours of sample collection, with a detection limit of 10 ppb. Total P was determined after persulfate digestion using Inductively Coupled Plasma mass spectrometry (ICP-MS) with a detection limit of 50 ppb. Additionally, we measured the pH of runoff samples in the first runoff event of the cold-warm experiment to determine the impact of manure application on runoff pH.

Soil and Manure Analysis:

After all simulated rainfall-runoff events, four soil cores to a depth of 5 cm were collected from each soil box and mixed thoroughly. The soil was air dried for one day, and then pulverized and sifted through a 1.168 mm sieve. Water extractable P (WEP) from soil cores was calculated by

oscillating 2 g of dry soil with 40 ml deionized water for two hours, filtering the liquid through a 0.45 um filter, and colorimetric analysis. Morgan-P was determined using a modified Morgan extraction (Gavlak et al., 2003) followed by colorimetric analysis. Manure WEP was determined using an extraction ratio of 100:1 by manure dry weight (Kleinman et al., (2007), within 24 hours of each manure application.

Results

Overall average runoff SRP concentrations were higher in the first experiment (April/May 2013) than the second (September/October 2013), which could be due in part to the higher WEP content in the manure applied in the first experiment. For both experiments, average runoff concentrations of total P and SPR tended to be highest in the first rain events after manure was spread, and declined over time (Figure 2.3). Additionally, in runoff events that occurred after manure application, average SRP concentration was highest in boxes spread most recently. The boxes that were spread on the day of first rain had a significantly higher overall average concentrations of SRP in runoff than the boxes fertilized 7 days prior to the first rain event ($p<0.01$), all other manure-treatment group pairings were not significantly different from each other (data not shown), but followed the trend of higher concentrations from more recently spread boxes relative to first rainfall.

We measured the pH of runoff in the first runoff event of the cold-warm experiment, and found that runoff pH varied by timing of manure application. The runoff pH was highest in the boxes spread on the day of rain (average pH = 8.4). All boxes that had been spread within three days of the rain event had runoff pH > 8 and were significantly different from control box runoff pH.

The pH of boxes spread 7 days before the first rain was not significantly different from control boxes; the average pH of the control group was 7.6, while the average for boxes spread 7 days before the first rain was 7.7 (Figure B.2.1). We would expect more mobility at lower pH values; thus, these results suggest that pH is not driving the differences in SRP concentrations in these systems.

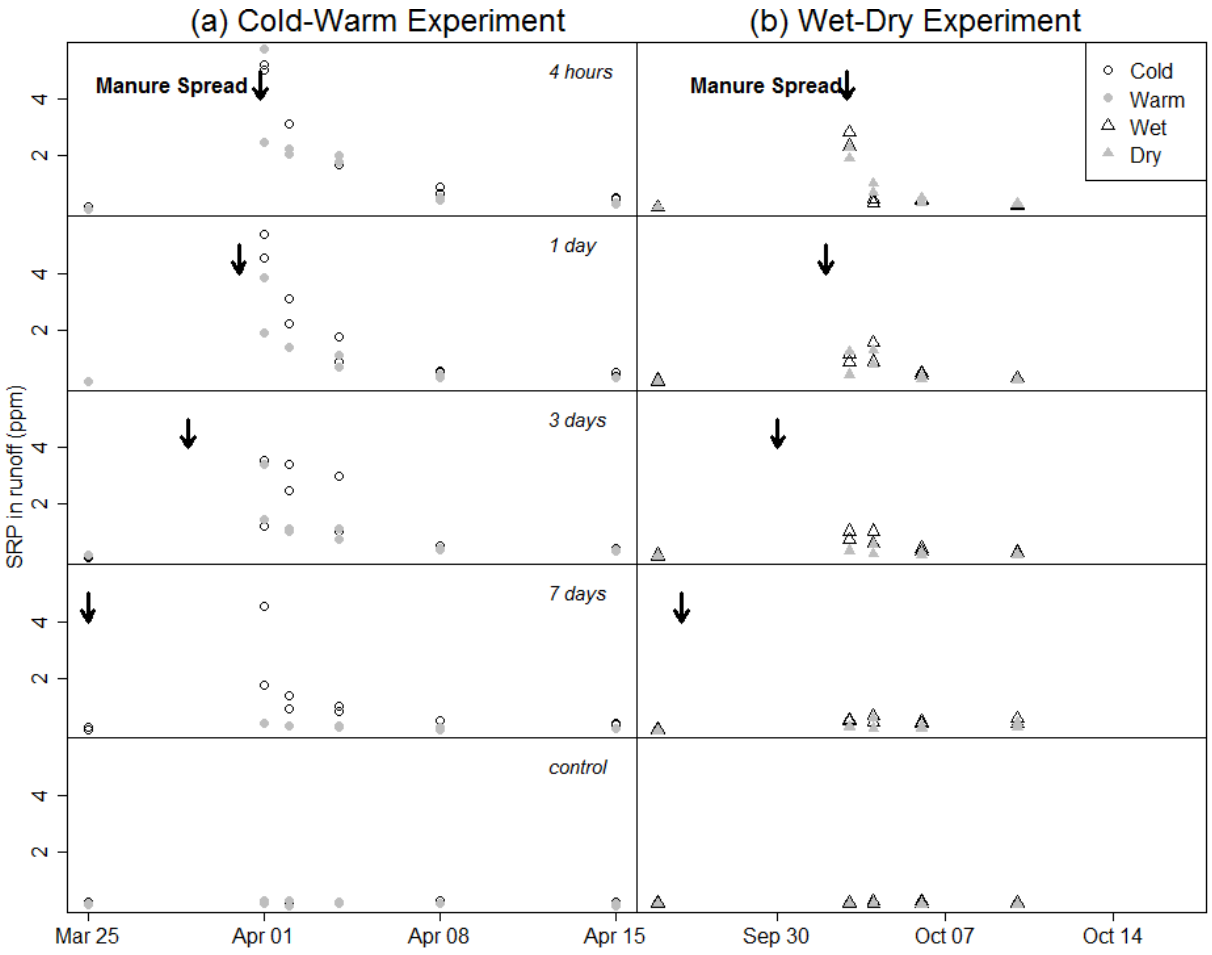

Figure 2.3: SRP runoff from the Cold-Warm experiment (a), and the Wet-Dry Experiment (a). Downward arrows represent the timing of manure spreading for that box grouping. Open circles represent the cold treatment group, grey filled circles are the warm treatment group, open triangles are the wet treatment group, and grey filled triangles are the dry treatment group.

In order to test the effect that previous infiltration was having on a specific runoff event's P export, we compared the concentration of SRP in runoff water to the infiltration since manure

application for each box (Figure 2.4a). Runoff SRP concentration was related to cumulative infiltration since manure application, with 34% of the variation explained with a best-fit power function (R^2 = 0.34, $p<0.01$), and a root mean square error (RMSE) of approximately 1 ppm. However, because the cumulative infiltration increased with each subsequent rain event, this analysis does not separate the effect of exposure-time from the effect of infiltration. In order to isolate the impact of infiltration depth before runoff on SRP, we compared the SRP in runoff from the wet-dry experiment for each rain event (Figure 2.5). For three of the four rain events, there was no significant ($p > 0.05$) relationship between infiltration and SRP concentration. In the third runoff event, there is a significant ($p<0.05$) linear relationship between the SRP in runoff and infiltration depth, but the maximum concentration of SRP in runoff is almost an order of magnitude less than the maximum SRP concentration of the first event.

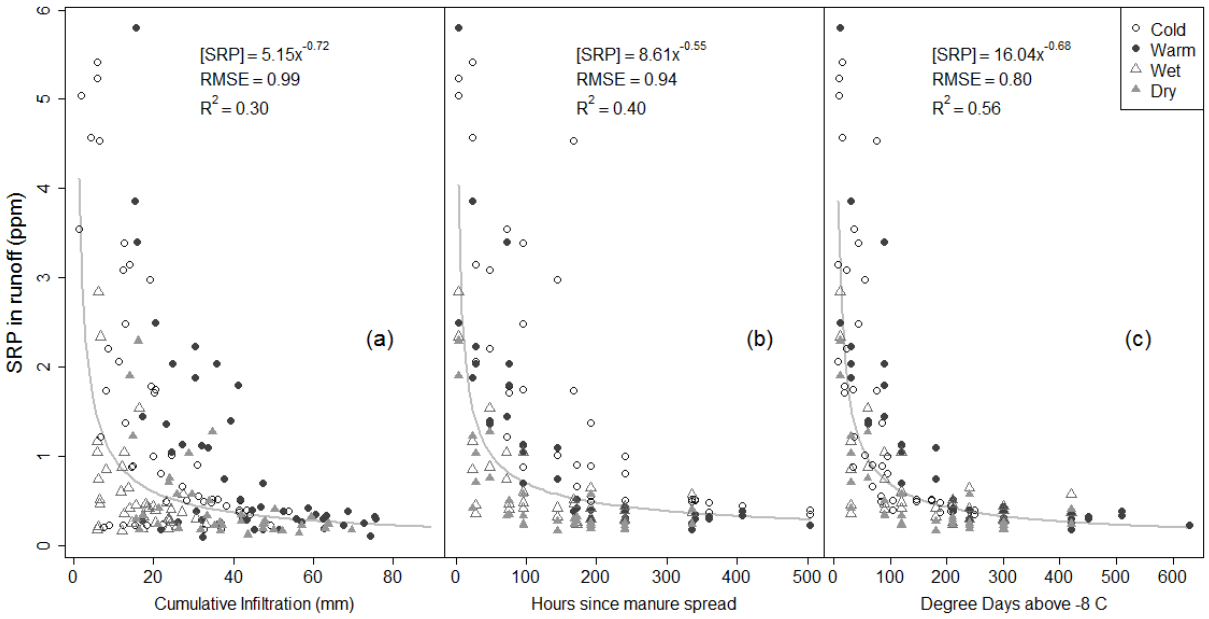

Figure 2.4 Runoff SRP plotted against cumulative infiltration depth (a), time since manure was applied (b) or degree days (c). Open circles represent cold boxes, closed circles are warm boxes, open triangles are wet boxes, and grey filled triangles are dry boxes.

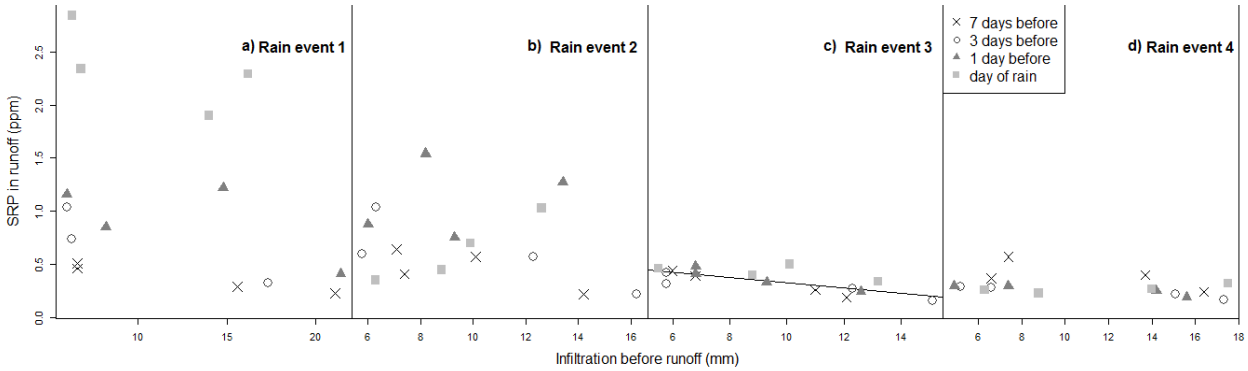

Figure 2.5 SRP concentration in the runoff from manure-fertilized boxes in the wet-dry experiment compared to the rain event infiltration (i.e. here infiltration was not cumulative over all events) before runoff was initiated for the four rain events following fertilization (a-d). There was a significant relationship ($p<0.05$) between runoff SRP concentration and infiltration depth only in the third runoff event, when SRP concentrations was closer to baseline level (c).

The models proposed by Walter et al. (2001) and Easton et al. (2009) suggests that P availability will decline over time after fertilization regardless of intervening infiltration. To see if this pattern could be observed in these data, we plotted SRP concentration in runoff against time since manure application in Figure 2.4b, giving a coefficient of determination of the best-fit power function of 0.39. As can be seen in Figure 2.4b, the decline in P availability over time is slower in the cold boxes from the first experiment. To get at a temperature difference, we calculated the degree days (DD) since manure was applied for each runoff event using:

$$DD = \sum \begin{cases} if\ T > T_B,\ \ T - T_B \\ if\ T \leq T_B,\ \ 0 \end{cases} \tag{2.1}$$

We tested a range of potential T_B values between -20°C and 20°C (1°C increments) and found that the calculated RMSE between the best-fit power curve and observed SRP concentration was minimized when T_B = -8 °C. This curve explained 56% of the variation in observed SRP concentration and suggests that temperature plays an important role in the decline in SRP concentration in runoff (Figure 2.4c). The best-fit value for T_B was unexpected because it does

not correlate to any obvious environmental threshold, such as the freezing point of water or a biological trigger of some sort; as such, this deserves further investigation.

Because the initial WEP in the manure varied among soil boxes, we scaled the best-fit SRP equation based on *DD* by the WEP applied to each box to determine a predictive equation for SRP based on *DD* (Eqn. 2.2)

$$SRP = \left(\frac{WEP}{M_o}\right) 16.04\ DD^{-0.68} \qquad (2.2)$$

Where WEP is in mg/m^2 and M_o is the average manure WEP (767 mg/m^2) applied to the boxes. This equation was able to explain 60% of the variation in observed runoff SRP concentration (R^2 = 0.60)

Because P that is not lost in runoff and drainage is expected to remain in the soil, we compared the amount of total P lost in runoff and drainage with the Morgan-extractable P remaining in the surface soil after the runoff events. There was a weak (R^2 = 0.17), but significant (p = 0.01) relationship between the total P lost from the soil boxes in runoff and drainage and the Morgan-extractable P in the soil after the runoff experiments (Figure 2.6). Additionally, there was a significant difference between the boxes that received manure within 24 hours of the first rain event, and those that had manure spread at least three days before the first rain event (boxplots in Figure 2.6, $p < 0.01$).

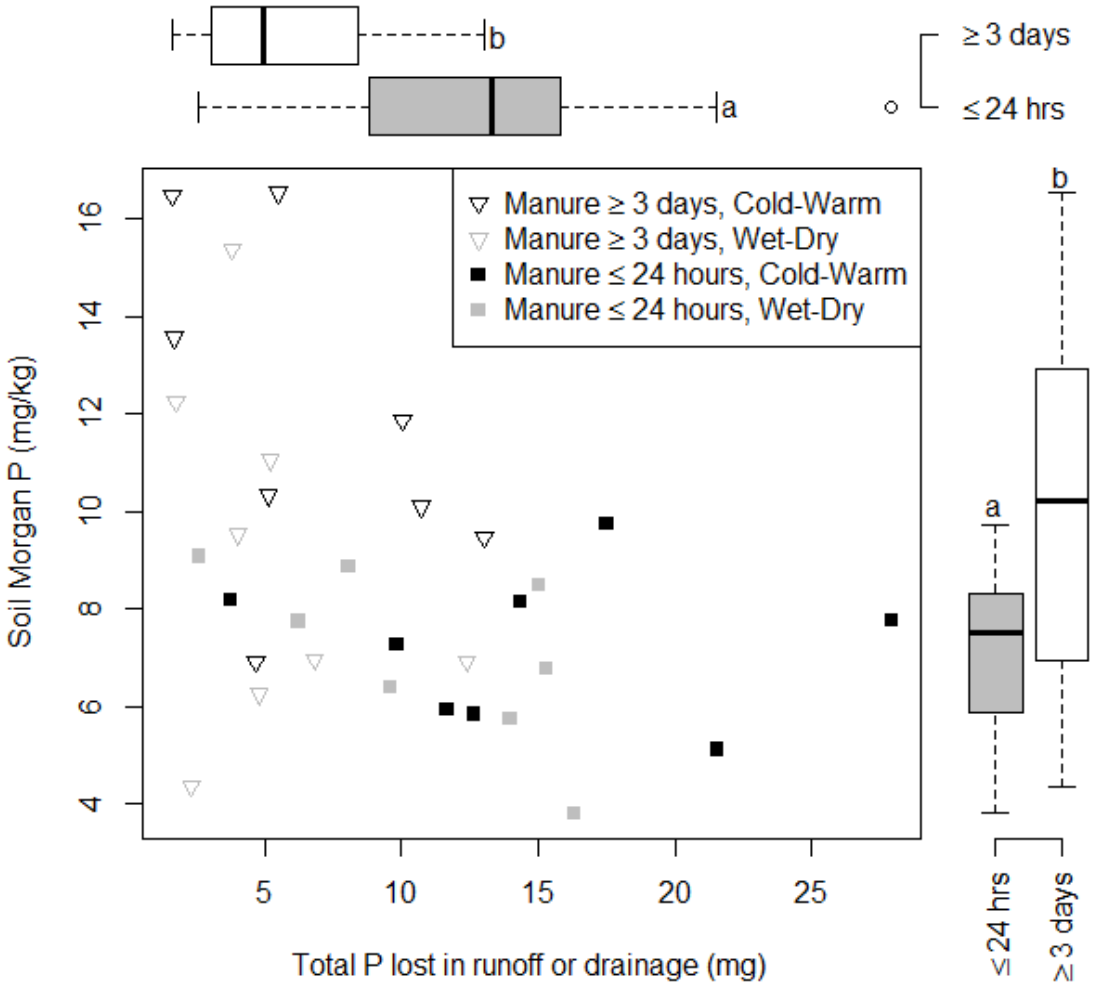

Figure 2.6 Final Morgan-extractable P in soil cores compared with the total P lost in runoff or drainage from soil boxes that were fertilized with manure. Black symbols are from the cold-warm experiment and grey symbols are from the wet-dry experiment. Filled squares represent boxes spread 24 or 4 hours before the first rain, while open triangles were spread 3 or 7 days before the first rain event. In the margins, the boxplots compare between boxes that were fertilized within 24 hours before the first rain event, with those that were fertilized 3 or 7 days before the first rain event; these groups are significantly different for both final Morgan-extractable P and total P lost in runoff and drainage.

We see a similar pattern between remaining soil WEP and Morgan-extractable P for the boxes after the rain experiments based on the timing of manure application. When broken up this way,

the only manure-fertilized treatments that were significantly different from each other were those spread within one day of the first rain event compared to boxes that were spread 7 days before the first rain (boxplots in Figure 2.7).

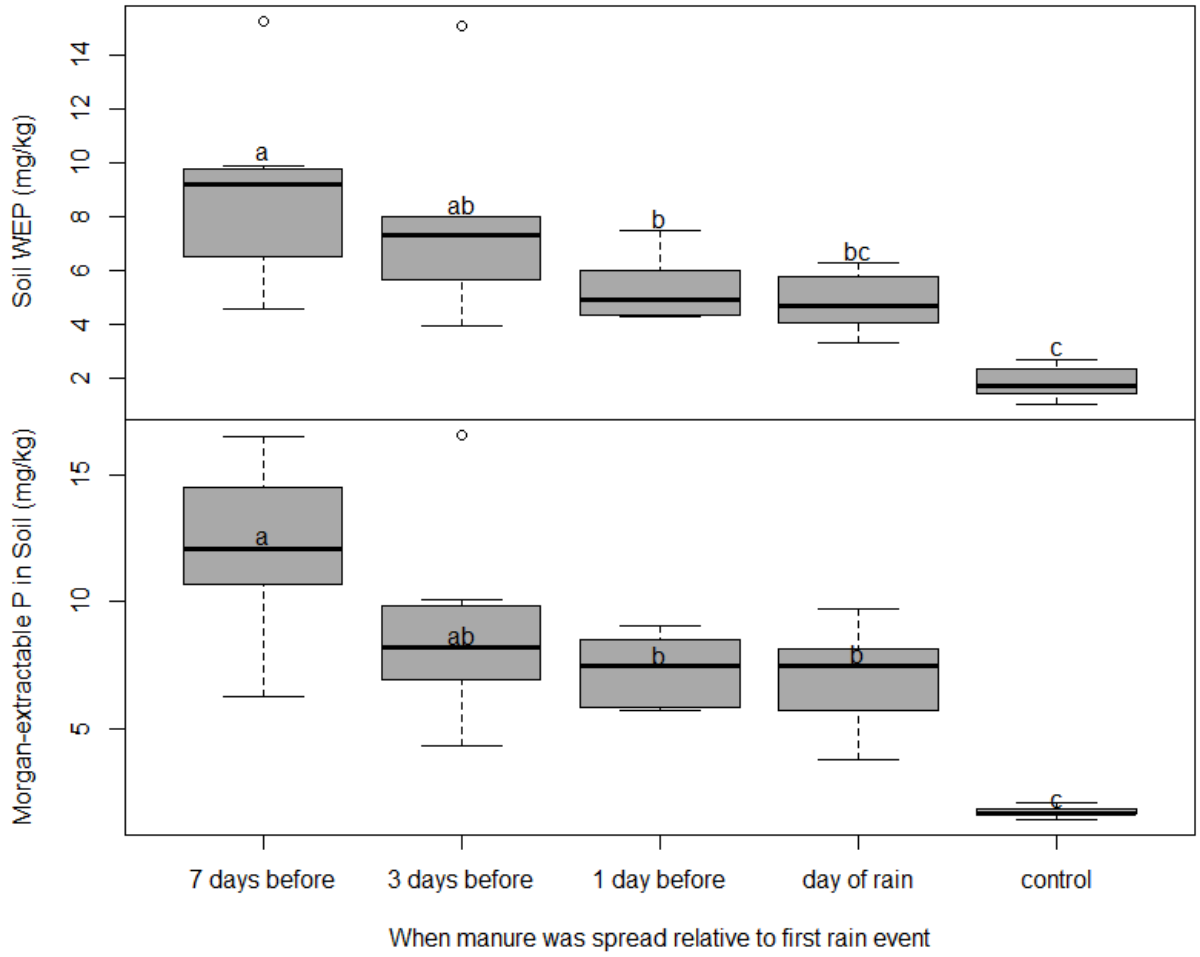

Figure 2.7 Soil WEP (mg/kg) in soil boxes after runoff experiments (top), and soil Morgan-extractable P (bottom). Within each plot (but not between plots), groups that share a letter are not significantly different from each other.

Gérard-Marchant et al. (2005) proposed a model of SRP loss in runoff proportionate to the total WEP applied based on filter paper experiments by (Sharpley and Moyer, 2000). Their model was based on the duration of rainfall. We compared the total mass of SRP lost in runoff from boxes spread with manure four hours before the first rain over the course of the experiment with this

model (Figure 2.8). We found that in all cases, less than 13% of the total mass of WEP applied was lost in runoff by the end of the two experiments for all treatments, and this was much less than what was predicted by the model proposed by Gérard-Marchant et al. (2005), implying that manure contact with soil is an important factor in how much P is actually lost in storm runoff.

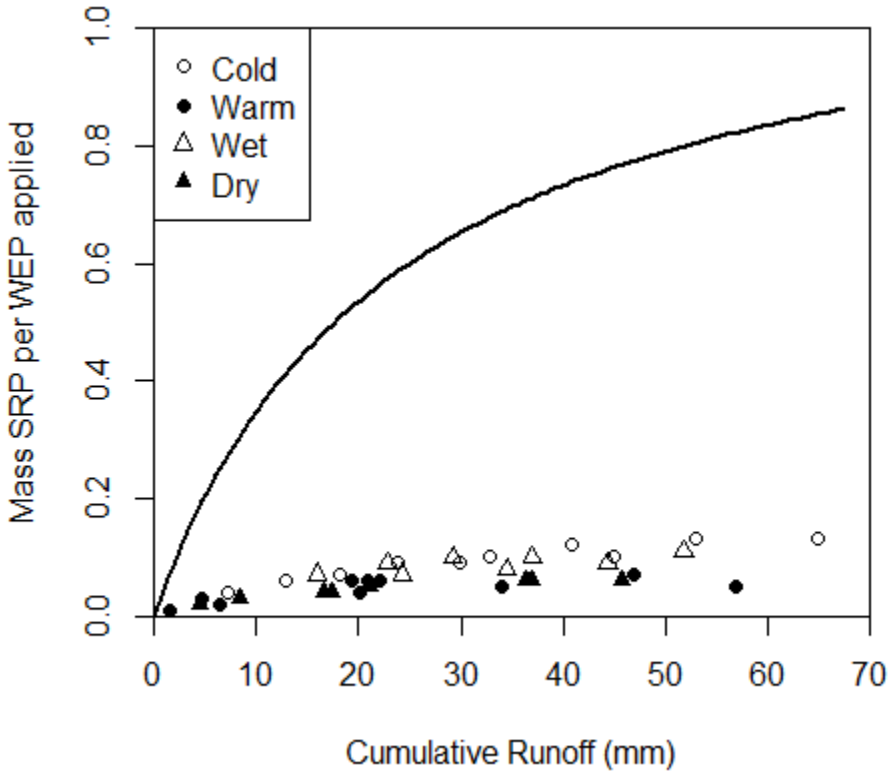

Figure 2.8 For soil boxes spread the day of first rain: total SRP lost in runoff per total mass of WEP applied per box against cumulative runoff depth from the box. Open circles represent cold boxes, closed circles are warm boxes, open triangles are wet boxes, and filled triangles are dry boxes. The curve is the model proposed by (Gérard-Marchant et al., 2005) based on filter paper experiments by (Sharpley and Moyer, 2000).

We also tried to account for the total mass of WEP applied to the soil boxes by comparing the WEP applied and not lost through SRP in runoff and drainage with the change in soil WEP for each box (Figure 2.9). If WEP were conserved, we would expect the losses to balance the WEP remaining in the soil, i.e., the data would lie along the 1:1 line in Figure 2.9. However, the data

generally lie below the line, suggesting that WEP is not conserved and probably subjected to transformations that reduce its water extractability.

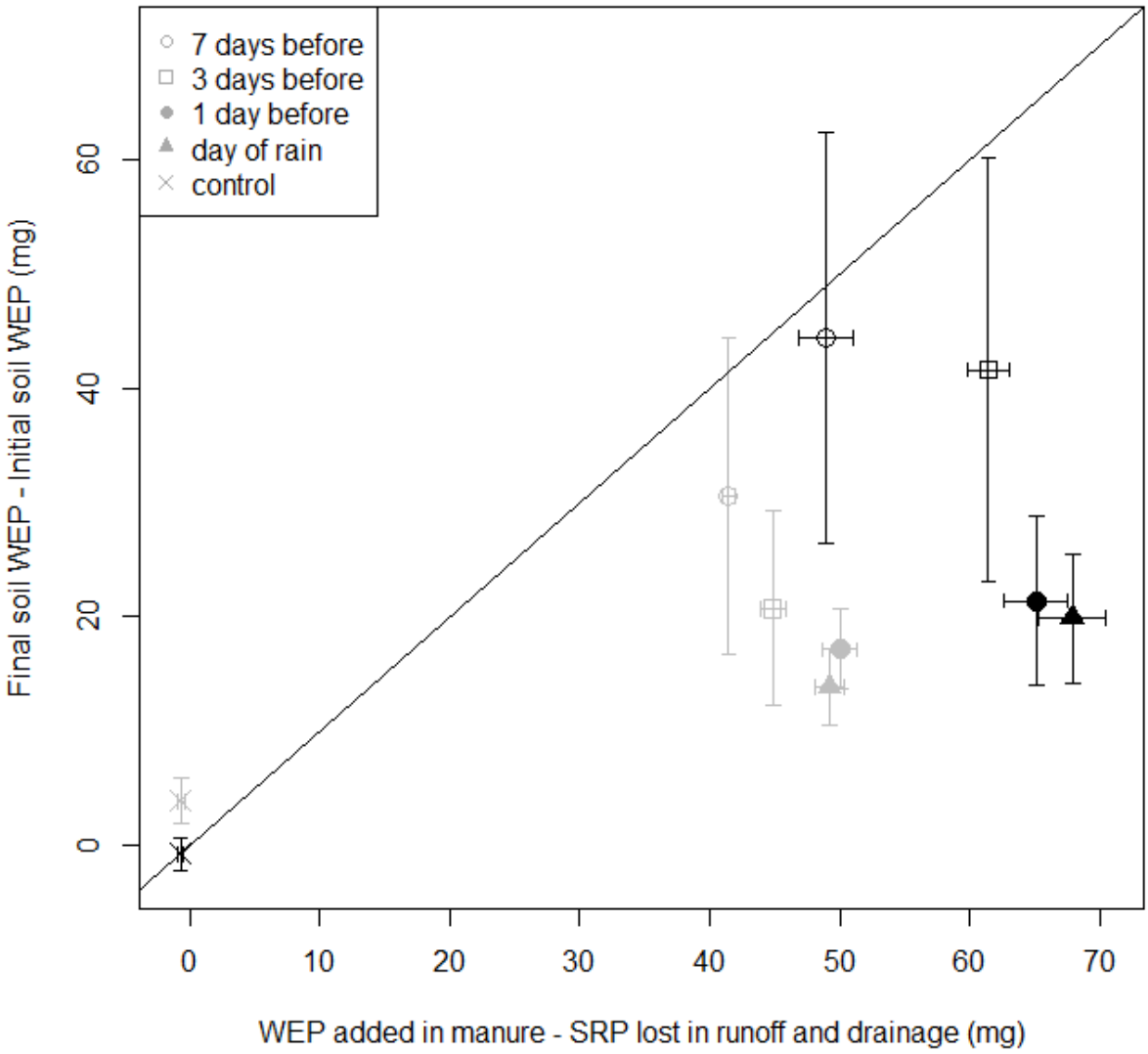

Figure 2.9 Change in soil WEP compared to the WEP added in manure application. Black symbols are from the cold-warm experiment, while grey symbols are from the wet-dry experiment. The solid line indicates a 1-1 relationship.

Discussion

Modeling Implications

Early, yet still commonly used models like the Generalized Watershed Loading Function (GWLF, Haith et al., 1992), model nonpoint source P pollution as a simple, static wash-off coefficient based on land use, i.e., each specific land use has a representative P concentration in its storm runoff. Researchers have been able to successfully calibrate wash-off coefficients such that watershed-scale P loads are well simulated. The likely reason for this is that storm runoff volumes vary by many orders of magnitude more than P concentrations so, as long as the storm runoff estimates are reasonably well estimated, the P load estimates are likely to also be reasonably well predicted (Shaw et al., 2010). This is the classic case of getting the right answer for the wrong reason, or at least partially the wrong reason (Kirchner, 2006; Schneiderman et al., 2007).

There have been a few models proposed that take a more mechanistic perspective on P concentrations in storm runoff, considering the interactions among various environmental P-pools among manure, soil, and biota (Arnold, 2006; Vadas et al., 2007; Easton et al., 2009). However, the large number of field measurements or calibrated parameters needed for these models makes it difficult to tease-out the impact of timing, temperature, and other factors on manure-leached P. This study suggests that a simplified approach to modeling P in runoff from fertilized (specifically manure-spread) fields could be used to estimate the impact of fertilizer timing on runoff P concentrations without having to work-out all the interactions between various environmental pools by considering the role of temperature on manure P leaching. Depth of infiltration before runoff, while related to SRP concentration, was not an important predictor of SRP concentrations in the early rain events following fertilization, when SRP concentrations can be up to an order of magnitude higher than in later events (Figure 2.5). This suggests that

models of P transport in fertilized systems should account for fertilization timing and temperature and perhaps place less emphasis on P-losses in infiltration and runoff prior to a specific rainfall-runoff event.

In addition, the amount of SRP that is lost in runoff is much less than the WEP added to the soil, even in boxes with the highest rates of P loss in overland runoff (Figure 2.8). This suggests chemical transformations of P in the soil-manure matrix are playing an important role in immobilization and that simple models based on P loss from manure placed on filter paper (e.g., Gerard-Marchant et al., 2005) do not necessarily apply to systems with a interactions between soil and P sources. In addition, it is likely that P transfers between soil, water and manure P forms are driving the apparent loss of WEP in the soil boxes (Figure 2.9).

Management Implications

One vexing challenge is how the chronic soil-manure interactions will manifest in higher P concentrations from long-term manure-amended soils above the growth requirements of crops (Sharpley et al., 2013). These substantially slower build-up processes are, to date, not well represented by current field datasets but are absolutely necessary for developing meaningful long-term mitigation strategies. In other words, are we developing measures to mitigate short-term nonpoint source pollution measures from field-spread manure only to reap long-term, more chronic and more difficult to address problems of leaching from historically P-loaded soils? How to capture this in models is not obvious.

This study provides evidence to support the recommendation that land applied manure-fertilization should be avoided right before rain-runoff events (e.g. Greenhill et al., 1983; Daniel et al., 1994; Schroeder et al., 2004). Our results suggest that manure P is immobilized in the soil over time, and the rate of immobilization increases with temperature. Thus, reduced nonpoint source P pollution can be mitigated by reducing the manure spread within three days of forecasted rain, especially during warm periods. However, we found that dairy manure WEP increased the longer its contact with soil was delayed (consistent with Shree K. Giri, personal communication), so there is a clear manure-storage vs. spread-immediately tension that needs further study. Our results corroborate the findings of (Gardner and Jones, 1973), who found that temperature increased the rate of P sorption in two types of Idaho soils in the absence of biological activity.

We found higher levels of WEP and Morgan-extractable P in soils fertilized with manure three or more days before first runoff than in soil boxes fertilized sooner to the first runoff event (Figure 2.6); this is not unexpected, because less P was lost in overland runoff from these boxes. Because of this, we expect that fields fertilized well before runoff events would retain more P that could later be available for crop growth. However, if the application of P in manure is not matched to the P uptake by crops, a continual build-up of P in the soil could convert the problem of P export from an acute, runoff-initiated problem, to a more chronic, low level problem of continual P export from enriched soils. This problem has been noted in many agricultural areas already where reduction in fertilizer application and best management practices have not corresponded with an improvement of water quality downstream (e.g. Meals, 1996; Sharpley et

al., 2009; Kleinman et al., 2011). Indeed, this is parallel to the last modeling challenge mentioned in the previous section.

Conclusion

Land application of manure within a few (~3 days) days of rainfall-runoff events has the potential to increase nonpoint source P loading significantly from agricultural land relative to applications made more than 3 days before runoff. Phosphorus immobilization is a function of temperature, with quicker immobilization expected during warmer periods. Phosphorus leaching from manure is notably higher for experiments for which manure is in contact with filter paper than those that place the manure in contact with soil. Models that are able to take into account the decline in P availability after fertilization are best suited to address the implications of P concentration timing on receiving water quality. There is still an unresolved issue of long-term impacts of soil-P build-up and P-leaching from soils. In the short-term, we recommend not spreading manure within 3-days of a forecasted rainfall event in order to avoid immediate P-loading to streams, although we acknowledge that this recommendation would have to be coupled with an overall reduction in P fertilization to avoid exacerbating a chronic problem.

Acknowledgements

We thank Bryan Finneran for his assistance in running some of the experiments used in this study. Funding for this research was from the USDA NIFA Land/Sea Grant number 2012-67019019434, Agriculture and Food Research Initiative Competitive Grant No. 2010-03869 from the USDA National Institute of Food and Agriculture, Rawlings Cornell Presidential Research Scholars (RCPRS) program, and Cornell Engineering Learning Initiatives (ELI)

undergraduate research grant. In addition, we would like to thank the Soil and Water Lab group at Cornell University.

WORKS CITED

Agnew, L.J., Lyon, S., Gérard-Marchant, P., Collins, V.B., Lembo, A.J., Steenhuis, T.S., Walter, M.T., 2006. Identifying hydrologically sensitive areas: Bridging the gap between science and application. J. Environ. Manage. 78, 63–76. doi:10.1016/j.jenvman.2005.04.021

Archibald, J.A., Buchanan, B.P., Fuka, D.F., Georgakakos, C.B., Lyon, S.L., Walter, M.T., 2014. A simple, regionally parameterized model for predicting nonpoint source areas in the Northeastern US. J. Hydrol. Reg. Stud. 1, 74–91. doi:10.1016/j.ejrh.2014.06.003

Arnold, I.C., 2006. V Phosphorus Modeling in Soil and Water Assessment Tool (SWAT) Model. Model. Phosphorus Environ. 163.

Austin, N.R., Prendergast, J.B., Collins, M.D., 1996. Phosphorus Losses in Irrigation Runoff from Fertilized Pasture. J Env. Qual 25, 63–68.

Bouldin, D., 2007. Water quality data for Fall Creek (Tompkins County, NY) sampling sites: 1972-1995 [WWW Document]. URL http://hdl.handle.net/1813/8148 (accessed 7.6.14).

Buchanan, B.P., Archibald, J.A., Easton, Z.M., Shaw, S.B., Schneider, R.L., Todd Walter, M., 2013. A phosphorus index that combines critical source areas and transport pathways using a travel time approach. J. Hydrol. 486, 123–135. doi:10.1016/j.jhydrol.2013.01.018

Chappell, B., 2014. Algae Toxins Prompt Toledo To Ban Its Drinking Water [WWW Document]. NPR.org. URL http://www.npr.org/blogs/thetwo-way/2014/08/03/337545914/algae-toxins-prompt-toledo-to-ban-its-drinking-water (accessed 8.13.14).

Cordell, D., Drangert, J.-O., White, S., 2009. The story of phosphorus: Global food security and food for thought. Glob. Environ. Change 19, 292–305. doi:10.1016/j.gloenvcha.2008.10.009

Cornell Soil and Water Lab, 2014. HSA-DSS Tool [WWW Document]. URL http://hsadss.bee.cornell.edu/OwascoLake/ (accessed 11.23.13).

Correll, D.L., 1998. The Role of Phosphorus in the Eutrophication of Receiving Waters: A Review. J Env. Qual 27, 261–266.

Dahlke, H., Easton, Z., Fuka, D., Walter, M., Steenhuis, T., 2013. Real-Time Forecast of Hydrologically Sensitive Areas in the Salmon Creek Watershed, New York State, Using an Online Prediction Tool. Water 5, 917–944. doi:10.3390/w5030917

Daniel, T.C., Sharpley, A.N., Wedepol, R., Lemunyon, J. L., 1994. Minimizing surface water eutrophication from agriculture by phosphorus management. J. Soil Water Conserv. 49, 30–38.

DATCP, 2013. Runoff Risk Advisory Forecast [WWW Document]. Wis. Manure Manag. Advis. Syst. URL http://144.92.93.196/app/events/runoff_forecast (accessed 10.14.13).

Easton, Z.M., Gérard-Marchant, P., Walter, M.T., Petrovic, A.M., Steenhuis, T.S., 2007. Identifying dissolved phosphorus source areas and predicting transport from an urban watershed using distributed hydrologic modeling: URBAN DISSOLVED PHOSPHOROUS SOURCE AREAS. Water Resour. Res. 43, n/a–n/a. doi:10.1029/2006WR005697

Easton, Z.M., Walter, M.T., Schneiderman, E.M., Zion, M.S., Steenhuis, T.S., 2009. Including source-specific phosphorus mobility in a nonpoint source pollution model for agricultural watersheds. J. Environ. Eng. 135, 25–35.

Gardner, B.R., Jones, J.P., 1973. Effects of temperature on phosphate sorption isotherms and phosphate desorption. Commun. Soil Sci. Plant Anal. 4, 83–93. doi:10.1080/00103627309366422

Gavlak, R., Horneck,, D., Miller, R., Kotuby-Amacher, J., 2003. Soil, Plant and Water Reference Methods for the Western Region.

Gburek, W.J., Drungil, C.C., Srinivasan, M.S., Needelman, B.A., Woodward, D.E., 2002. Variable-source-area controls on phosphorus transport: Bridging the gap between research and design. J. Soil Water Conserv. 57, 534–543.

Gérard-Marchant, P., Walter, M.T., Steenhuis, T.S., 2005. Simple Models for Phosphorus Loss from Manure during Rainfall. J. Environ. Qual. 34, 872. doi:10.2134/jeq2003.0097

Greenhill, N.B., Peverill, K.I., Douglas, L.A., 1983. Nutrient concentrations in runoff from pasture in Westernport, Victoria. Soil Res. 21, 139–145.

Haith, D.A., Mandel, R., Wu, R.S., 1992. GWLF, generalized watershed loading functions, version 2.0, user's manual. Dept Agric. Biol. Eng. Cornell Univ. Ithaca NY.

Kirchner, J.W., 2006. Getting the right answers for the right reasons: Linking measurements, analyses, and models to advance the science of hydrology. Water Resour. Res. 42, doi:10.1029/2005WR004362

Kleinman, P., Sullivan, D., Wolf, A., Brandt, R., Dou, Z., Elliott, H., Kovar, J., Leytem, A., Maguire, R., Moore, P., Saporito, L., Sharpley, A., Shober, A., Sims, T., Toth, J., Toor, G., Zhang, H., Zhang, T., 2007. Selection of a Water-Extractable Phosphorus Test for Manures and Biosolids as an Indicator of Runoff Loss Potential. J. Environ. Qual. 36, 1357. doi:10.2134/jeq2006.0450

Kleinman, P.J., Sharpley, A.N., Moyer, B.G., Elwinger, G.F., 2002. Effect of mineral and manure phosphorus sources on runoff phosphorus. J. Environ. Qual. 31, 2026–2033.

Kleinman, P.J., Sharpley, A.N., Veith, T.L., Maguire, R.O., Vadas, P.A., 2004. Evaluation of phosphorus transport in surface runoff from packed soil boxes. J. Environ. Qual. 33, 1413–1423.

Kleinman, P.J.A., Sharpley, A.N., 2003. Effect of broadcast manure on runoff phosphorus concentrations over successive rainfall events. J. Environ. Qual. 32, 1072–1081.

Kleinman, P.J.A., Sharpley, A.N., McDowell, R.W., Flaten, D.N., Buda, A.R., Tao, L., Bergstrom, L., Zhu, Q., 2011. Managing agricultural phosphorus for water quality protection: principles for progress. Plant Soil 349, 169–182. doi:10.1007/s11104-011-0832-9

Meals, D.W., 1996. Watershed-scale response to agricultural diffuse pollution control programs in Vermont, USA. Water Sci. Technol. 33, 197–204. doi:10.1016/0273-1223(96)00231-4

Murphy, J., Riley, J.P., 1962. A modified single solution method for the determination of phosphate in natural waters. Anal. Chim. Acta 27, 31–36.

Northeast Regional Climate Center (NRCC), 2014. [WWW Document]. URL http://www.nrcc.cornell.edu/ (accessed 7.30.14)

Olander, L., Vitousek, P., 2005. Short-term controls over inorganic phosphorus during soil and ecosystem development. Soil Biol. Biochem. 37, 651–659. doi:10.1016/j.soilbio.2004.08.022

Schneiderman, E.M., Steenhuis, T.S., Thongs, D.J., Easton, Z.M., Zion, M.S., Neal, A.L., Mendoza, G.F., Todd Walter, M., 2007. Incorporating variable source area hydrology into a curve-number-based watershed model. Hydrol. Process. 21, 3420–3430. doi:10.1002/hyp.6556

Schroeder, P.D., Radcliffe, D.E., Cabrera, M.L., 2004. Rainfall timing and poultry litter application rate effects on phosphorus loss in surface runoff. J. Environ. Qual. 33, 2201–2209.

Sharpley, A., Jarvie, H.P., Buda, A., May, L., Spears, B., Kleinman, P., 2013. Phosphorus Legacy: Overcoming the Effects of Past Management Practices to Mitigate Future Water Quality Impairment. J. Environ. Qual. 42, 1308. doi:10.2134/jeq2013.03.0098

Sharpley, A., Moyer, B., 2000. Phosphorus forms in manure and compost and their release during simulated rainfall. J. Environ. Qual. 29, 1462–1469.

Sharpley, A.N., Herron, S., West, C., Daniel, T., 2009. Outcomes of phosphorus-based nutrient management in the Eucha-Spavinaw watershed. Farming Grass Sustain. Mix. Agric. Landsc. Grassl. Environ. Soil Water Conserv. Soc. Press Ankeny IA 192–204.

Shaw, S., Stedinger, J., Walter, M., 2010. Evaluating Urban Pollutant Buildup/Wash-Off Models Using a Madison, Wisconsin Catchment. J. Environ. Eng. 136, 194–203.

Shigaki, F., Sharpley, A., Prochnow, L.I., 2006. Source-Related Transport of Phosphorus in Surface Runoff. J. Environ. Qual. 35, 2229. doi:10.2134/jeq2006.0112

Vadas, P.A., Aarons, S.R., Butler, D.M., Dougherty, W.J., 2011. A new model for dung decomposition and phosphorus transformations and loss in runoff. Soil Res. 49, 367. doi:10.1071/SR10195

Vadas, P.A., Gburek, W.J., Sharpley, A.N., Kleinman, P.J.A., Moore, P.A., Cabrera, M.L., Harmel, R.D., 2007. A Model for Phosphorus Transformation and Runoff Loss for Surface-Applied Manures. J. Environ. Qual. 36, 324.

Vadas, P.A., Kleinman, P.J.A., Sharpley, A.N., 2004. A Simple Method to Predict Dissolved Phosphorus Runoff from Surface-Applied Manures. J. Environ. Qual. 33, 749.

Walter, M.T., Brooks, E.S., Walter, M.F., Steenhuis, T., Scott, C.A., Boll, J., 2001. Evaluation of soluble phosphorus loading from manure-applied fields under various spreading strategies. J. Soil Water Conserv. 56, 329–335.

Walter, M.T., Walter, M.F., Brooks, E.S., Steenhuis, T.S., Boll, J., Weiler, K., 2000. Hydrologically sensitive areas: Variable source area hydrology implications for water quality risk assessment. J. Soil Water Conserv. 55, 277–284.

Walter, M. Todd, M., Brooks, E.S., McCool, D.K., King, L.G., Molnau, M., Boll, J., 2005. Process-based snowmelt modeling: does it require more input data than temperature-index modeling? J. Hydrol. 300, 65–75. doi:10.1016/j.jhydrol.2004.05.002

CHAPTER 3

Optimizing Timing of Manure Fertilization to Decrease Phosphorus Loading[3]

Introduction

Excess phosphorus (P) in runoff from agriculture is a major contributor to water quality impairments in freshwater and coastal ecosystems (Carpenter et al., 1998). Increasingly, water quality experts are recognizing that P management strategies need to be explicitly linked to an understanding of hydrologic pathways (Walter et al., 2000; Buda et al., 2009; Kleinman et al., 2011; Buchanan et al., 2013). A trend towards water quality websites and apps targeting watershed residents offers new opportunities for innovative small scale actions that could help to protect water quality by giving residents information about hydrologically sensitive moments. For example, The Wisconsin Manure Management Advisory System allows residents so see if runoff is expected in their watershed in the upcoming three to ten days (DATCP, 2013), and similar tools have been created in agricultural watersheds in New York State (Cornell Soil and Water Lab, 2014; Dahlke et al., 2013). These tools can help farmers to avoid spreading manure on fields when runoff is likely, and has the potential to be a low-cost method of reducing P loading from agriculture. However, we do not yet understand how the widespread use of such tools could impact P loading in watersheds dominated by dairy agriculture such as upstate New York or Wisconsin.

Understanding what controls the extent of P loss from agricultural systems is a complex problem, as P release is influenced by a number of factors including soil physical and biogeochemical properties, dominant hydrologic pathways, in-stream processes, biological uptake and release, "legacy P" in soils and aquatic sediments from historical land practices, and

[3] Archibald, J., D.R. Fuka, B.K.Richards, R. Schneider, Z.M Easton, M.T. Walter. (in prep). Optimizing Timing of Manure Fertilization to Decrease Phosphorus Loading. *Agriculture, Ecosystems and Environment*

current management strategies. Complex models that try to incorporate all these factors necessarily have burdensome data requirements, making model runs possible only through extensive calibration, or for small idealized situations such as laboratory experiments.

Although many processes are involved in P transport, a number of studies have shown that it is often a small fraction of the landscape (Buda et al., 2009; Easton et al., 2008; Kleinman et al., 2011; Ulén et al., 2001) or a small percentage of time (Hart et al., 2004; McDowell and Srinivasan, 2009; Sharpley et al., 2008) that have a disproportionately large impact on P loading. In addition, DeLaune et al (2004) found that fertilizer effects dominate all other factors contributing to soluble reactive phosphorus (SRP) in field-plot runoff in the first three rain events following poultry manure fertilization. These findings suggest that in agricultural systems where we are interested in the implications of manure management strategies, models of P transport can be simplified to focus on the interaction of runoff patterns and fertilizer application timing.

Here we are interested in examining the impact of manure application timing strategies on water quality in a rural watershed in upstate New York, USA. To do this, we use a simplified watershed model to determine where and when runoff is occurring on the landscape (Archibald et al., 2014) combined with a modified version of the SRP model proposed by Easton et al. (2007). We parameterized this model using data for Fall Creek watershed from the 1970s (Bouldin, 2007). We use the model to predict the impact on P transport for scenarios in which farmers modify the timing of manure fertilization in order to avoid the intersection of manure application with runoff generating times.

Methods

Model Design

We modeled P transport from the Fall Creek watershed near Ithaca, NY by running a daily runoff model (Archibald et al., 2014, Chapter 1) that partitions flow into baseflow and saturation-excess overland runoff triggered by rain or snowmelt. When runoff occurs in fields fertilized with manure, we approximate the readily mobile manure-derived SRP in that portion of the watershed using equations 3.1 and 3.2, below (Archibald et al., in preparation, Chapter 2). In areas that have not been spread with manure, runoff SRP concentration is determined by equation 3.3. The baseflow SRP concentration is determined by equation 3.4.

SRP from manure-applied fields is modeled based on a simple timing model in which the SRP concentration in overland runoff is related to degree days (*DD*) since manure application occurred:

$$DD = \sum \begin{cases} 0\,, if\ T < -8℃ \\ T + 8,\ if\ T \geq -8℃ \end{cases} \quad (3.1)$$

where *T* is the average daily air temperature (°C) for days after manure was applied.

When and where runoff occurs, we then model the SRP concentration in runoff from fertilized areas (ppm) using an empirical relationship (Equation 3.2) (Archibald et al., in prep, chapter 2):

$$SRP_{Manured\ Areas} = \left(\frac{WEP}{M_o}\right) 16.04\ DD^{-0.68} \quad (3.2)$$

where *WEP* is the water-extractible P (mg/m^2) most recently applied in that location; and M_o is 767 mg/m^2.

In land that did not have a recent application of manure (i.e. either no manure had been applied, or DD > 680 °C-d), we used the soil P equation proposed by Easton et al (2007):

$$SRP_{Soil} = STP\ \mu_{TS}\ Q_S^{\frac{T-T_S}{10}} \quad (3.3)$$

where *STP* is Morgan-extractable Soil Test Phosphorus (mg/kg) ; Q_S is a factor change rate for a 10°C change in temperature (dimensionless); and μ_{TS} is the reference export coefficient (dimensionless, calibrated).

The values used in this modeling exercise are reported in table 3.1:

Table 3.1: Parameter values used in equations 3 and 4

Parameter	Value	Description	Reference for value used
STP	1.8 kg/m^2	Morgan-extractable soil test P	Eqn 3.3, (Chapter 2)
Q_S	1.7	Temperature factor for soil P	Eqn 3.3, (Easton et al., 2009)
μ_{TS}	0.018	Soil P export coefficient	Eqn 3.3, (Hively et al., 2005)
T_S	20.5 °C	Base temperature for soil P	Eqn 3.3, (Easton et al., 2009)
T_B	17 °C	Base temperature for baseflow P	Eqn 3.4, (Easton et al., 2007)
Q_B	2.2	Temperature factor for baseflow P	Eqn 3.4, (Easton et al., 2007)
μ_{TB}	5 x 10^{-3}	Baseflow export coefficient	Eqn 3.4, Calibrated from water quality data-set (Bouldin, 2007)

During baseflow, P is typically desorbed from stream bed sediments. We estimated SRP in baseflow using equation 3.4, based on the methodology of Easton et al. (2007):

$$SRP_{baseflow} = \mu_{TB}\ Q_B^{\frac{T-T_B}{10}} \quad (3.4)$$

where T was the average air temperature for the day (°C), μ_{TB} is the baseflow export coefficient (dimensionless) Q_B is the temperature factor for baseflow (dimensionless) and T_B is the base temperature used to determine equation 4 (°C) (Table 3.1). We calculated overall SRP concentration using equation 3.5:

$$SRP = \frac{SRP_{baseflow} Q_{BF} + SRP_{Soil} Q_{UA} + SRP_{Manured\ Areas} Q_{FA}}{Q} \quad (3.5)$$

Where Q_{BF} is baseflow (m^3); Q_{UA} is the runoff from unfertilized areas (m^3); Q_{FA} is runoff from manure fertilized areas (m^3); and Q is total streamflow (m^3) = Q_{BF} + Q_{FA} + Q_{FA}

Model inputs and verification data

Precipitation and temperature data used to run the watershed model were accessed from the National Climate Data Center (NOAA, 2014). For scenarios where farmer behavior was dependent on forecast weather or model output, we used archived 72-hour forecasts from the National Oceanic and Atmospheric Administration (NOAA) Global Forecast System Model Output Statistic (NOAA, 2014) which are available for 2002-present. For the scenario where farmers are reacting to modeled runoff forecast, we ran the model using the 3-day precipitation forecast to simulate the knowledge that farmers would have had if they had access to a watershed forecast tool (e.g., DATCP, 2013; Cornell Soil and Water Lab, 2014). Because forecast data are probabilistic with a range of a precipitation, we ran the model based on the maximum value predicted for that day, except on days when precipitation was predicted to be "2.00 inches or greater" (~5 cm or greater) – in these cases the model assumed that 6.4 cm (2.5 inches) of precipitation would occur. Because we chose the highest precipitation value in a range, we expected the forecasted streamflow to over-predict compared to modeled streamflow based on precipitation observations, which it does (Figure 3.1).

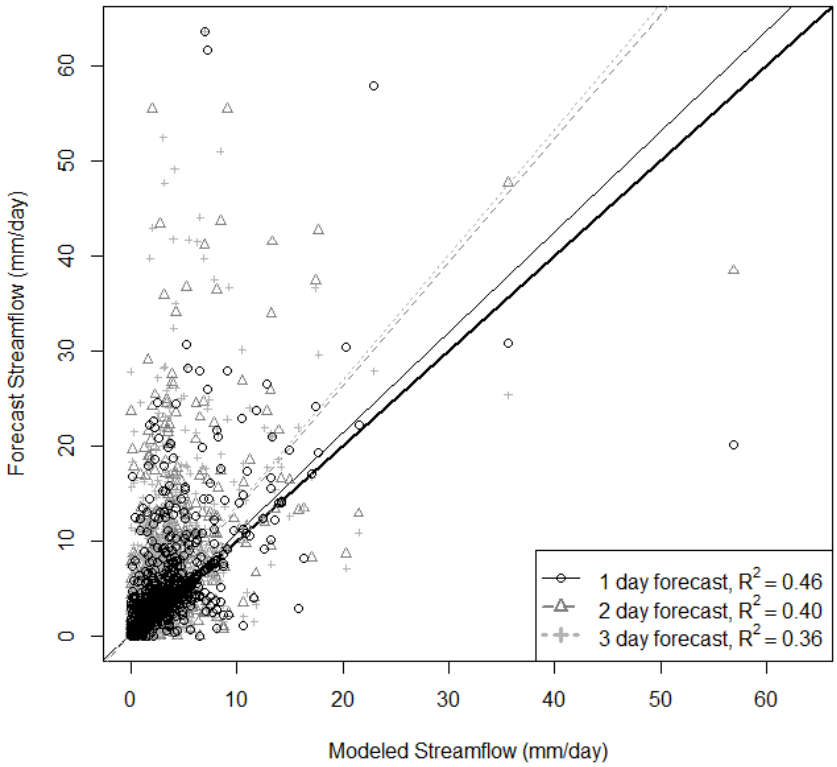

Figure 3.1. Forecast vs. modeled streamflow for the one-day forecast (black open circles, best-fit line is the thin solid line), two-day forecast (grey triangles and dashed grey line for the best-fit), and three day forecast (light grey cross symbol, dotted light grey line for the best fit). The thick solid line is the 1-1 line.

Watershed Description

Fall Creek watershed is a 326 km^2 watershed in upstate NY, with predominantly forest (47%) and agricultural (46%) land uses (U.S. Geological Survey, 2011). Researchers at Cornell University have been monitoring water quality and flow intermittently since the 1970s, and SRP measurements were made every 3-14 days, with some more frequent storm samples during 1972 – 1976 (Bouldin, 2007; Johnson, Arthur H. et al., 1976). We use these measurements to verify that our model estimations of phosphorus loads are reasonable; we used a flow-weighted mean

SRP concentration for days with multiple measurements for SRP concentration during storm events.

Scenarios

We ran the model for a variety of potential management scenarios using weather data from Fall Creek watershed between 2002 and 2011. For all scenarios we assumed the land use breakdown was similar to current conditions, with unfertilized pastures in 14% of the watershed, manure-fertilized pastures or hay fields in 15%, and row crop in 17% of the watershed. We assumed that row crops only received manure fertilization in April, May, October, or November, while pasture fields were fertilized throughout the year (Tompkins and Cortland Co. Soil and Water Conservation Districts and NYS Soil and Water Conservation Committee, personal communication). Runoff SRP loads from manure-applied fields were modeled using Eqn 3.2, while runoff-SRP from the rest of the watershed was modeled using Eqn 3.3. In all scenarios, we assumed that farmers only applied manure as fertilizer to a particular field or pasture location once per year, with an annual rate of application equal to 500 mg-WEP/m^2 for manure-fertilized pasture fields, and 1000 mg-WEP/m^2 for all row crops. These application rates are consistent with manure application rates to meet the crop P requirements for dairy and cash crop systems, respectively (Sharpley and Wang, 2014), assuming a ratio of WEP to total P of 0.29 (Kleinman et al., 2002)

Scenario 0: Approximating the period of record, 1972 – 1976:

We approximated farmer behavior in the 1970s to evaluate the model uncertainties. During this period we assume that farmers were spreading a subset of their manure-fertilized pasture fields

daily throughout the year, and spreading row crops before spring planting in April and May or after fall harvesting during October and November.

Scenario 1: Maximum-Reduction Scenario (2002-20011)

In the maximum-reduction scenario, we assume that no manure is applied anywhere in the watershed.

Scenario 2: Approximation of current practices (2002-20012)

To approximate current practices in the watershed, we consulted with agricultural professionals from Tompkins and Cortland Co. Soil and Water Conservation Districts and NYS Soil and Water Conservation Committee (personal communication). Based on their input, we assumed that for any given year, half of the pasture lands were not spread with any manure (14% of total watershed area). The rest of the pasture land was split between larger farms with manure storage (8% of watershed area), which allows avoidance of winter (December – March) manure application, and smaller farms without manure storage, where land application of manure is year-round (7% of watershed). Row crop fields (17% of watershed area) received manure application only during the months of April, May, October and November (spring and fall spreading).

Scenario 3: Avoiding spreading within 3 days of any rain or snowmelt, assuming perfect knowledge (2002-20011)

In this scenario, row crops were only spread in spring and fall when no rain or snowmelt occurred in the 3 days following any particular day. For all scenarios, we estimated snowmelt using daily temperature range to estimate daily radiation using the methodology described by

Walter et al (2005). In addition, the farmers with significant storage continued to avoid spreading pasture fields in winter (Dec – March), and all farmers avoided spreading within 3 days of rain or snowmelt.

Scenario 4: Avoiding spreading within 3 days of runoff, assuming perfect prediction of precipitation to inform the model (2002-20011)

In this scenario, we assumed that farmers would refrain from spreading manure on days when runoff would occur within three days following the current day anywhere in the watershed. The number of days available for manure application was approximately double that of scenario 3 for both pasture with storage and row crop fields (Table 3.2)

Scenario 5: Avoiding spreading within 3 days of "forecast" rain (2002-20011)

Farmers avoided spreading manure any day that rain or snowmelt occurred, or had rain or snowmelt forecast in the following three days in row or manure-fertilized pasture fields.

Scenario 6: Avoiding spreading within 3 days of forecast runoff (2002-20011)

Farmers avoided spreading in manure-fertilized fields when runoff was modeled for that day, or forecast for the next 3 days.

Scenario 7: Preferentially spreading before rainfall (2002-20011)

In this scenario, we assumed farmers were four times more likely to spread any type of field when rain is forecast for the following day. This reflects the antidotal observation by several researchers who have worked on agricultural nonpoint source pollution in the region (personal

communication) that farmers will often try to spread before rain because they know that it will be hard to get the tractor onto the field after rain, and could be considered an alternative model for current practices.

Determining the impact of management window size on SRP transport (2002-20011)

The three-day cut-off for forecasting scenarios is based on Archibald et al. (in preparation, Chapter 2), and attempts to balance between maintaining forecast accuracy and creating a large enough window to allow biogeochemical immobilization of P from the manure. However, we recognize that the 3-day window is still a bit arbitrary. So we simulated a number of scenarios where we looked at the expected change to SRP loads considering zero to five day window sizes for avoiding manure spreading. The "Day of" scenario assumes that farmers would only avoid spreading manure when runoff is modeled for that day, while the "1d" – "5d" scenarios assume that farmers would avoid spreading for the given number of days before a runoff event, as well as during the period of modeled runoff.

Results

Comparison to Measured SRP concentrations at Fall Creek Outlet in 1972 - 1976

Modeled and measured SRP loads and concentrations are shown in Figure 3.2a-b. While SRP loads are reasonably-well modeled (Nash-Sutcliffe efficiency (NSE) = 0.53, Figure 3.2c), the stream water SRP concentration was not well modeled (R^2 = 0.04, figure 3.2b), so modeled SRP loads seem to be driven by modeled streamflow (NSE = 0.70, figure 3.2a) (Nash and Sutcliffe, 1970). Using the average SRP concentration over the period of measurement reduces the accuracy of the load model, giving a NSE value of 0.46. Because we do not know where manure

was actually applied in the watershed on any given day and instead use very general guidelines on how it is distributed, it is perhaps not surprising that we cannot predict the day-to-day concentrations well. Additionally, we assume mobilized SRP is conserved, e.g., we do not consider biological uptake of SRP moving through the landscape. However, the modeled range of concentrations matches the observed ranges.

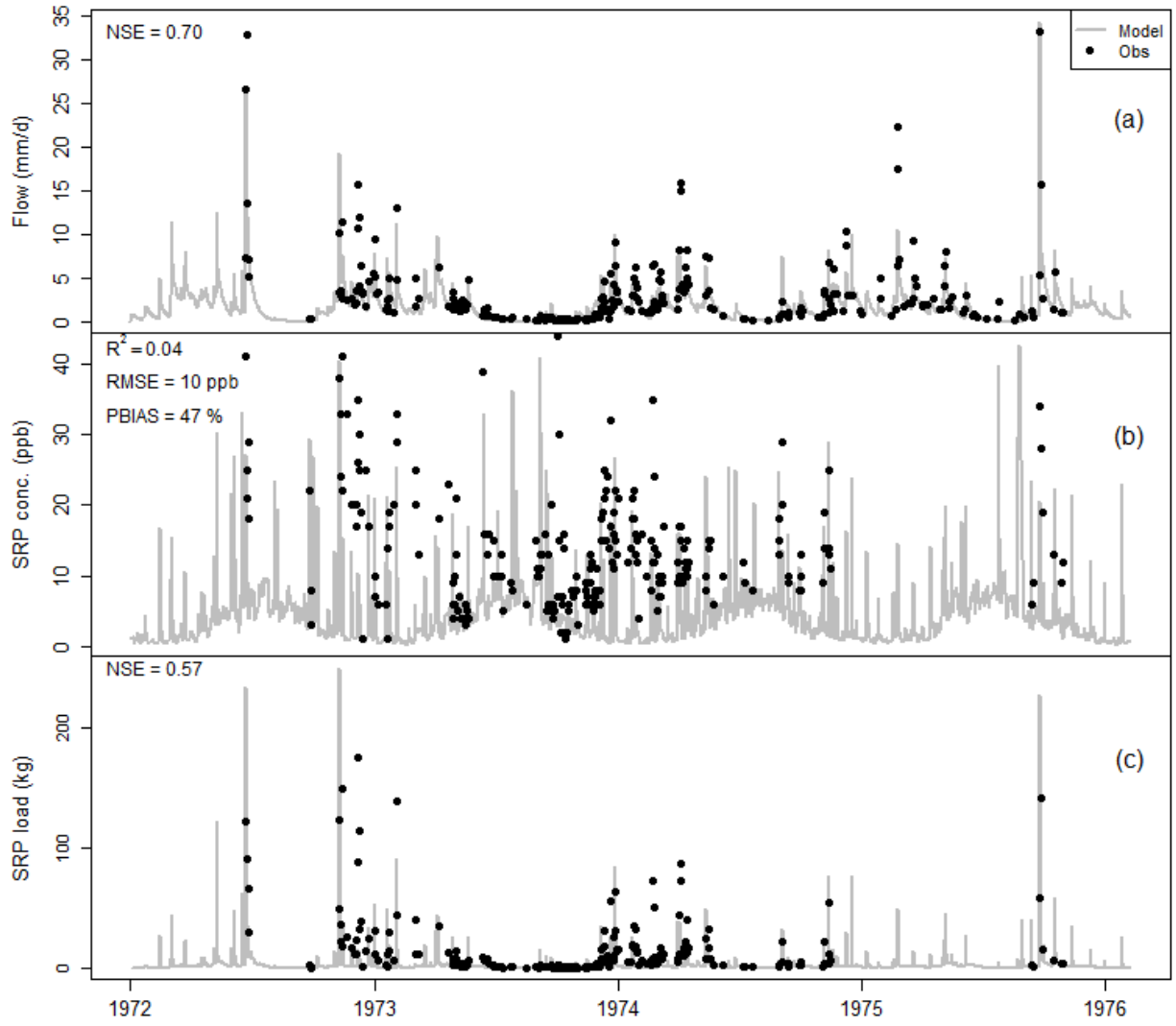

Figure 3.2. Model (grey line) SRP and measured (black circle), (a) streamflow at the Fall Creek outlet (mm/day) (b) SRP concentrations (ppm), and (c) SRP load (kg/day)

Scenario results (2002-2011)

As we will show, the different scenarios had different impacts on P loadings from agricultural lands, but these came at a cost of increased restrictions on farmers of the days they had available to deal with their animal wastes. Of the days that were available for row crop spreading in baseline Scenario 2, Scenario 3 resulted in an 85% reduction in the number of days that were suitable for manure spreading in cropland, a 78% reduction in potential days for year-round fertilized pasture fields, and an 84% reduction in potential spreading days for non-winter pasture spreading (Table 3.2, Figure 3.3). The number of days available for the forecast rain or snowmelt avoidance scenario (Scenario 5) was slightly less, while the runoff and runoff forecasts scenarios had many more days available for spreading (Table 3.2).

Table 3.2. Average number of days per year that farmers would be able to spread manure based on the different spreading plans using on observed and predicted data from 2002 - 2011. Values in parentheses indicate the percentage of days available for spreading compared to current practices.

Scenario	Pasture with Minimal Storage	Pasture with Storage	Row Crop
1. Maximum-Reduction, no manure	0	0	0
2. Approximation of current practices	365	244	122
3. No spreading before rain or snowmelt	79 (22%)	39 (16%)	18 (15%)
4. No spreading before runoff	165 (45%)	109 (45%)	44 (36%)
5. No spreading before rain or snowmelt forecast	91 (25%)	49 (20%)	20 (17%)
6. No spreading before runoff forecast	143 (39%)	96 (40%)	33 (27%)
7. Increased spreading before rain forecast	365	244	122

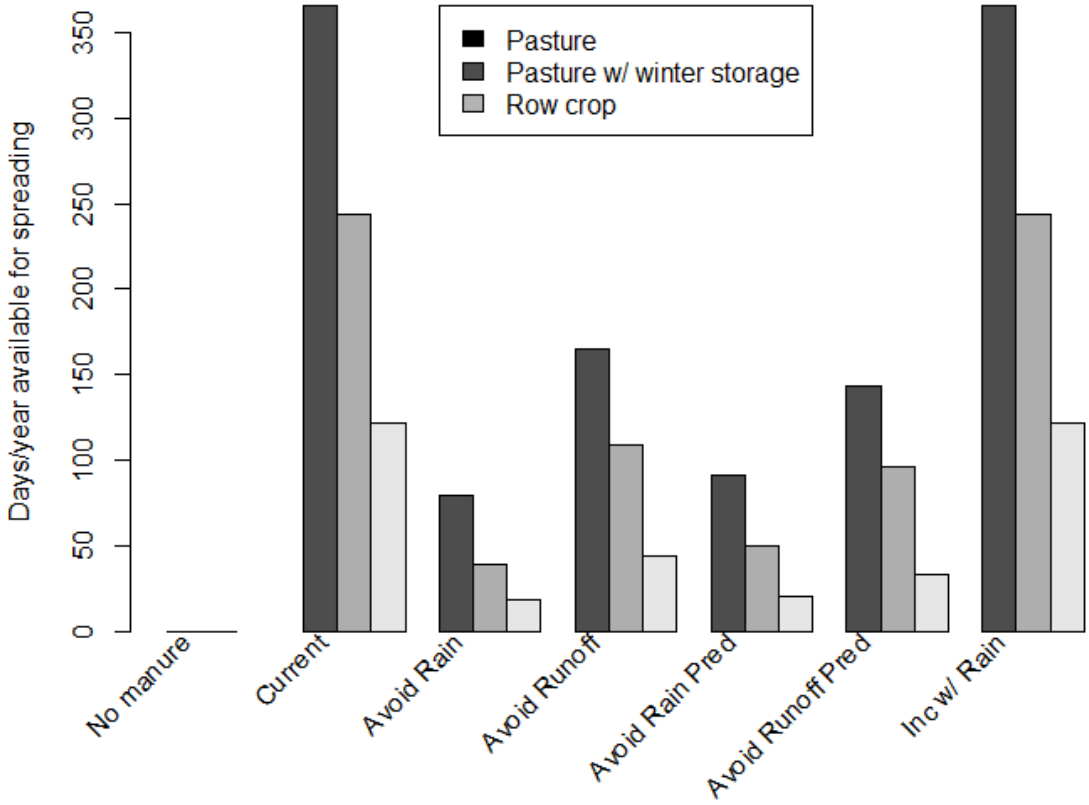

Figure 3.3. Average number of days available for spreading manure under the scenarios considered in this study.

The model predicted that under current manure spreading practices, 32% of SRP loads are delivered through baseflow, with the remainder from runoff: 15% from fertilized pasture land (8% without storage, 7% with storage), 25% from row crops, and 28% from unfertilized area overland runoff. The seasonal breakdown of SRP loads for the various scenarios are reported in Table 3.3.

Table 3.3. Average seasonal loads (kg/km^2) for each management scenario. Values in parentheses are the percentage of total yearly load occurring in each season.

Scenario	Winter	Spring	Summer	Fall	Total load
1. Maximum Reduction, no manure	0.35 (11%)	1.03 (31%)	0.79 (24%)	1.16 (35%)	3.33
2. Approximation of current practices	0.59 (13%)	1.46 (32%)	0.84 (18%)	1.68 (37%)	4.57
3. No spreading before rain or snowmelt	0.55 (13%)	1.38 (33%)	0.80 (19%)	1.42 (34%)	4.14
4. No spreading before runoff	0.58 (13%)	1.29 (32%)	0.82 (20%)	1.44 (35%)	4.06
5. No spreading before rain and snowmelt forecast	0.58 (14%)	1.29 (31%)	0.82 (20%)	1.45 (35%)	4.14
6. No spreading before runoff forecast	0.53 (13%)	1.28 (31%)	0.85 (21%)	1.44 (35%)	4.09
7. Increased (4 x) probability of spreading before rain forecast	0.60 (13%)	1.54 (34%)	0.85 (18%)	1.73 (37%)	4.72

Reductions in predicted P loads are similar, between 35 – 41% of the maxim reduction scenario (Scenario 1) reductions, for all scenarios of avoiding runoff spreading (assuming perfect foresight of rain or snowmelt, runoff, or using precipitation or runoff forecasts) (Figure 3.4). This is surprising, because there were large differences in the number of potential days for spreading among these scenarios (between 39 – 109 days for pasture with major storage, 79-164 days for pasture without major storage, and 18-44 days for row crops per year) (Table 3.2). If reductions of P loads are calculated in relation to the reduction in days of spreading per year, we see that the most effective way to reduce P loading from recently spread manure is to use a forecasting runoff model; for a similar reductions in P loading, a farmer basing spreading schedules on a watershed model forecast would have a 65% reduction in potential days for manure application, while using rain forecasts directly would require an 81% reduction of potential spreading days from current practices. In the case of farmers preferentially spreading before forecast rain (Scenario 7), annual SRP loading increased by approximately 3% from Scenario 2.

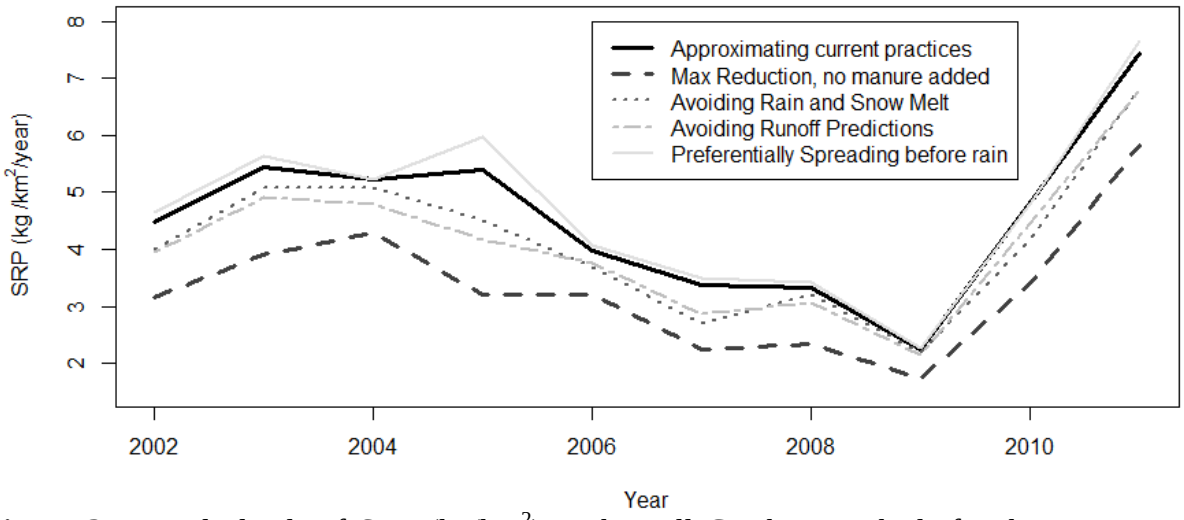

Figure 3.4 Yearly loads of SRP (kg/km^2) in the Fall Creek watersheds for the scenarios of : approximating current practices (solid black line), hypothetically removing all manure P inputs to the watershed (dashed dark grey line), avoiding all rain and snowmelt days (dotted line) , avoiding runoff predictions (dashed grey), and if farmers preferentially spread before rain (light grey line)

Impact of management window size on SRP transport (2002-2011)

As expected, a larger management window before runoff events results in lower SRP export from the watershed (Figure 3.5), however with diminishing returns as the window gets larger. Avoiding rain or snowmelt gives a less consistent decrease in SRP load than avoiding modeled runoff, which is not surprising, since many days with rain or snowmelt do not produce runoff. (Figure 3.6).

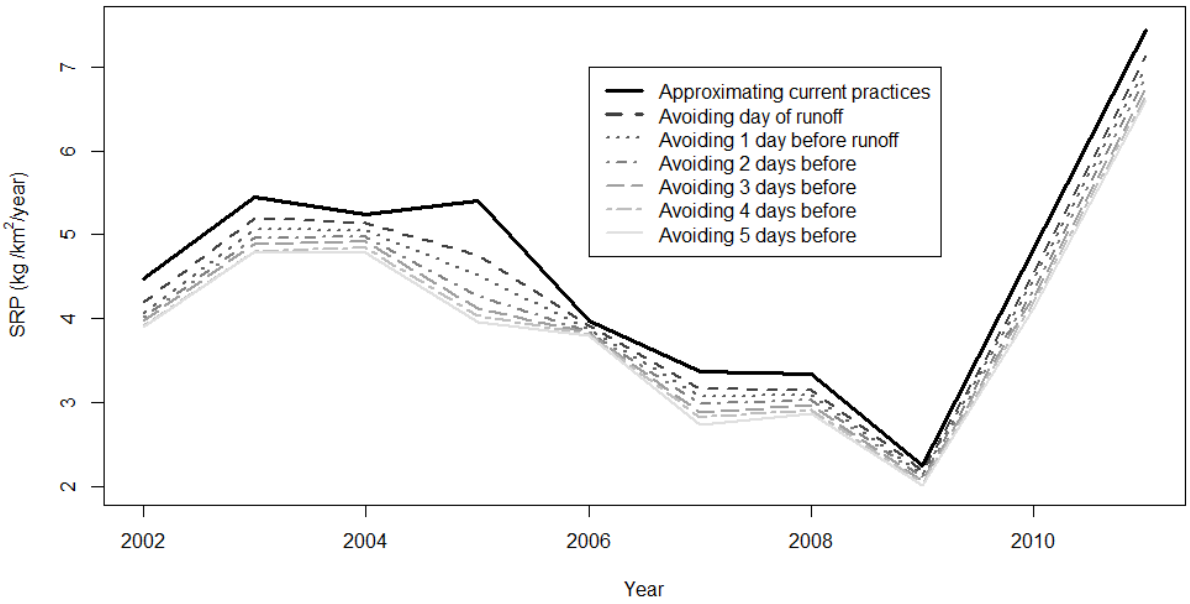

Figure 3.5: Yearly SRP loads using a variety of management window sizes to restrict manure spreading before or during runoff events.

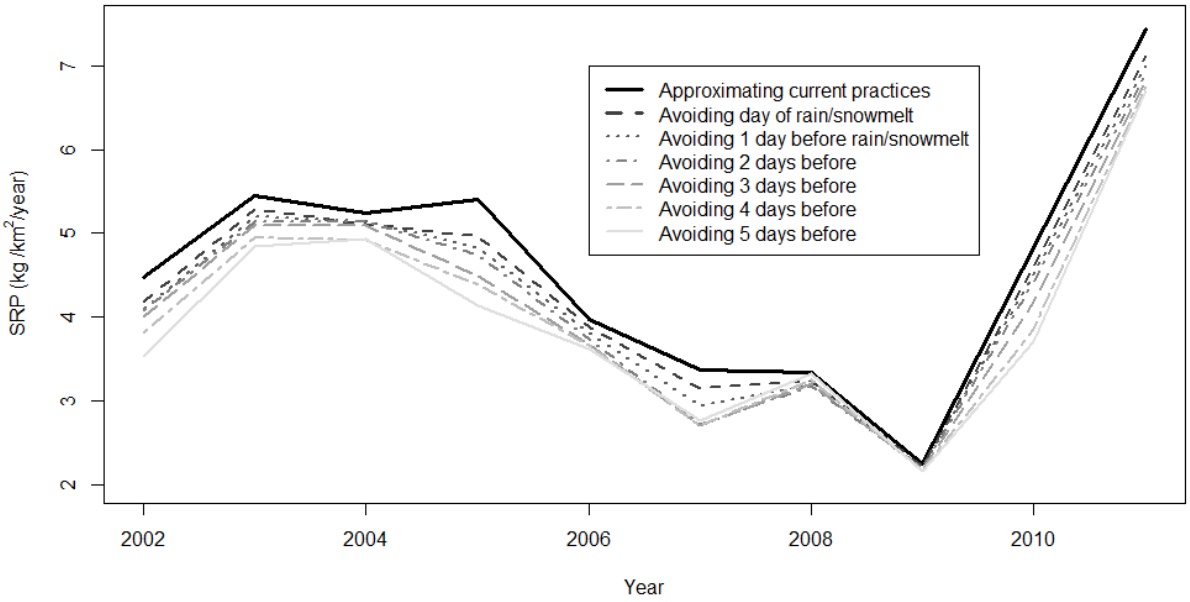

Figure 3.6. Yearly SRP loads using variable management window sizes to avoid rain or snowmelt.

In the scenario where farmers have perfect knowledge and are able to avoid spreading manure within 5 days of a runoff event, a 12 -15% reduction in days available to spread leads to only a 3% reduction in manure-derived SRP loading from the scenario where they avoid within 4 days

of runoff. This is in contrast to the difference between avoiding spreading one day before runoff verses the day of, where 12-14% less days are available to spread, but manure-derived SRP in runoff is reduced by 9% (Figure 3.7).

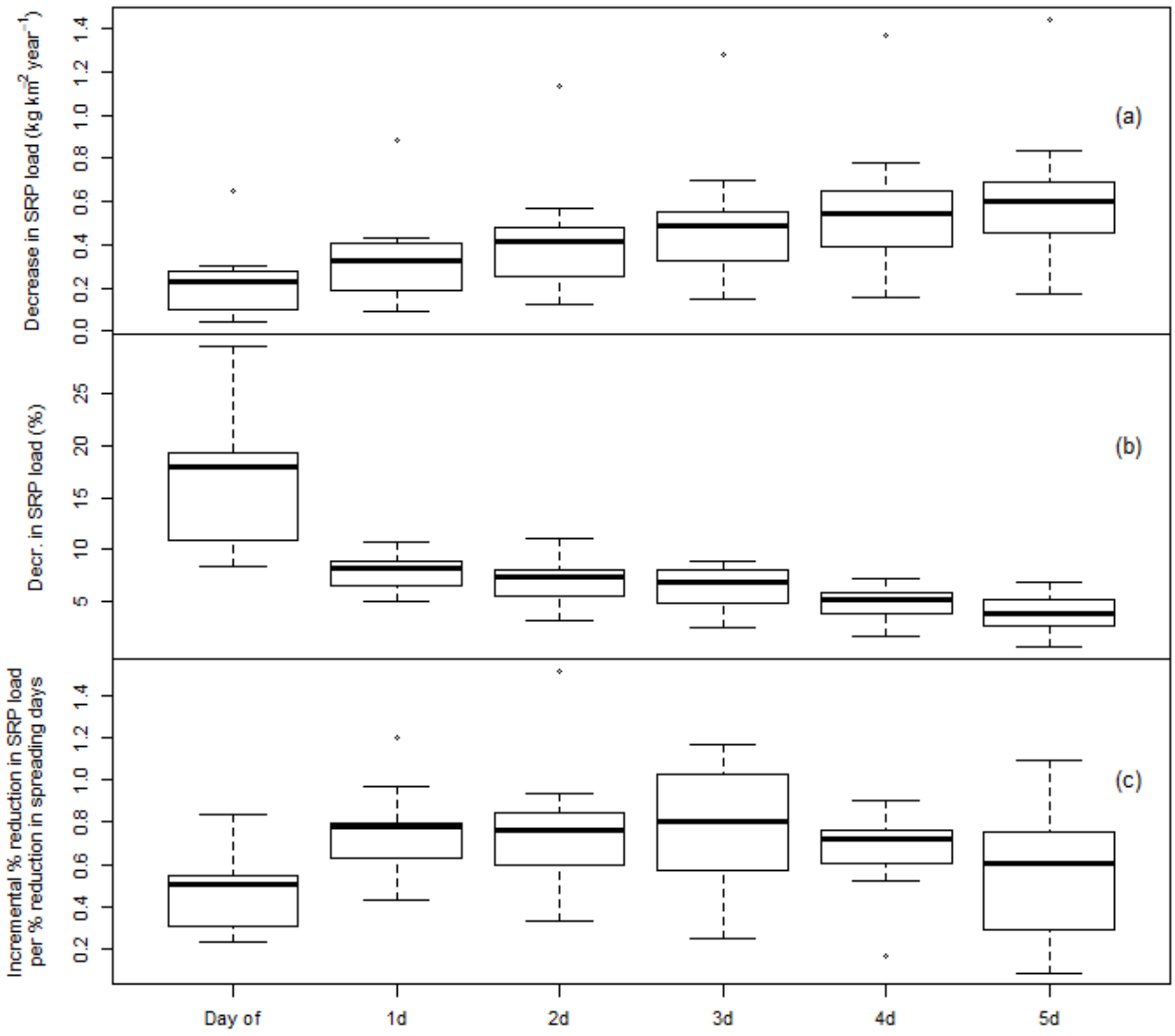

Figure 3.7. The impact of window size on avoiding manure application during and before runoff. In the "Day of" scenario, manure application is only avoided on days that runoff is modeled, while "1d" avoids spreading manure within one day of runoff and during runoff days, similarly for 2d – 5d. (a) The change in yearly SRP load delivered compared to current practices. (b) The decrease in load compared to the next scenario practice (e.g. the "2d" boxplot refers to the difference in between SRP load delivered using the "1d" and the "2d" scenario) expressed as a percentage of the max possible reduction if all manure was removed from the watershed. (c) The % decrease in manure-derived SRP load delivered divided by the % decrease in number of days available to farmers to spread manure using the current scenario.

Discussion

Modeling SRP concentration accurately is a notoriously difficult task, in part because SRP changes through interaction with soil, sediment, biota, and suspended particles, and exhibits a first flush hysteresis effect that can be difficult to capture in such a simple daily model (Bowes et al., 2005). For this reason, almost all P modeling studies report SRP or total P loads, and usually in larger than daily time steps, such as event-based, monthly or yearly loads (e.g., Kirsch et al., 2002; Easton et al., 2008). Here we find that we were able to reasonably-well predict the daily SRP loads even though SRP concentration was poorly modeled. SRP concentrations could be mismatched because of the difficulty in accurately capturing unexpected farmer behavior, such as an accidental manure spill in a ditch, allowing cows to access a stream (e.g. James et al., 2007), or manure storage failures (e.g., Easton et al. 2008); these behaviors could have a disproportionate impact on stream SRP concentration and are not simulated in our model.

In addition, the percent bias of SRP concentration and loads is high – 47% for concentration and 46% for load, suggesting that we are under-predicting SRP concentration during low flow periods. This could be due to the fact that we are not incorporating point sources of pollution, which would increase P concentration during loading during low-flow periods, but not in higher flow periods. These would be expected to have a higher impact during the earlier period of modeling (1970s) than in the present day, when more advanced tertiary treatment options are in use and P-based detergents have been banned.

Not all scenarios used here are currently feasible – for example, the perfect foresight of rain/snowmelt or runoff is not possible, however these scenarios let us know how perfect knowledge of future weather could help us in reducing P from agricultural runoff. The surprising result here is that more accurate forecasts would have a negligible impact on water quality

protection under these scenarios. Currently available forecasts allow for a similar level of protection from P loading, although using watershed model predictions requires 12 – 15% more days of abstaining from manure application than a perfect knowledge of the weather would provide.

Using a forecasting watershed model would allow more flexibility for spreading and reduce the burden of manure storage requirements, since runoff is not expected in all cases of rain, particularly during dry periods of the year. A step further in this analysis would be to consider the impact of a spatially explicit model that could pinpoint the locations of areas likely to produce runoff in the next three days (Cornell Soil and Water Lab, 2014; Dahlke et al., 2013). This would give farmers further flexibility in their ability to spread manure even on days when runoff is predicted, although the impact of such a model are beyond the scope of this analysis. Walter et al. (2001) found that by limiting manure spreading to areas that are less likely to generate runoff in general had the potential to reduce SRP loading from an agricultural field in the New York City watershed by approximately 50% of the maximal rate of reduction, so the rates of reduction are comparable but slightly greater than what we found here.

An important assumption made in this model is that P additions to agricultural land are not more than is needed for crop growth. We know that this is not the case for many agricultural systems in which manure is added according to nitrogen (N) requirements and because farmers recognize that there will be unavoidable N losses due to leaching and volatilization, the effective ratio of N:P in applied manure is lower than that used by crops. In situations where an excess of P is being added to agricultural land, we would expect to see the background level of P from soil/plant interaction increasing, and might find the problem of P transport from agricultural fields becomes more of a long-term chronic problem rather than an acute problem tied mainly to

overland runoff and fertilization regimes. In addition, the model reported here is sensitive to the amount of WEP applied to fields. If farmers add more manure than we are accounting for here, we could expect to see significantly larger changes in the expected loads if runoff avoiding strategies are employed.

Conclusions

Changing fertilization timing has potential to reduce SRP loading from agriculture without the need for large capital investments. In the Fall Creek watershed in NY, we found that a change in fertilizer application timing had the potential to reduce manure-fertilization-caused SRP runoff by up to 41%. The use of runoff models as a prediction tool gave marginal improvements in SRP loadings over direct use of weather forecasts; the main benefit of runoff models was that they farmers would be able to spread more frequently using these tools. The reductions in SRP loading by avoiding high-runoff periods were substantial, but they do not address the problem of chronic P build-up in the watershed if too much P is being applied.

Acknowledgements

We'd like to thank Aaron Ristow and Jon Negley (Tompkins Co. SWCD), Greg Albrecht (NYS Soil and Water Conservation Committee), and Karl Czymmek (NYS ProDairy), for their thoughtful insight into farmer manure management strategies within the watershed. Funding for this research was from the USDA NIFA Land/Sea Grant number 2012-67019019434.

WORKS CITED

Archibald, J.A., Buchanan, B.P., Fuka, D.F., Georgakakos, C.B., Lyon, S.L., Walter, M.T., 2014. A simple, regionally parameterized model for predicting nonpoint source areas in the Northeastern US. J. Hydrol. Reg. Stud. 1, 74–91. doi:10.1016/j.ejrh.2014.06.003

Bouldin, D., 2007. Water quality data for Fall Creek (Tompkins County, NY) sampling sites: 1972-1995 [WWW Document]. URL http://hdl.handle.net/1813/8148 (accessed 7.6.14).

Bowes, M.J., House, W.A., Hodgkinson, R.A., Leach, D.V., 2005. Phosphorus–discharge hysteresis during storm events along a river catchment: the River Swale, UK. Water Res. 39, 751–762. doi:10.1016/j.watres.2004.11.027

Buchanan, B.P., Archibald, J.A., Easton, Z.M., Shaw, S.B., Schneider, R.L., Todd Walter, M., 2013. A phosphorus index that combines critical source areas and transport pathways using a travel time approach. J. Hydrol. 486, 123–135. doi:10.1016/j.jhydrol.2013.01.018

Buda, A.R., Kleinman, P.J.A., Srinivasan, M.S., Bryant, R.B., Feyereisen, G.W., 2009. Effects of Hydrology and Field Management on Phosphorus Transport in Surface Runoff. J. Environ. Qual. 38, 2273. doi:10.2134/jeq2008.0501

Carpenter, S.R., Caraco, N.F., Correll, D.L., Howarth, R.W., Sharpley, A.N., Smith, V.H., 1998. Nonpoint pollution of surface waters with phosphorus and nitrogen. Ecol. Appl. 8, 559–568.

Cornell Soil and Water Lab, 2014. HSA-DSS Tool [WWW Document]. URL http://hsadss.bee.cornell.edu/OwascoLake/ (accessed 11.23.13).

Dahlke, H., Easton, Z., Fuka, D., Walter, M., Steenhuis, T., 2013. Real-Time Forecast of Hydrologically Sensitive Areas in the Salmon Creek Watershed, New York State, Using an Online Prediction Tool. Water 5, 917–944. doi:10.3390/w5030917

DATCP, 2013. Runoff Risk Advisory Forecast [WWW Document]. Wis. Manure Manag. Advis. Syst. URL http://144.92.93.196/app/events/runoff_forecast (accessed 10.14.13).

DeLaune, P.B., Moore, P.A., Carman, D.K., Sharpley, A.N., Haggard, B.E., Daniel, T.C., 2004. Development of a phosphorus index for pastures fertilized with poultry litter—Factors affecting phosphorus runoff. J. Environ. Qual. 33, 2183–2191.

Easton, Z.M., Fuka, D.R., Walter, M.T., Cowan, D.M., Schneiderman, E.M., Steenhuis, T.S., 2008. Re-conceptualizing the soil and water assessment tool (SWAT) model to predict runoff from variable source areas. J. Hydrol. 348, 279–291. doi:10.1016/j.jhydrol.2007.10.008

Easton, Z.M., Gérard-Marchant, P., Walter, M.T., Petrovic, A.M., Steenhuis, T.S., 2007. Identifying dissolved phosphorus source areas and predicting transport from an urban watershed using distributed hydrologic modeling: URBAN DISSOLVED

PHOSPHOROUS SOURCE AREAS. Water Resour. Res. 43, n/a–n/a. doi:10.1029/2006WR005697

Easton, Z.M., Walter, M.T., Schneiderman, E.M., Zion, M.S., Steenhuis, T.S., 2009. Including source-specific phosphorus mobility in a nonpoint source pollution model for agricultural watersheds. J. Environ. Eng. 135, 25–35.

Hart, M.R., Quin, B.F., Nguyen, M., 2004. Phosphorus runoff from agricultural land and direct fertilizer effects. J. Environ. Qual. 33, 1954–1972.

Hively, W.D., Bryant, R.B., Fahey, T.J., 2005. Phosphorus Concentrations in Overland Flow from Diverse Locations on a New York Dairy Farm. J. Environ. Qual. 34, 1224. doi:10.2134/jeq2004.0116

James, E., Kleinman, P., Veith, T., Stedman, R., Sharpley, A., 2007. Phosphorus contributions from pastured dairy cattle to streams of the Cannonsville Watershed, New York. J. Soil Water Conserv. 62, 40–47.

Johnson, Arthur H., David R. Bouldin, Edward A. Goyette, Anne M. Hedges, 1976. Phosphorus Loss by Stream Transport from a Rural Watershed: Quantities, Processes, and Sources 5, 148–157.

Kirsch, K., Kirsch, A., Arnold, J.G., 2002. Predicting sediment and phosphorus loads in the Rock River basin using SWAT. Forest 971, 10.

Kleinman, P.J., Sharpley, A.N., Moyer, B.G., Elwinger, G.F., 2002. Effect of mineral and manure phosphorus sources on runoff phosphorus. J. Environ. Qual. 31, 2026–2033.

Kleinman, P.J.A., Sharpley, A.N., McDowell, R.W., Flaten, D.N., Buda, A.R., Tao, L., Bergstrom, L., Zhu, Q., 2011. Managing agricultural phosphorus for water quality protection: principles for progress. Plant Soil 349, 169–182. doi:10.1007/s11104-011-0832-9

McDowell, R.W., Srinivasan, M.S., 2009. Identifying critical source areas for water quality: 2. Validating the approach for phosphorus and sediment losses in grazed headwater catchments. J. Hydrol. 379, 68–80. doi:10.1016/j.jhydrol.2009.09.045

Nash, Je., Sutcliffe, J.V., 1970. River flow forecasting through conceptual models part I—A discussion of principles. J. Hydrol. 10, 282–290.

NOAA, 2014. National Climatic Data Center (NCDC) | The world's largest active archive of weather and climate data producing and supplying data and publications for the world. [WWW Document]. URL http://www.ncdc.noaa.gov/ (accessed 7.20.14).

Sharpley, A., Wang, X., 2014. Managing agricultural phosphorus for water quality: Lessons from the USA and China. J. Environ. Sci. doi:10.1016/j.jes.2014.06.024

Sharpley, A.N., Kleinman, P.J.A., Heathwaite, A.L., Gburek, W.J., Folmar, G.J., Schmidt, J.P., 2008. Phosphorus Loss from an Agricultural Watershed as a Function of Storm Size. J. Environ. Qual. 37, 362. doi:10.2134/jeq2007.0366

U.S. Geological Survey, 2011. NLCD 2006 Land Cover [WWW Document]. URL http://nationalmap.gov/index.html

Ulén, B., Johansson, G., Kyllmar, K., 2001. Model predictions and long-term trends in phosphorus transport from arable lands in Sweden. Agric. Water Manag. 49, 197–210.

USDA-NRCS, 2004. National Engineering handbook (NEH), Section 4, Hydrology. US Government Press, USDA.

Walter, M.T., Brooks, E.S., Walter, M.F., Steenhuis, T., Scott, C.A., Boll, J., 2001. Evaluation of soluble phosphorus loading from manure-applied fields under various spreading strategies. J. Soil Water Conserv. 56, 329–335.

Walter, M.T., Walter, M.F., Brooks, E.S., Steenhuis, T.S., Boll, J., Weiler, K., 2000. Hydrologically sensitive areas: Variable source area hydrology implications for water quality risk assessment. J. Soil Water Conserv. 55, 277–284.

Walter, M. Todd, M., Brooks, E.S., McCool, D.K., King, L.G., Molnau, M., Boll, J., 2005. Process-based snowmelt modeling: does it require more input data than temperature-index modeling? J. Hydrol. 300, 65–75. doi:10.1016/j.jhydrol.2004.05.002

CONCLUSION

A simple lumped watershed model has the ability to predict runoff location and timing in non-urban watersheds in the Northeastern USA. This model provides the basis for a decision support tool for identifying runoff source areas which allow watershed residents to avoid polluting activity before runoff is expected. P runoff is of particular concern in inland aquatic ecosystems, and land application of manure can contribute to P contamination. Results from laboratory soil box experiments found that SRP concentration in runoff decreased exponentially over time; this reduction was amplified by higher temperatures. This suggests that use of runoff identifying tools such as the one developed in Chapter 1 have the potential to significantly reduce SRP loading to receiving waters if farmers avoid spreading during high-risk runoff periods. We found that up to 40% of the manure-derived SRP loads from agriculture could be avoided if farmers avoid spreading manure within three days of runoff prediction.

APPENDIX

Appendix A.
The Runoff Hydrograph

The synthetic hydrograph used here has a linear increase to peak followed by an exponential decrease (Figure A.1.1) and is defined by two parameters, time to peak, T_P, and a shape parameter, b, which determines the height of the peak and the length of the tail with respect to T_P.

$$q = \begin{cases} \frac{2t}{(1+b)\,T_P{}^2}, & t < T_P \\ \frac{2e^{-2(t-T_P)/(bT_P)}}{T_P(b+1)}, & t \geq T_P \end{cases} \quad \text{(A.1.1)}$$

where q is the instantaneous runoff fraction [time^{-1}], and t is time since runoff began (same units as T_P , here, hours). Because we are modeling runoff on a daily time-step, we use the integral of Eq. A.1.1 with respect to t to determine the cumulative runoff fraction:

$$\frac{Q}{Q_{tot}} = \begin{cases} \frac{t^2}{T_P{}^2(1+b)}, & t < T_P \\ 1 - \frac{be^{-\frac{2(t-T_P)}{bT_P}}}{b+1}, & t \geq T_P \end{cases} \quad \text{(A.1.2)}$$

where Q is runoff depth at time t (defined as the time since runoff began, hours), Q_{tot} is the total runoff depth for this runoff event , b is the shape parameter of the curve (dimensionless). Eq. (A.1.2) can take very different shapes depending on the length of T_P in relation to the daily time step (Figure A.1.1).

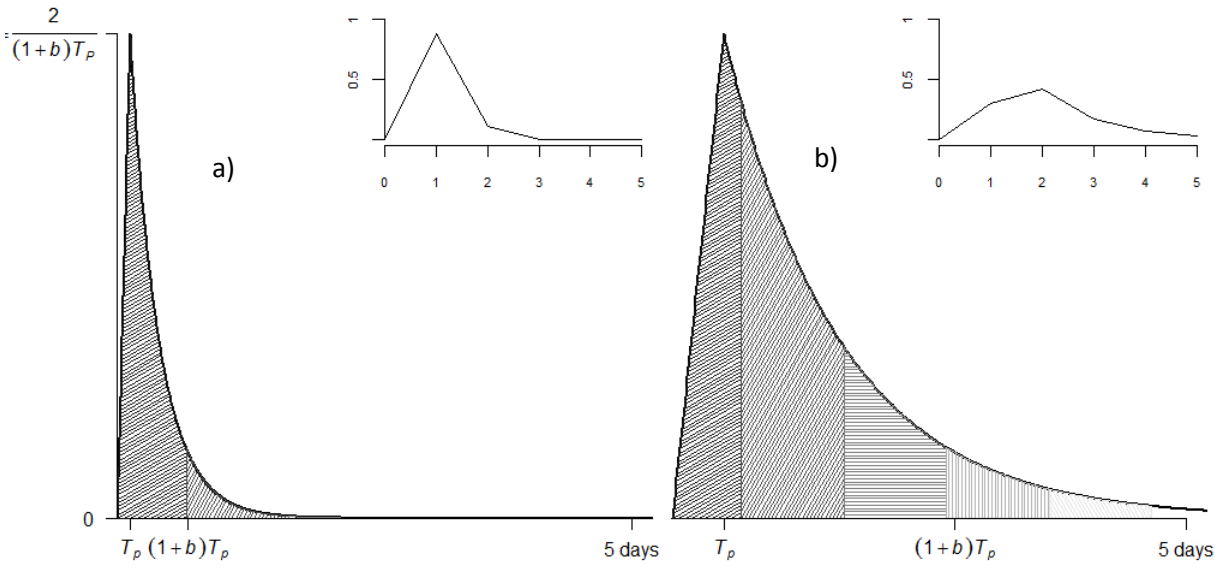

Figure A.1.1. Integrating the continuous hydrograph over a daily time step allows us to see the daily runoff pattern (insets). Watersheds with a quick response time as in (a) (T_P = 3 hours), will see most of the runoff generated from a single storm reach the outlet on the first day. A longer T_P as in (b), (T_P = 12 hours), creates a more dampened runoff pattern. To handle the timing mismatch between USGS gauges (being from midnight to midnight) and most NOAA gauges (approximately 8 am – 8 am), we summed the first 16 hours of the hydrograph for the first day of runoff and summed the full 24-hour periods for subsequent days.

Estimating T_P and b

We calculated the event-based daily runoff fraction for each watershed over the five-day period following isolated rain events by dividing the amount of runoff from a particular day following rain input by the total runoff over the five day period. The daily runoff fractions were then averaged over all events for each day following runoff initiation. From these, we determined the average T_P for each watershed by minimizing the root mean square error (RMSE) between the 5-day runoff patterns observed with the expected runoff breakdown determined by Eq. A.2. A representative subset of the resulting best-fit runoff patterns and the observed runoff patterns are shown in Figure A.1.2.

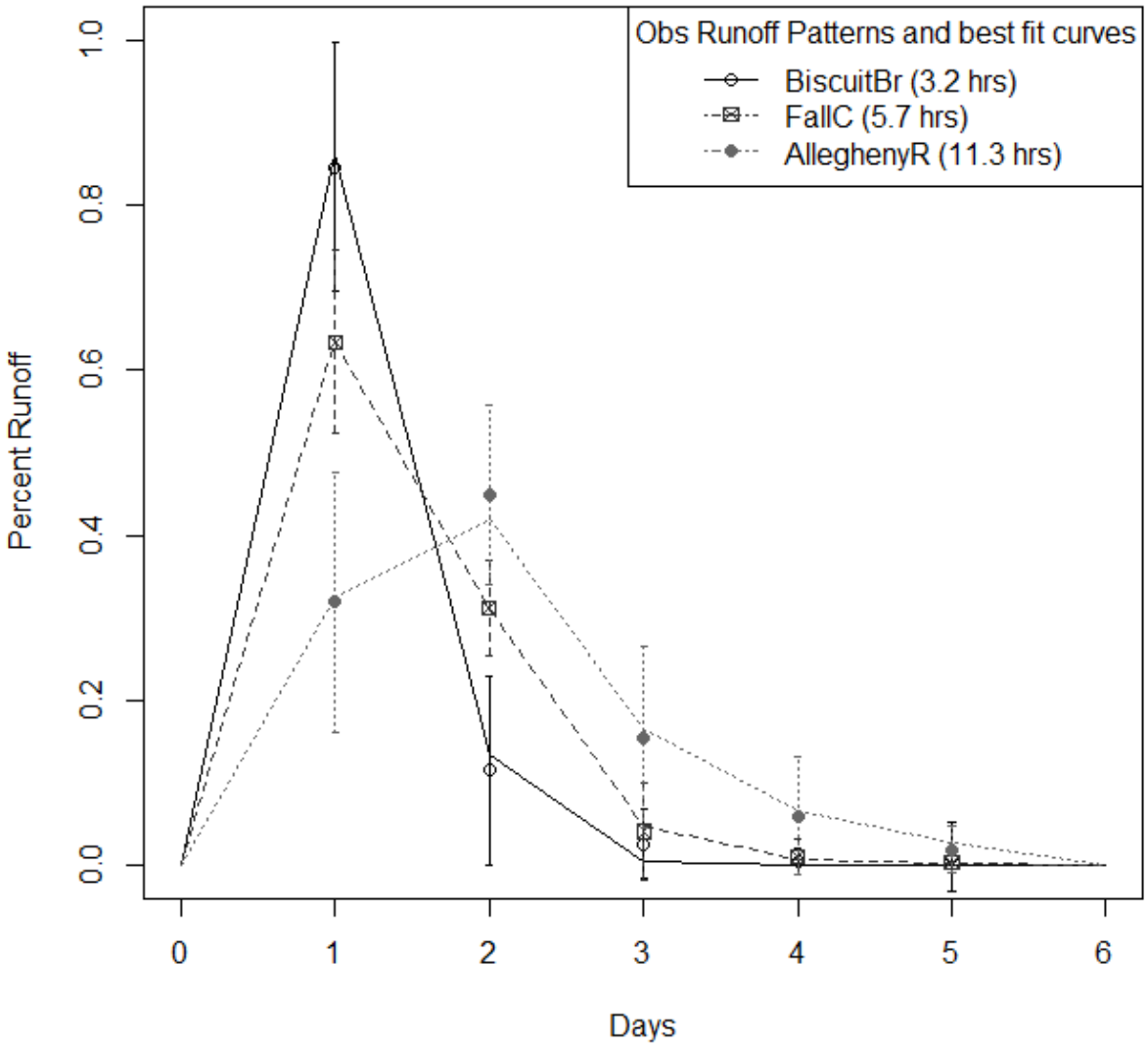

Figure A.1.2: Observed (symbols; error bars represent the standard deviation from the mean of all events for that watershed) and best-fit (lines) daily runoff patterns for three watersheds (the smallest, an intermediate, and largest area watersheds). The best-fit T_P values, indicated in parentheses, were determined by minimizing the RMSE between the observed runoff pattern and the runoff pattern calculated from Eq. A.2 by varying T_P.

T_P was not constant across watersheds. We investigated two potential predictors of T_P: T_c and watershed area. In calculating T_c, we determined the longest flowpath, L, using ArcHydro's longest flowpath tool with 10m DEMs from the USGS (ESRI, 2009; USGS, 2013). The relationship between T_c and T_P are reported in Results Section 4.1.2. The linear relationship

found between T_P and watershed area ($T_{P,A}$ = 0.002A + 4.7; A = watershed area, km^2) was also significant, with R^2 = 0.62 and could be useful when information on longest flow path is not easily obtainable.

We also compared the observed cumulative runoff fraction against time since storm runoff began normalized by the calculated T_P, (i.e. $T_{P,C}$, Eq. 1.7, with C_2 = 0.33 and C_3 = 3.4 hrs) (Figure A.1.3). Normalizing time since runoff began (t) by $T_{P,C}$ allows all observations to be compared against the predicted cumulative runoff curve (Eq. A.1.2). The observed runoff fractions from all watersheds compared well with the predicted runoff pattern, with an R^2 of 0.94, and RMSE of 0.05.

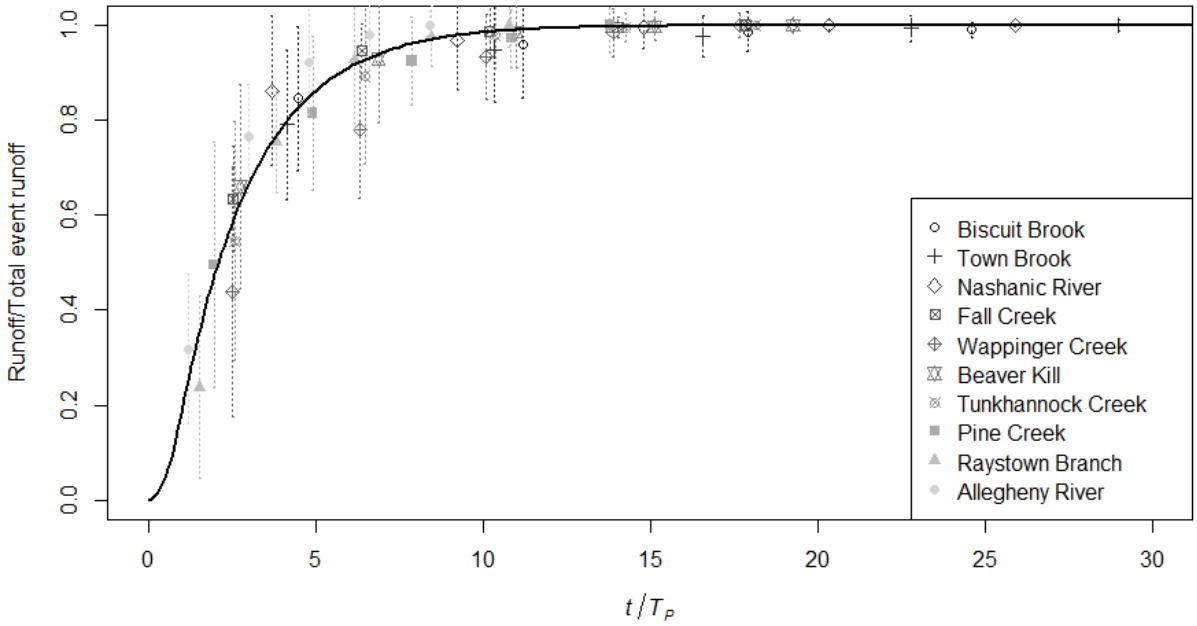

Figure A.1.3. Observed cumulative runoff proportion vs. time since runoff began (t) normalized for $T_{P,C}$ (Eq. 7) for all ten watersheds (symbols); R^2 = 0.94 and RMSE = 0.05 (fraction of total runoff, unitless). Symbols are measured runoff fractions, and error bars on the observations indicate one standard deviation from the mean. The smooth curve represents the expected runoff fraction based on Equation A.1.2

Choosing runoff events for SWD_d - S_d relationship determination.

The rainfall/snowmelt-runoff events used to determine the coefficients in Eq. 6 were chosen with the following requirements. The rain or snowmelt triggering the event was at least 20 mm and the rain or snowmelt within two days before and four days after this trigger was less than 10 mm. We calculated the runoff that occurred after that rainfall/snowmelt trigger by using a one-pass baseflow separation filter (Lyne and Hollick, 1979) and summing the quickflow that occurred after the rain event until it returned to zero or up to four days of runoff, which-ever was shorter. This window was chosen to maximize the amount of events that could be included in the analysis, while minimizing the impact of additional runoff from previous or subsequent events. Our runoff hydrograph analysis (Appendix A.1) indicated that at least 97% of the runoff following an event reached the outlet in these ten watersheds within a four day period. We also removed events which had runoff values greater than 10% of baseflow before the precipitation event, and if no streamflow peak occurred within 4 days of runoff starting to further ensure that the relationship was not influenced by other storm events. These criteria further allowed us to exclude events that were likely to have been influenced by runoff from other rain or snowmelt events.

Appendix B

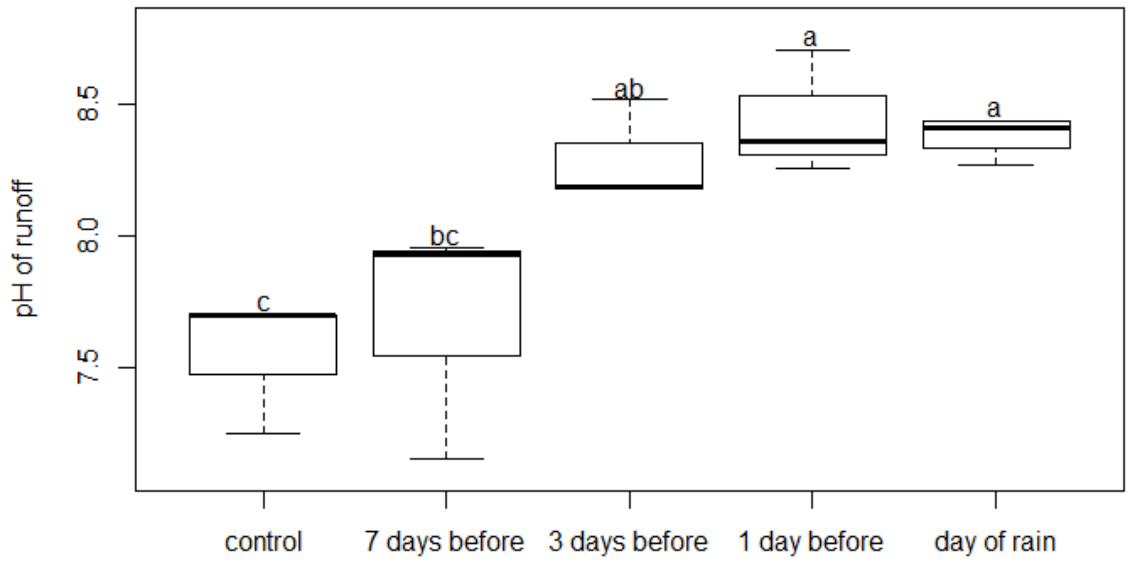

Figure B.2.1. The pH of runoff water from the first rain event in the Wet-Dry experiment. Boxplots that do not share the same letter are significantly different from each other using a Tukey means test ($p<0.05$).

Appendix C

Table C 2.1 Rain event measurements, Cold-Warm Experiment.

Box	Date	Treatment	Condition	Hours Since Manure Spread	Length of rain (min)	Rain (mm)	Runoff (mm)	Infiltration (mm)	Drainage (mm)
1	3/25/2013	control	Outside		34	42.4	5.7	36.7	
2	3/25/2013	7 days before	Outside		35	30.6	0.8	29.9	
3	3/25/2013	3 days before	Outside		35	29.5	1.3	28.2	
4	3/25/2013	1 day before	Outside		17.5	30.7	1.6	29.0	
5	3/25/2013	day of rain	Outside		35	29.3	6.1	23.3	
6	3/25/2013	control	Outside		35	36.7	9.3	27.4	
7	3/25/2013	7 days before	Outside		35	34.5	3.8	30.7	
8	3/25/2013	3 days before	Outside		34	32.8	5.1	27.7	
9	3/25/2013	1 day before	Outside		35	34.7	3.2	31.5	
10	3/25/2013	day of rain	Outside		35	27.9		27.9	
11	3/25/2013	control	Inside		30	39.7	7.7	32.1	
12	3/25/2013	7 days before	Inside		30	18.6		18.6	
13	3/25/2013	3 days before	Inside		30	25.2		25.2	
14	3/25/2013	1 day before	Inside		30	41.5	9.2	32.3	
15	3/25/2013	day of rain	Inside		30	22.2		22.2	
16	3/25/2013	control	Inside		30	39.4	10.1	29.3	
17	3/25/2013	7 days before	Inside		30	18.9		18.9	
18	3/25/2013	3 days before	Inside		30	42.1	9.5	32.6	
19	3/25/2013	1 day before	Inside		30	14.8		14.8	
20	3/25/2013	day of rain	Inside		30	32.3	0.5	31.8	
1	4/1/2013	control	Outside		15	13.4	5.7	7.7	9.6
2	4/1/2013	7 days before	Outside	168	15	13.1	6.5	6.6	9.3
3	4/1/2013	3 days before	Outside	72	15		0.3	1.4	2.7
4	4/1/2013	1 day before	Outside	24	15	11.2	5.1	6.0	8.2
5	4/1/2013	day of rain	Outside	4	15	14.7	12.8	1.9	4.9
6	4/1/2013	control	Outside		15	14.2	5.2	9.0	11.0
7	4/1/2013	7 days before	Outside	168	15	12	3.8	8.2	11.2
8	4/1/2013	3 days before	Outside	72	15	12.3	5.5	6.8	8.5
9	4/1/2013	1 day before	Outside	24	15	17.5	13.1	4.4	7.4
10	4/1/2013	day of rain	Outside	4	15	13.1	7.1	6.0	8.8
11	4/1/2013	control	Inside		31	34.4	12.5	21.9	12.3

12	4/1/2013	7 days before	Inside	168	31	39.9	9.2	30.7	14.0
13	4/1/2013	3 days before	Inside	72	31	22.9	5.7	17.3	10.7
14	4/1/2013	1 day before	Inside	24	31	20.7	5.3	15.3	8.5
15	4/1/2013	day of rain	Inside	4	31	22.1	1.6	20.5	10.1
16	4/1/2013	control	Inside		31	20.9	3.7	17.3	10.1
17	4/1/2013	7 days before	Inside	168	31	22.2		22.2	4.7
18	4/1/2013	3 days before	Inside	72	31	27.1	11.2	15.9	10.4
19	4/1/2013	1 day before	Inside	24	31	35.7	5.3	30.4	9.3
20	4/1/2013	day of rain	Inside	4	31	20.3	4.7	15.6	8.8
1	4/2/2013	control	Outside		15	17.2	12.6	4.7	6.3
2	4/2/2013	7 days before	Outside	192	15	15.8	9.5	6.3	7.7
3	4/2/2013	3 days before	Outside	96	15	16.3	5.1	11.2	11.5
4	4/2/2013	1 day before	Outside	48	15	11.6	5.3	6.3	7.7
5	4/2/2013	day of rain	Outside	28	15	14.7	5.3	9.3	10.1
6	4/2/2013	control	Outside		15	16.6	10.3	6.3	8.2
7	4/2/2013	7 days before	Outside	192	15	12	5.4	6.6	9.3
8	4/2/2013	3 days before	Outside	96	15	15.6	9.6	6.0	7.9
9	4/2/2013	1 day before	Outside	48	15	11.8	7.4	4.4	6.0
10	4/2/2013	day of rain	Outside	28	15	24.6	16.7	7.9	10.1
11	4/2/2013	control	Inside		20.8	12	1.6	10.4	9.3
12	4/2/2013	7 days before	Inside	192	20.8	21	8.4	12.6	11.8
13	4/2/2013	3 days before	Inside	96	20.8	15.2	5.3	9.9	10.4
14	4/2/2013	1 day before	Inside	48	20.8	14.4	6.4	7.9	8.5
15	4/2/2013	day of rain	Inside	28	20.8	14.6	4.8	9.9	9.9
16	4/2/2013	control	Inside		20.8	29.7	20.9	8.8	9.0
17	4/2/2013	7 days before	Inside	192	20.8	14.6	4.8	9.9	9.3
18	4/2/2013	3 days before	Inside	96	20.8	16.1	7.6	8.5	9.3
19	4/2/2013	1 day before	Inside	48	20.8	12.7	3.9	8.8	9.3
20	4/2/2013	day of rain	Inside	28	20.8	23.7	14.7	9.0	8.5
1	4/4/2013	control	Outside		20.33	19.9	13.9	6.0	4.9
2	4/4/2013	7 days before	Outside	240	20.33	19.2	12.1	7.1	7.1
3	4/4/2013	3 days before	Outside	144	20.33	19	7.2	11.8	11.0
4	4/4/2013	1 day before	Outside	96	20.33	20.3	12.1	8.2	8.2
5	4/4/2013	day of rain	Outside	76	20.33	20.9	11.8	9.0	9.0
6	4/4/2013	control	Outside		20.33	19	11.9	7.1	7.7

7	4/4/2013	7 days before	Outside	240	20.33	30.1	23	7.1	7.9
8	4/4/2013	3 days before	Outside	144	20.33	14.5	8.2	6.3	6.8
9	4/4/2013	1 day before	Outside	96	20.33	16.8	11.1	5.8	6.8
10	4/4/2013	day of rain	Outside	76	20.33	22.5	17	5.5	6.3
11	4/4/2013	control	Inside		22.25	17.7	4.8	12.9	9.3
12	4/4/2013	7 days before	Inside	240	22.25	16.6	2.9	13.7	11.2
13	4/4/2013	3 days before	Inside	144	22.25	16.5	5.8	10.7	9.6
14	4/4/2013	1 day before	Inside	96	22.25	24.1	15.3	8.8	7.4
15	4/4/2013	day of rain	Inside	76	22.25	24.4	13.7	10.7	9.0
16	4/4/2013	control	Inside		22.25	16.2	6.1	10.1	9.3
17	4/4/2013	7 days before	Inside	240	22.25	26.8	16.7	10.1	8.8
18	4/4/2013	3 days before	Inside	144	22.25	12.7	3.4	9.3	8.5
19	4/4/2013	1 day before	Inside	96	22.25	15.1	6.8	8.2	7.1
20	4/4/2013	day of rain	Inside	76	22.25	12.6	1.4	11.2	9.3
1	4/8/2013	control	Outside		27.1	27.1	12.9	14.2	4.1
2	4/8/2013	7 days before	Outside	336	27.1	26.4	11.6	14.8	6.4
3	4/8/2013	3 days before	Outside	240	27.1	26.6	9.6	17.0	10.1
4	4/8/2013	1 day before	Outside	192	27.1	21	10.3	10.7	7.7
5	4/8/2013	day of rain	Outside	172	27.1	13.6	2.9	10.7	7.5
6	4/8/2013	control	Outside		27.1	25.3	10.8	14.5	7.4
7	4/8/2013	7 days before	Outside	336	27.1	16.2	5.5	10.7	6.8
8	4/8/2013	3 days before	Outside	240	27.1	31	21.9	9.0	6.0
9	4/8/2013	1 day before	Outside	192	27.1	18.9	10.1	8.8	6.4
10	4/8/2013	day of rain	Outside	172	27.1	19.9	12.2	7.7	5.1
11	4/8/2013	control	Inside		30.5	11	0	11.0	9.5
12	4/8/2013	7 days before	Inside	336	30.5	26.2	10.6	15.6	9.9
13	4/8/2013	3 days before	Inside	240	30.5	17.7	2.9	14.8	8.6
14	4/8/2013	1 day before	Inside	192	30.5	14.2	1.6	12.6	7.8
15	4/8/2013	day of rain	Inside	172	30.5	31.4	13.9	17.5	8.8
16	4/8/2013	control	Inside		30.5	14.1	2.8	11.2	8.5
17	4/8/2013	7 days before	Inside	336	30.5	14.7	5.3	9.3	8.2
18	4/8/2013	3 days before	Inside	240	30.5	38	24.9	13.2	8.1
19	4/8/2013	1 day before	Inside	192	30.5	9.5	1.3	8.2	7.9
20	4/8/2013	day of rain	Inside	172	30.5	7	1.3	5.8	8.9
1	4/15/2013	control	Outside		23.5	20.1	15.8	4.4	3.3

2	4/15/2013	7 days before	Outside	504	23.5	24.9	16.4	8.5	5.8
3	4/15/2013	3 days before	Outside	408	23.5	16.8	4.5	12.3	9.3
4	4/15/2013	1 day before	Outside	360	23.5	22.3	12.1	10.1	7.1
5	4/15/2013	day of rain	Outside	340	23.5	22.8	12.1	10.7	6.0
6	4/15/2013	control	Outside		23.5	18.8	6.5	12.3	7.1
7	4/15/2013	7 days before	Outside	504	23.5	26.4	14.9	11.5	5.8
8	4/15/2013	3 days before	Outside	408	23.5	20	9.9	10.1	5.2
9	4/15/2013	1 day before	Outside	360	23.5	18.6	7.3	11.2	6.0
10	4/15/2013	day of rain	Outside	340	23.5	20.8	11.8	9.0	3.8
11	4/15/2013	control	Inside		30.25	18.8	0.7	18.1	9.6
12	4/15/2013	7 days before	Inside	504	30.25	16.7	0	16.7	8.5
13	4/15/2013	3 days before	Inside	408	30.25	38.6	22.7	15.9	7.7
14	4/15/2013	1 day before	Inside	360	30.25	22.9	5.1	17.8	8.2
15	4/15/2013	day of rain	Inside	340	30.25	39.9	22.9	17.0	8.5
16	4/15/2013	control	Inside		30.25	17.9	2.5	15.3	7.7
17	4/15/2013	7 days before	Inside	504	30.25	18.9	2.7	16.2	7.7
18	4/15/2013	3 days before	Inside	408	30.25	20.3	3.8	16.4	7.7
19	4/15/2013	1 day before	Inside	360	30.25	20.7	1	19.7	8.8
20	4/15/2013	day of rain	Inside	340	30.25	43.6	24.7	18.9	8.5

Table C 2.2. Chemical analysis of runoff and drainage water, Cold-Warm Experiment. Note, pH measurements marked with an asterisk (*) were measured >24 hours after sample was collected, which could have affected the reading.

Box	Date	Runoff SRP (ppm)	Runoff Total P (ppm)	Drained SRP (pm)	Air temp (°C)	Manure WEP (mg/box)	pH runoff
1	3/25/2013	0.12	0.72	0.02	0	0.00	7.17
2	3/25/2013	0.25	0.56	0.04	0	51.24	7.79
3	3/25/2013	0.11	0.78	0.02	0	65.05	7.21
4	3/25/2013	0.19	0.47	0.02	0	69.65	7.48
5	3/25/2013	0.2	0.83	0.02	0	74.56	7.43
6	3/25/2013	0.21	0.73	0.02	0	0.00	7.52
7	3/25/2013	0.15	0.62	0.03	0	51.24	7.5
8	3/25/2013	0.15	0.55	0.02	0	65.05	7.53
9	3/25/2013	0.18	0.69	0.02	0	69.65	7.55
10	3/25/2013			0.02	0	74.56	
11	3/25/2013	0.2	0.85	0.02	22	0.00	7.54
12	3/25/2013			0.02	22	51.24	
13	3/25/2013			0.02	22	65.05	

14	3/25/2013	0.18	1.15	0.02	22	69.65	7.59
15	3/25/2013			0.02	22	74.56	
16	3/25/2013	0.14	1.48	0.02	22	0.00	7.45
17	3/25/2013			0.02	22	51.24	
18	3/25/2013	0.19	1.38	0.03	22	65.05	7.41
19	3/25/2013				22	69.65	
20	3/25/2013	0.1		0.02	22	74.56	7.48
1	4/1/2013	0.2	0.54	0.01	2	0.00	7.25
2	4/1/2013	4.54	12.22	0.02	2	51.24	7.93
3	4/1/2013	3.55		0.07	2	65.05	
4	4/1/2013	5.41	14.32	0.11	2	69.65	8.36
5	4/1/2013	5.04	25.79	0.01	2	74.56	8.44
6	4/1/2013	0.22	0.39	0.01	2	0.00	7.7
7	4/1/2013	1.74	3.81	0.04	2	51.24	7.96
8	4/1/2013	1.22	5.17	0.01	2	65.05	8.19
9	4/1/2013	4.57	10.29	0.03	2	69.65	8.26
10	4/1/2013	5.23	25.47	0.02	2	74.56	8.4
11	4/1/2013	0.18	0.51	0.02	22	0.00	7.7
12	4/1/2013	0.38	0.92	0.02	22	51.24	7.16
13	4/1/2013	1.45	4.32	0.07	22	65.05	8.18
14	4/1/2013	3.86	11.19	0.12	22	69.65	8.71
15	4/1/2013	2.5	4.85	0.18	22	74.56	8.27
16	4/1/2013	0.27	0.34	0.02	22	0.00	7.7
17	4/1/2013			0.03	22	51.24	
18	4/1/2013	3.4	10.4	0.07	22	65.05	8.52
19	4/1/2013	1.88	3.57	0.04	22	69.65	8.36
20	4/1/2013	5.8	12.46	0.15	22	74.56	8.43
1	4/2/2013	0.22	0.62	0.01	1	0.00	7.65*
2	4/2/2013	1.37	1.71	0.06	1	51.24	7.96*
3	4/2/2013	3.39	7.76	0.05	1	65.05	8.4*
4	4/2/2013	3.09	4.72	0.08	1	69.65	7.6*
5	4/2/2013	2.06	1.83	0.05	1	74.56	7.89*
6	4/2/2013	0.22	0.57	0.02	1	0.00	7.51*
7	4/2/2013	0.89	1.29	0.05	1	51.24	7.58*
8	4/2/2013	2.48	3.81	0.03	1	65.05	8.04*
9	4/2/2013	2.21	3.55	0.04	1	69.65	7.93*
10	4/2/2013	3.15	2.53	0.03	1	74.56	7.88*
11	4/2/2013	0.09	0.23	0.02	22	0.00	7.22*
12	4/2/2013	0.28	0.69	0.03	22	51.24	7.37*
13	4/2/2013	1.13	3.66	0.05	22	65.05	7.84*
14	4/2/2013	1.36	4.53	0.05	22	69.65	7.75*

15	4/2/2013	2.23	5.77	0.08	22	74.56	7.49*
16	4/2/2013	0.26	0.79	0.03	22	0.00	7.56*
17	4/2/2013	0.29	0.67	0.04	22	51.24	7.4*
18	4/2/2013	1.05	2.68	0.05	22	65.05	7.8*
19	4/2/2013	1.4	4.27	0.03	22	69.65	7.71*
20	4/2/2013	2.04	10.32	0.03	22	74.56	7.38*
1	4/4/2013	0.22	0.42	0.02	15	0.00	7.4*
2	4/4/2013	1	1.54	0.03	15	51.24	7.9*
3	4/4/2013	1.01	1.74	0.06	15	65.05	8*
4	4/4/2013	1.75	3.22	0.08	15	69.65	8.26*
5	4/4/2013	1.71	2.19	0.04	15	74.56	8.13*
6	4/4/2013	0.24	0.52	0.02	15	0.00	7.99*
7	4/4/2013	0.81	1.46	0.05	15	51.24	7.95*
8	4/4/2013	2.98	6.47	0.07	15	65.05	8.62*
9	4/4/2013	0.88	1.49	0.31	15	69.65	8.48*
10	4/4/2013	1.78	2.61	0.02	15	74.56	8.34*
11	4/4/2013	0.18	0.39	0.01	22	0.00	7.91*
12	4/4/2013	0.26	0.65	0.02	22	51.24	7.74*
13	4/4/2013	0.75	1.62	0.03	22	65.05	8.01*
14	4/4/2013	1.12	4.99	0.03	22	69.65	8.19*
15	4/4/2013	1.79	5.02	0.07	22	74.56	8.34*
16	4/4/2013	0.24	0.37	0.01	22	0.00	8.08*
17	4/4/2013	0.31	0.82	0.04	22	51.24	7.42*
18	4/4/2013	1.1	2.63	0.03	22	65.05	7.84*
19	4/4/2013	0.7	2	0.02	22	69.65	8.31*
20	4/4/2013	2.03	4.55	0.04	22	74.56	8.34*
1	4/8/2013	0.18	0.63	0.02	15	0.00	7.74*
2	4/8/2013	0.51	0.83	0.04	15	51.24	7.78*
3	4/8/2013	0.39	0.67	0.05	15	65.05	7.75*
4	4/8/2013	0.55	0.99	0.07	15	69.65	7.81*
5	4/8/2013	0.9	1.19	0.06	15	74.56	7.99*
6	4/8/2013	0.25	0.44	0.03	15	0.00	7.99*
7	4/8/2013	0.49	0.75	0.05	15	51.24	7.94*
8	4/8/2013	0.5	0.89	0.1	15	65.05	7.9*
9	4/8/2013	0.49	0.94	0.17	15	69.65	8.16*
10	4/8/2013	0.66	1.25	0.01	15	74.56	8.17*
11	4/8/2013	0	0	0.01	23	0.00	
12	4/8/2013	0.25	0.53	0.02	23	51.24	7.04*
13	4/8/2013	0.38	0.8	0.03	23	65.05	7.33*
14	4/8/2013	0.4	0.91	0.02	23	69.65	
15	4/8/2013	0.42	0.94	0.04	23	74.56	7.75*

16	4/8/2013	0.18	0.35	0.02	23	0.00	7.77*
17	4/8/2013	0.18	0.51	0.03	23	51.24	7.33*
18	4/8/2013	0.43	1.17	0.04	23	65.05	7.74*
19	4/8/2013	0.3	0.7	0.02	23	69.65	
20	4/8/2013	0.51	1.23	0.02	23	74.56	
1	4/15/2013	0.18	0.3	0.02	16	0.00	7.61*
2	4/15/2013	0.4	0.76	0.03	16	51.24	7.7*
3	4/15/2013	0.38	0.77	0.04	16	65.05	7.76*
4	4/15/2013	0.37	0.78	0.06	16	69.65	7.69*
5	4/15/2013	0.5	0.96	0.06	16	74.56	7.7*
6	4/15/2013	0.22	0.42	0.02	16	0.00	7.79*
7	4/15/2013	0.35	0.63	0.04	16	51.24	7.6*
8	4/15/2013	0.44	0.79	0.09	16	65.05	7.74*
9	4/15/2013	0.48	0.78	0.08	16	69.65	7.89*
10	4/15/2013	0.52	1.12	0.03	16	74.56	7.87*
11	4/15/2013	0.1	0.23	0.02	22	0.00	7.66*
12	4/15/2013	0	0	0.02	22	51.24	
13	4/15/2013	0.38	0.77	0.03	22	65.05	7.37*
14	4/15/2013	0.3	0.86	0.02	22	69.65	7.38*
15	4/15/2013	0.3	0.62	0.03	22	74.56	7.45*
16	4/15/2013	0.19	0.38	0.02	22	0.00	7.66*
17	4/15/2013	0.22	0.42	0.03	22	51.24	7.49*
18	4/15/2013	0.33	0.58	0.03	22	65.05	7.6*
19	4/15/2013	0.32	0.61	0.02	22	69.65	7.85*
20	4/15/2013	0.35	0.82	0.02	22	74.56	7.7*

Table C 2.3 Rain event measurements, Wet-Dry Experiment

Box	Date	Treatment	Condition	Hours Since Manure Spread	Length of rain (min)	Rain (mm)	Runoff (mm)	Infiltration (mm)	Drainage (mm)
1	9/25/2013	control	wet		21	17.1	8.9	8.2	7.4
2	9/25/2013	7 days before	wet		21	27.7	20.3	7.4	7.1
3	9/25/2013	3 days before	wet		21	17	9.3	7.7	7.7
4	9/25/2013	1 day before	wet		21	18.1	11.5	6.6	6.3
5	9/25/2013	day of rain	wet		21	20.8	12.6	8.2	8.2
6	9/25/2013	control	wet		21	19.6	10.8	8.8	8.2
7	9/25/2013	7 days before	wet		21	32.5	25.6	6.8	6.6
8	9/25/2013	3 days before	wet		21	18.9	11.8	7.1	6.6
9	9/25/2013	1 day before	wet		21	21.5	10.3	11.2	10.4
10	9/25/2013	day of rain	wet		21	19.5	7.4	12.1	11.5

11	9/25/2013	control	dry		43	38.9	4.4	34.5	14.2
12	9/25/2013	7 days before	dry		43	35	3.8	31.2	14.5
13	9/25/2013	3 days before	dry		43	59.4	24	35.3	17
14	9/25/2013	1 day before	dry		43	42.3	8.6	33.7	14
15	9/25/2013	day of rain	dry		43	64.8	34.9	29.9	13.4
16	9/25/2013	control	dry		43	36.3	4	32.3	12.1
17	9/25/2013	7 days before	dry		43	34.8	1.4	33.4	12.9
18	9/25/2013	3 days before	dry		43	39	4.5	34.5	14.5
19	9/25/2013	1 day before	dry		43	37.7	7.5	30.1	10.1
20	9/25/2013	day of rain	dry		43	47.9	16.2	31.8	10.7
1	10/3/2013	control	wet		19.3	16.4	10.4	6	6
2	10/3/2013	7 days before	wet	168	19.3	14.9	8.4	6.6	6.6
3	10/3/2013	3 days before	wet	72	19.3	14.2	8.2	6	6
4	10/3/2013	1 day before	wet	24	19.3	16.2	10.1	6	6.6
5	10/3/2013	day of rain	wet	4	19.3	22.2	15.9	6.3	7.4
6	10/3/2013	control	wet		19.3	25.9	19.6	6.3	6.3
7	10/3/2013	7 days before	wet	168	19.3	17.9	11.4	6.6	6.3
8	10/3/2013	3 days before	wet	72	19.3	15.5	9.2	6.3	6
9	10/3/2013	1 day before	wet	24	19.3	16.2	8	8.2	8.2
10	10/3/2013	day of rain	wet	4	19.3	29.7	22.9	6.8	9
11	10/3/2013	control	dry		26.7	19.7	0	19.7	10.4
12	10/3/2013	7 days before	dry	168	26.7	26.6	5.5	21.1	13.7
13	10/3/2013	3 days before	dry	72	26.7	21.1	0	21.1	12.6
14	10/3/2013	1 day before	dry	24	26.7	22.5	1.2	21.4	11.8
15	10/3/2013	day of rain	dry	4	26.7	20.7	4.5	16.2	11.5
16	10/3/2013	control	dry		26.7	38.6	22.2	16.4	10.7
17	10/3/2013	7 days before	dry	168	26.7	34.5	18.9	15.6	10.7
18	10/3/2013	3 days before	dry	72	26.7	20.6	3.3	17.3	12.1
19	10/3/2013	1 day before	dry	24	26.7	32.1	17.3	14.8	11.5
20	10/3/2013	day of rain	dry	4	26.7	22.3	8.4	14	10.4
1	10/4/2013	control	wet		18.9	26.2	20.2	6	5.8
2	10/4/2013	7 days before	wet	192	18.9	18.8	11.7	7.1	6.8
3	10/4/2013	3 days before	wet	96	18.9	15.6	9.8	5.8	5.8
4	10/4/2013	1 day before	wet	48	18.9	30.8	24.8	6	6
5	10/4/2013	day of rain	wet	28	18.9	14.7	8.4	6.3	6

6	10/4/2013	control	wet		18.9	16.5	8.3	8.2	7.7
7	10/4/2013	7 days before	wet	192	18.9	15.4	8	7.4	6.8
8	10/4/2013	3 days before	wet	96	18.9	23	16.7	6.3	5.8
9	10/4/2013	1 day before	wet	48	18.9	15.5	7.3	8.2	7.7
10	10/4/2013	day of rain	wet	28	18.9	15.1	6.3	8.8	8.2
11	10/4/2013	control	dry		19.3	14.7	2.7	12.1	10.4
12	10/4/2013	7 days before	dry	192	19.3	15.9	1.6	14.2	12.9
13	10/4/2013	3 days before	dry	96	19.3	31.2	15	16.2	14.5
14	10/4/2013	1 day before	dry	48	19.3	17.6	4.2	13.4	11.8
15	10/4/2013	day of rain	dry	28	19.3	25.4	12.8	12.6	11
16	10/4/2013	control	dry		19.3	15.6	5.8	9.9	9
17	10/4/2013	7 days before	dry	192	19.3	14.6	4.5	10.1	9.3
18	10/4/2013	3 days before	dry	96	19.3	22.1	9.7	12.3	11.5
19	10/4/2013	1 day before	dry	48	19.3	29.5	20.1	9.3	8.8
20	10/4/2013	day of rain	dry	28	19.3	18.1	8.2	9.9	8.8
1	10/6/2013	control	wet		20.7	16.2	11	5.2	4.7
2	10/6/2013	7 days before	wet	240	20.7	26.2	19.3	6.8	6.6
3	10/6/2013	3 days before	wet	144	20.7	16.9	11.2	5.8	5.2
4	10/6/2013	1 day before	wet	96	20.7	20.8	13.9	6.8	6.3
5	10/6/2013	day of rain	wet	76	20.7	15.7	10.2	5.5	5.2
6	10/6/2013	control	wet		20.7	18.5	12.5	6	5.5
7	10/6/2013	7 days before	wet	240	20.7	37.1	31.1	6	5.8
8	10/6/2013	3 days before	wet	144	20.7	31	25.3	5.8	5.5
9	10/6/2013	1 day before	wet	96	20.7	16.7	9.9	6.8	6.6
10	10/6/2013	day of rain	wet	76	20.7	16.6	7.8	8.8	8.2
11	10/6/2013	control	dry		22.3	15.2	3.4	11.8	9.9
12	10/6/2013	7 days before	dry	240	22.3	17.1	5.1	12.1	10.4
13	10/6/2013	3 days before	dry	144	22.3	17.3	2.3	15.1	13.2
14	10/6/2013	1 day before	dry	96	22.3	17.4	4.8	12.6	10.4
15	10/6/2013	day of rain	dry	76	22.3	17	3.8	13.2	11.5
16	10/6/2013	control	dry		22.3	22.1	11.6	10.4	8.5
17	10/6/2013	7 days before	dry	240	22.3	34.3	23.4	11	9
18	10/6/2013	3 days before	dry	144	22.3	40.1	27.7	12.3	10.4
19	10/6/2013	1 day before	dry	96	22.3	19.5	10.2	9.3	7.9
20	10/6/2013	day of rain	dry	76	22.3	30.5	20.3	10.1	9

1	10/10/2013	control	wet		19.9	16.6	10.1	6.6	6.3
2	10/10/2013	7 days before	wet	336	19.9	15.1	8.5	6.6	6.3
3	10/10/2013	3 days before	wet	240	19.9	28.9	22.3	6.6	5.5
4	10/10/2013	1 day before	wet	192	19.9	15.8	10.8	4.9	4.9
5	10/10/2013	day of rain	wet	172	19.9	16.2	9.9	6.3	6.3
6	10/10/2013	control	wet		19.9	16.4	11.2	5.2	4.4
7	10/10/2013	7 days before	wet	336	19.9	19.7	12.3	7.4	7.4
8	10/10/2013	3 days before	wet	240	19.9	31.4	26.2	5.2	4.7
9	10/10/2013	1 day before	wet	192	19.9	16.4	9	7.4	7.1
10	10/10/2013	day of rain	wet	172	19.9	23.6	14.8	8.8	8.8
11	10/10/2013	control	dry		27	21.8	9	12.9	9.3
12	10/10/2013	7 days before	dry	336	27	42.8	26.4	16.4	12.9
13	10/10/2013	3 days before	dry	240	27	39.7	22.5	17.3	13.2
14	10/10/2013	1 day before	dry	192	27	26	10.4	15.6	10.7
15	10/10/2013	day of rain	dry	172	27	32.7	15.2	17.5	12.9
16	10/10/2013	control	dry		27	21.5	8.1	13.4	8.5
17	10/10/2013	7 days before	dry	336	27	22.7	9	13.7	8.8
18	10/10/2013	3 days before	dry	240	27	22.6	7.5	15.1	10.1
19	10/10/2013	1 day before	dry	192	27	22.9	8.6	14.2	8.8
20	10/10/2013	day of rain	dry	172	27	22.8	8.8	14	7.9

Table C. 2.4 Chemical analysis of runoff and drainage water, Wet-Dry Experiment

Box	Date	Runoff SRP (ppm)	Runoff TP (ppm)	Drainage SRP (ppm)	Soil moist (vol. %)	Air temp (^{o}C)	Manure WEP (mg/box)
1	9/25/2013	0.16	0.53	0.03	51	21	
2	9/25/2013	0.14	0.57	0.03	52	21	44
3	9/25/2013	0.14	0.53	0.03	52	21	43
4	9/25/2013	0.22	0.44	0.03	50	21	49
5	9/25/2013	0.18	0.67	0.02	49	21	48
6	9/25/2013	0.2	0.47	0.03	54	21	
7	9/25/2013	0.18	0.5	0.03	52	21	44
8	9/25/2013	0.19	0.4	0.02	54	21	44
9	9/25/2013	0.18	0.55	0.02	47	21	50
10	9/25/2013	0.18	0.42	0.02	45	21	47
11	9/25/2013	0.16	0.26	0.03	8	21	
12	9/25/2013	0.1	0.21	0.04	8	21	44
13	9/25/2013	0.11	0.18	0.04	7	21	44
14	9/25/2013	0.17	0.3	0.04	9	21	47

15	9/25/2013	0.17	0.28	0.04	9	21	48
16	9/25/2013	0.15	0.32	0.03	9	21	
17	9/25/2013	0.14	0.5	0.04	7	21	44
18	9/25/2013	0.17	0.29	0.04	8	21	43
19	9/25/2013	0.17	0.3	0.04	9	21	50
20	9/25/2013	0.19	0.46	0.04	8	21	47
1	10/3/2013	0.18	0.58	0.03	54	21	
2	10/3/2013	0.51	2.68	0.05	56	21	44
3	10/3/2013	1.04	5.53	0.07	62	21	43
4	10/3/2013	1.16	6.06	0.1	69	21	49
5	10/3/2013	2.84	10.23	0.07	89	21	48
6	10/3/2013	0.21	0.5	0.07	57	21	
7	10/3/2013	0.46	1.91	0.06	61	21	44
8	10/3/2013	0.74	2.93	0.08	62	21	44
9	10/3/2013	0.85	4.79	0.08	63	21	50
10	10/3/2013	2.34	7.97	0.15	107	21	47
11	10/3/2013	0	0	0.05	22	21	
12	10/3/2013	0.23	1.11	0.08	25	21	44
13	10/3/2013	0	0	0.06	21	21	44
14	10/3/2013	0.41	4.13	0.12	26	21	47
15	10/3/2013	2.29	6.72	0.35	77	21	48
16	10/3/2013	0.17	0.33	0.06	39	21	
17	10/3/2013	0.29	1.25	0.08	47	21	44
18	10/3/2013	0.33	1.46	0.13	40	21	43
19	10/3/2013	1.22	7.64	0.79	47	21	50
20	10/3/2013	1.9	5.21	0.28	74	21	47
1	10/4/2013	0.16	0.32	0.03	50	21	
2	10/4/2013	0.64	1.59	0.05	62	21	44
3	10/4/2013	0.6	2.05	0.06	57	21	43
4	10/4/2013	0.88	4.01	0.09	58	21	49
5	10/4/2013	0.35	2.04	0.08	57	21	48
6	10/4/2013	0.25	0.3	0.04	56	21	
7	10/4/2013	0.41	0.83	0.1	59	21	44
8	10/4/2013	1.04	4.9	0.04	60	21	44
9	10/4/2013	1.54	6.75	0.18	57	21	50
10	10/4/2013	0.45	2.77	0.42	56	21	47
11	10/4/2013	0.17	0.21	0.05	47	21	
12	10/4/2013	0.22	0.76	0.07	46	21	44
13	10/4/2013	0.22	1.16	0.08	41	21	44
14	10/4/2013	1.27	3.63	0.1	38	21	47
15	10/4/2013	1.03	2.99	0.12	45	21	48

16	10/4/2013	0.19	0.23	0.05	46	21	
17	10/4/2013	0.57	0.7	0.2	47	21	44
18	10/4/2013	0.57	1.96	0.37	51	21	43
19	10/4/2013	0.75	2.59	0.23	51	21	50
20	10/4/2013	0.7	3.24	0.28	54	21	47
1	10/6/2013	0.19	0.3	0.08	52	21	
2	10/6/2013	0.39	0.92	0.09	53	21	44
3	10/6/2013	0.32	0.94	0.09	60	21	43
4	10/6/2013	0.41	1.41	0.16	56	21	49
5	10/6/2013	0.46	1.7	0.2	54	21	48
6	10/6/2013	0.25	0.26	0.09	58	21	
7	10/6/2013	0.44	1	0.08	53	21	44
8	10/6/2013	0.42	1.77	0.1	57	21	44
9	10/6/2013	0.48	1.36	0.08	60	21	50
10	10/6/2013	0.4	0.96	0.11	59	21	47
11	10/6/2013	0.12	0.18	0.04	35	21	
12	10/6/2013	0.19	0.5	0.09	34	21	44
13	10/6/2013	0.16	0.69	0.09	43	21	44
14	10/6/2013	0.24	1.21	0.07	32	21	47
15	10/6/2013	0.34	0.75	0.11	43	21	48
16	10/6/2013	0.16	0.26	0.06	40	21	
17	10/6/2013	0.26	0.78	0.05	47	21	44
18	10/6/2013	0.27	0.75	0.12	49	21	43
19	10/6/2013	0.33	1.02	0.07	43	21	50
20	10/6/2013	0.5	2.41	0.12	41	21	47
1	10/10/2013	0.19	0.28	0.03	52	21	
2	10/10/2013	0.37	0.62	0.04	51	21	44
3	10/10/2013	0.28	0.73	0.05	57	21	43
4	10/10/2013	0.3	0.79	0.04	55	21	49
5	10/10/2013	0.26	0.72	0.03	56	21	48
6	10/10/2013	0.21	0.31	0.04	57	21	
7	10/10/2013	0.57	0.81	0.05	57	21	44
8	10/10/2013	0.29	0.56	0.02	58	21	44
9	10/10/2013	0.3	0.74	0.04	51	21	50
10	10/10/2013	0.23	0.67	0.05	51	21	47
11	10/10/2013	0.14	0.18	0.03	30	21	
12	10/10/2013	0.24	0.4	0.05	37	21	44
13	10/10/2013	0.17	0.43	0.04	33	21	44
14	10/10/2013	0.19	0.56	0.06	35	21	47
15	10/10/2013	0.32	0.46	0.04	33	21	48
16	10/10/2013	0.17	0.42	0.03	41	21	

17	10/10/2013	0.4	0.46	0.04	42	21	44
18	10/10/2013	0.22	0.41	0.05	36	21	43
19	10/10/2013	0.25	0.4	0.05	38	21	50
20	10/10/2013	0.27	0.66	0.05	46	21	47